

Cassiana Mendes

**ESTRATÉGIAS PARA A MELHORIA DAS PROPRIEDADES
BIOFARMACÊUTICAS DE FÁRMACOS CLASSE IV:
DESENVOLVIMENTO DE SISTEMAS NANOESTRUTURADOS
PARA A HIDROCLOROTIAZIDA E NORFLOXACINO**

Tese submetida ao Programa de Pós-
Graduação em Farmácia da Universidade
Federal de Santa Catarina.

Orientador: Prof. Dr. Marcos Antônio
Segatto Silva

Coorientador: Prof. Dr. Gilles Ponchel

Florianópolis
2016

Ficha de identificação da obra elaborada pelo autor,
através do Programa de Geração Automática da Biblioteca Universitária da UFSC.

Mendes, Cassiana

Estratégias para a melhoria das propriedades biofarmacêuticas de fármacos classe IV: desenvolvimento de sistemas nanoestruturados para a hidroclorotiazida e norfloxacino / Cassiana Mendes ; orientador, Marcos Antônio Segatto Silva ; coorientador, Gilles Ponchel. - Florianópolis, SC, 2016.

178 p.

Tese (doutorado) - Universidade Federal de Santa Catarina, Centro de Ciências da Saúde. Programa de Pós-Graduação em Farmácia.

Inclui referências

1. Farmácia. 2. Fármacos classe IV. 3. Nanotecnologia. 4. Solubilidade. 5. Permeabilidade. I. Silva, Marcos Antônio Segatto. II. Ponchel, Gilles. III. Universidade Federal de Santa Catarina. Programa de Pós-Graduação em Farmácia. IV. Título.

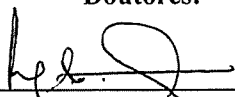
**“Estratégias para melhoria das propriedades
biofarmacêuticas de fármacos Classe IV:
desenvolvimento de sistemas nanoestruturados para a
hidroclorotiazida e norfloxacino”**

POR

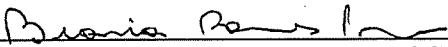
Cassiana Mendes

Tese julgada e aprovada em sua
forma final pelo(a) Orientador(a) e
membros da Banca Examinadora,
composta pelos Professores
Doutores:

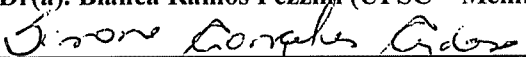
Banca Examinadora:




Prof(a). Dr(a). Angela Machado de Campos (UFSC – Membro
Titular)



Prof(a). Dr(a). Bianca Ramos Pezzini (UFSC – Membro Titular)



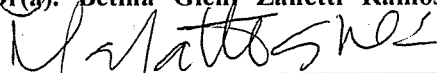
Prof(a). Dr(a). Simone Gonçalves Cardoso (UFSC – Membro
Titular)



Prof(a). Dr(a). Franceline Reynaud (UFRJ – Membro Titular)



Prof(a). Dr(a). Betina Giehl Zanetti Ramos (UFSC – Membro
Titular)



Prof(a). Dr(a). Marcos Antônio Segatto Silva (UFSC – Orientador)

Prof(a). Dra. Tânia Beatriz Creczynski Pasa
Coordenadora do Programa de Pós-Graduação em Farmácia da
UFSC

Florianópolis, 30 de novembro de 2016.

Dedico este trabalho aos meus pais,
que sempre iluminaram meu caminho com
a luz mais brilhante que puderam
encontrar, o estudo.

AGRADECIMENTOS

Aos meus pais, Elisabeth e Ildemar, por todo incentivo, apoio e preocupação, bem como à toda minha família, Rafael, Luciana e Arthur.

Ao meu amor, Diego Furtado, por ser meu companheiro de todas as horas, pelo ombro amigo, por todo amor, paciência, carinho e conselhos.

Ao meu orientador Marcos Segatto, por me aceitar em toda minha trajetória acadêmica sempre apoiando e acreditando no meu trabalho.

Ao meu coorientador Gilles Ponchel, *pour ouvrir les portes de Paris-Sud et pour tous les réflexions scientifique et de la vie.*

Às minhas ICs Aline e Jéssica por toda a ajuda, esforço, dedicação, e principalmente, por assumirem o trabalho como de vocês.

Às meninas da Farmacologia, Clarissa, Patricia e Flora, pela ajuda essencial nos experimentos *in vivo*, sempre acompanhados de boas risadas.

A todos os meus amigos de coração, Tábata, Nakita, Ana Paula, Heloísa, Clarissa, Gabriela, Juliana Munari, Mariana, Patricia, Aline e Rafael Nicolay, por estarem de alguma forma sempre presentes me incentivando. À minha amiga Luana, que me acolheu em Paris e me fez enxergar o lado bom depois da tempestade. Vocês tornaram a caminhada mais leve e divertida!

Aos meus colegas do LabCQ, Aline Farias, Aline Leão, Ana Karolina, Amarilis, Brenda, Daia, Fabi, Ju, Juli, Maria, Manuela, Paola, Rafael, Tati, Roberta, Yasmin, às professoras Simone e Hellen e também aos meus colegas Equipe 6, Gabriela, Sarah, Henrique, Any Taylor, Sophie, Herman, Raul por toda ajuda, risadas e momentos de descontração.

Aos professores Thiago Caon, Elenara Lemos-Senna e Jamil Assreuy pela colaboração e discussão fundamentais para este trabalho.

Ao CNPq, CAPES, PGfar, UFSC, UPSud. UMRS pelo apoio financeiro e por possibilitar a realização deste trabalho.

A todos que mesmo não citados, contribuíram para a realização deste sonho.

Every now and then a man's mind is stretched by a new idea or sensation, and never shrinks back to its former dimensions.

(Oliver Wendell Holmes Sr, 1873)

RESUMO

Para a efetividade terapêutica após a administração oral é imprescindível a dissolução do fármaco no meio gastrointestinal e sua consequente permeação pelas membranas biológicas para atingir a corrente sanguínea. Fármacos classe biofarmacêutica IV exibem propriedades inadequadas de absorção, não só pela baixa dissolução aquosa, mas também pela sua baixa permeabilidade, de modo que níveis muito baixos de fármaco dissolvido levarão a uma baixa biodisponibilidade. Um dos desafios encontrados no desenvolvimento de formulações contendo fármacos da classe IV situa-se na dificuldade de desenvolver sistemas de liberação capazes de aperfeiçoar ambas as propriedades em deficiência. Este trabalho trata-se de uma progressão do mestrado para o doutorado e tem por objetivo a continuação com os estudos para melhora das propriedades biofarmacêuticas de fármacos classe IV. A nanotecnologia é uma área proeminente no desenvolvimento de formas farmacêuticas para fármacos com limitações de biodisponibilidade, como o diurético hidroclorotiazida. Foi proposto neste trabalho, portanto, o desenvolvimento de duas estratégias nanoestruturadas para liberação da hidroclorotiazida: (1) um sistema de liberação autonanoemulsionável e (2) uma nanoemulsão formada por emulsificação espontânea revestida com agente mucoadesivo e seca em *spray-dryer* (partículas Trojan). O sistema de liberação autonanoemulsionável com reduzida quantidade de surfactante foi composto por triglicerídeos de cadeia média, Cremophor EL e Transcutol P que resultou em uma nanoemulsão com potencial zeta altamente negativo. Todas as caracterizações foram realizadas em meio biorelevante de forma a predizer melhor o comportamento *in vivo*. A melhora do perfil de dissolução refletiu na atividade diurética, apresentando uma natriurese, caliurese e cloriurese nos estágios iniciais e um aumento do volume total de urina em comparação com o fármaco puro. O sistema autonanoemulsionável apresentou-se, portanto, eficiente na modulação da absorção da hidroclorotiazida. Outro sistema inovador desenvolvido foram as partículas Trojan mucoadesivas. Para tanto, nanoemulsões foram desenvolvidas pelo método de formação espontânea compostas por triglicerídeos de cadeia média, Lipoid® S75 e Pluronic® F68 com alta eficiência de encapsulação. Esta nanoemulsão foi revestida com quitosana para adicionar as propriedades mucoadesivas à formulação. A microencapsulação da nanoemulsão foi realizada em *spray-dryer* com Aerosil® com material de parede para englobar as gotículas de óleo de hidroclorotiazida, originando então as partículas denominadas de Trojan. A rápida solubilização do material de parede seguida da redispersão da nanoemulsão revestida nos fluidos gastrointestinais simulados levou a

uma completa dissolução no meio gástrico. O sistema Trojan incrementou a atividade farmacodinâmica da hidroclorotiazida bem como suas propriedades biofarmacêuticas, estendendo a atividade diurética do fármaco. Ambos sistemas desenvolvidos apresentam abordagens cientificamente fundamentadas capazes de superar as limitações apresentadas pela hidroclorotiazida e consequentemente melhorar a eficácia terapêutica. No mesmo contexto, pesquisas com o norfloxacino foram realizadas de modo a guiar o desenvolvimento de um sistema nanoestruturado direcionado para este fármaco, um antibiótico classe biofarmacêutica IV também objeto de estudo deste trabalho. O norfloxacino é um fármaco pouco solúvel e pouco permeável, o que reflete na sua absorção oral e, consequentemente, altas doses são necessárias para um tratamento efetivo. A literatura sugere mecanismos de efluxo intestinal do norfloxacino, o que pode estar associado com a baixa biodisponibilidade relatada para este fármaco. Portanto, durante estágio sanduíche foi realizada a determinação dos fatores de permeabilidade intestinal do norfloxacino. O efluxo intestinal foi confirmado e foi possível identificar os transportadores que o norfloxacino serve de substrato, tanto para ligação para permear como para inibição do transportador, podendo influenciar na absorção de outros fármacos. Desta forma este estudo serviu de base para o desenvolvimento de um nanocarreador que pode aperfeiçoar as características de solubilidade e permeabilidade do norfloxacino. A nanoesponja de norfloxacino é um sistema mucoadesivo que foi capaz de estender a atividade antibacteriana do fármaco. Esta melhora na farmacodinâmica pode levar a uma possível redução de dose com consequente aumento de adesão do paciente ao tratamento e diminuição do surgimento de novos microrganismos resistentes.

Palavras-chave: câmaras de Ussing, hidroclorotiazida; mucoadesão; nanoemulsão; nanoesponja, norfloxacino; partículas Trojan; sistemas de liberação de fármacos autonanoemulsionáveis; solubilidade; permeabilidade.

ABSTRACT

Aiming the therapeutic effectivity after oral administration, it is fundamental drug dissolution in the gastrointestinal medium and its consequent permeation across biological membranes to reach blood circulation. Drugs belonging to class biopharmaceutical IV present inappropriate absorption properties, not only because of low aqueous dissolution but also because of low permeability, generating low level of dissolved drug that leads a low bioavailability. One challenge faced in the pharmaceutical development of drugs class IV is the development of drug delivery systems able to improve both deficient properties. This work is a progression from master to PhD degree and it aims, continuously, the study of class IV biopharmaceutical properties improvement. Nanotechnology is a prominent area in the drug delivery development target to drugs with bioavailability limitations, as diuretic hydrochlorothiazide. Therefore, it was proposed in this work the development of two different nanostructured strategies to hydrochlorothiazide delivery: (1) self-nanoemulsifying drug delivery system and (2) nanoemulsion formed by spontaneous emulsification coated with mucoadhesive agent and dried in spray-dryer (Trojan particles). The self-nanoemulsifying drug delivery system with reduced amount of surfactant was composed of medium chain triglycerides, Cremophor EL and Transcutol P. This system was stabilized by the nanoscale globules and high negative zeta potential. All the physicochemical characterization assays were performed in biorelevant media to better predict the *in vivo* performance. The enhanced dissolution rate of the system reflected in the *in vivo* diuretic activity, presenting a natriuresis, kaliuresis and chlориuresis at early stages and an increased volume of total urine compared with hydrochlorothiazide alone. The designed system showed to be an efficient approach to modulate the absorption of hydrochlorothiazide. Another innovative system developed was Trojan-type mucoadhesive systems. Nanoemulsions were firstly formed spontaneously by combining medium chain triglycerides, Lipoid® S75 and Pluronic® F68 and high encapsulation efficiency was observed. The mucoadhesive properties were provided by chitosan and microencapsulation of nanoemulsions in spray-dryer was successfully achieved by using Aerosil® as wall material to entrap the oil-droplets of hydrochlorothiazide generating Trojan particles. The rapid solubilization of wall material followed by redispersion of coated-nanoemulsion in simulated fluids led to a fast and complete release of HCTZ in gastric medium. The pharmacodynamic of HCTZ was improved by Trojan-type system as biopharmaceutical properties, extending the diuretic activity. Both developed systems present scientific approaches able to overcome limitations of

hydrochlorothiazide and consequently improve therapeutic efficacy. In the same context, norfloxacin researches were done aiming to guide the development of nanostructured system target to this drug, an antibiotic class IV, also study object of this work. Norfloxacin is a drug that presents low solubility and low permeability, which reflects in the low bioavailability and consequently high daily doses are required to treatment effectiveness. Data from literature suggest the intestinal efflux of norfloxacin which could be associated with the low bioavailability reported to this drug. Therefore, during international doctoral stage, it was determinate intestinal permeability factors of norfloxacin. The intestinal efflux was confirmed and it was possible to identify intestinal transporters that norfloxacin is substrate, even to link to permeate or as inhibitor transporter, which could influence in other drugs absorption. In this way, this study provides a base to the development of nanocarrier able to improve both solubility and permeability of norfloxacin. Nanosponges of norfloxacin is a mucoadhesive system able to extend antibacterial activity of the drug. This pharmacodynamic improvement could lead to dose reduction and, as a consequence, it could improve patient compliance and decrease the appearance of new resistant microorganisms.

Keywords: hydrochlorothiazide; mucoadhesion; nanoemulsion; nanosponge, norfloxacin; self-nanoemulsifying drug delivery systems; solubility; permeability; Trojan particles; Ussing chambers.

LISTA DE FIGURAS

Capítulo 1

Figura 1 – Sistema de classificação Biofarmacêutica como definido por Amidon e colaboradores (1995).....	33
Figura 2 – Esquema do modelo de câmara de Ussing.....	36
Figura 3 – Estrutura química da hidroclorotiazida.....	37
Figura 4 – Transporte de íons no túbulo distal, mostrando o local de ação da hidroclorotiazida, diurético tiazídico.....	39
Figura 5 – Estrutura química do norfloxacino.....	42
Figura 6 – Representação esquemática do mecanismo de ação das quinolonas.....	42
Figura 7 – Estrutura da nanoesponja de ciclodextrina proposta por Swaminathan (2007).....	50

Capítulo 2

Figure 1 – Ternary phase diagram of system A (MCT/Cremophor EL/Transcutol).....	65
Figure 2 – TEM images of the reconstituted nanoemulsion from SNEDDS F1 (A and B) and F2 (C and D).....	69
Figure 3 – Dissolution profiles of HCTZ and SNEDDS F1 and F2 obtained in FASSGF (pH 1.6) during 120 min and in FASSIF (pH 6.5) for more 180 min.....	72
Figure 4 – Effects of acute oral administration of SNEDDS containing HCTZ on urine output (Panel A) and electrolyte excretion (Panel B, C, D). The graphs show the urinary volume (A), concentration of Na ⁺ , K ⁺ and Cl ⁻ (B, C and D, respectively) in samples collected 2, 4, 8 and 24 h after the treatment. The results show the mean ± S.E.M of 3-6 animals per group. Statistical analyses were performed by means of one-way analysis of variance (ANOVA) followed by Tukey post-test. * P < 0.05; when compared with the control group and # P < 0.05 significantly different from corresponding SNEDDS-HCTZ group.....	74

Capítulo 3

Figure 1 – Hydrodynamic diameter (nm) of nanoemulsions obtained with different oils (castor, cotton, olive or MCT) and surfactants (Pluronic® F68, Lipoid® and Tween 20). P25 and P05 correspond to Pluronic® F68 at 0.25% and 0.5%, T05 and T1 to Tween 20 at 0.5% and 1%, L1, L2 and L4 to Lipoid® at 1, 2 and 4 mg/mL.....	95
---	----

Figure 2 – Hydrodynamic diameter variation (nm) of the mucin colloidal system at 125 µg/mL (A) or 250 µg/mL (B) as a function of added chitosan coated NE (% v/v).....98

Figure 3 – Photomicrographs of the powders of spray-dried pure wall materials (scale bar 100 µm) and NE microencapsulated with the respective wall material (scale bar 30 µm): (A) Aerosil® , (B) F1 (microencapsulated NE Aerosil®), (C) Maltodextrin: Aerosil® 1:1 w, (D) F2 (microencapsulated NE Maltodextrin: Aerosil® 1:1 w/w), (E) Maltodextrin: Aerosil® 1:2 w/w, (F) F3 (microencapsulated NE Maltodextrin: Aerosil® 1:2 w/w).....100

Figure 4 – DSC curves obtained to HCTZ (A), Aerosil® (B), HCTZ:Aerosil® (1:1 w/w) (C), maltodextrin (D), HCTZ:maltodextrin (1:1 w/w) (E), F1 HCTZ-loaded (F) F1 unloaded (G), F2 HCTZ-loaded (H), F2 unloaded (I), F3 HCTZ-loaded (J), F3 HCTZ unloaded (K).....101

Figure 5 – FTIR spectrum of HCTZ (A), Aerosil® (B), HCTZ:Aerosil® (1:1 w/w) (C), maltodextrin (D), HCTZ:maltodextrin (1:1 w/w) (E), MCT (F), HCTZ:MCT (1:1 w/w) (G), F1 unloaded (H), F1 HCTZ-loaded (I), F2 unloaded (J), F2 HCTZ-loaded (K), F3 HCTZ unloaded (L), F3 HCTZ-loaded (M).....102

Figure 6. Dissolution profile of HCTZ (A) and NE microencapsulated systems: F1 (B) F2 (C) and F3 (D) obtained in FASSGF (pH 1.6) during 120 min and in FASSIF (pH 6.5) for more 180 min.....103

Figure 7– Effects of acute oral treatment of Trojan on urine output (Panel A) and electrolyte excretion (Panel B, C, D). The graphs show the urinary volume (A), concentration of Na+ K+ Cl- (B, C and D, respectively) in urine samples collected 2, 4, 8 and 24 h after the treatment. The results show the mean ± S.E.M of 3-6 animals per group. One-way analysis of variance (ANOVA) followed by Tukey post-test was used for statistical analysis. * P < 0.05; when compared with the control group and # P < 0.05 significantly different from corresponding Trojan-HCTZ group.....104

Capítulo 4

Figure 1–NFX quantity (%) that permeates during 180 minutes at 37 °C mucosal-to-serosal and serosal-to-mucosal and at 4 °C.....119

Figure 2 – NFX intestinal passage (%) at different portions of rat intestine: duodenum, jejunum, ileum and colon.....120

Figure 3– NFX and its species distributions according to pH value. The pH of 7.4 is highlighted because is the pH of the medium used in the Ussing chamber experiments. (Based on Mendes et al., 2015).....122

Figure 4 – Total quantity of NFX (NFX) in mucosal and serosal side of Ussing chamber experiment in the presence of levofloxacin (LVF, Panel A) or budesonide (BUD, Panel B).....126

Figure 5 – Schematic summary representation of main efflux (blue) and uptake (yellow) intestinal transporters and their involvement in NFX intestinal permeability. P-glycoprotein (P-gp), breast cancer resistance protein (BCRP), multidrug resistance-associated protein (MRP1/MRP2), peptide protein (PEPT-1), organic cation transporter (OCT1/OCT2), organic cation carnitine transporters (OCTN1/OCTN2), plasma membrane monoamine transporter (PMAT), organic anion transporter polypeptide (OATP2B1/OATP1A2), monocarboxylate transporter (MCT1).....128

Capítulo 5

Figure 1– Differential scanning calorimetry curves of Norfloxacin (NFX), β -cyclodextrin (β CD), diphenyl carbonate (DC), Nanosponge (NS), NFX-loaded Nanosponge (NFX NS).....146

Figure 2 – Fourier transform infrared spectroscopy spectra of Norfloxacin (NFX), β -cyclodextrin (β CD), diphenyl carbonate (DC), Nanosponge (NS), NFX-loaded Nanosponge (NFX NS).....147

Figure 3– TEM observations of nanosponges (NS).....148

Figure 4 – Norfloxacin (NFX) and NFX-loaded nanosponge (NS) (%) that permeates during 180 minutes at 37 °C: (A) mucosal-to-serosal (M-S) and serosal-to-mucosal (S-M), (B) in mucosal and serosal side and in presence and absence of semi-permeable membrane. (A) * P < 0.05 when compared NS with NFX M-S or S-M. (B) * P < 0.05 when compared NS with NS membrane, NFX or NFX membrane. # P < 0.05 when compared NS mucosal to NFX mucosal.....149

Figure 5 – Norfloxacin intestinal flow ($\times 10^{-12}$ nmol/cm²/s) at different portions of rat intestine (duodenum, jejunum, ileum and colon) from Norfloxacin drug alone (NFX) or NFX-loaded Nanosponge.....150

Figure 6– Norfloxacin-loaded Nanosponge attached to the mucus layer (% attached) at jejunum and colon during 60 min.....150

Figure 7– Release profile of norfloxacin (NFX) from nanosponge (NS) in intestinal simulated fluid (pH 6.8).....151

Figure 8– Effects of oral treatment of Nanosponge on bacterial growth. The graph show the bacterial growth in kidney harvested 24 h after the treatment of animal treated 1h after sepsis induction by CLP. The results show the mean \pm S.E.M of 5-6 animals per group (CLP+Veh: 5; NFX: 5; NS: 6 animals). The results not showed normal distribution, Kruskal-Wallis followed by Dunn’s post-test was used for statistical analysis. * P < 0.05 when compared

NS with the CLP+Veh group and # P < 0.05 when compared NS with the corresponding NFX group (NFX NS).....152

LISTA DE TABELAS

Capítulo 2

Table 1. Emulsifying ability between oils, surfactants and cosurfactants.....	64
Table 2. Mean globule size, polydispersity index and drug content of SNEDDS diluted in distilled water, FaSSGF and FaSSIF at a ratio of 1:1000 after the preparation (time zero), 1 and 3 months at room temperature (25°C) and refrigerator temperature (4°C)	67

Capítulo 3

Table 1. Hydrodynamic diameter and polydispersity index (PDI) of HCTZ-loaded NE after chitosan coating.....	96
Table 2. Nanoemulsion size distribution, after preparation (raw nanoemulsion), mixed with wall material before spray-drying (NE + WM before spray-drying), and mixed with wall material after spray-drying and resuspended in the same volume of water.....	97

Capítulo 4

Table 1. Apparent permeability values (P_{app}) of NFX determined from Ussing chamber experiments in mucosal-to-serosal (M-S) and serosal-to-mucosal (S-M) at 37 °C, and mucosal-to-serosal at 4 °C, both experiments realized with duodenal portions.....	120
Table 2. Flow obtained to NFX alone or in presence of transporter inhibitor at duodenum (duod), jejunum (jej), ileum or colon.....	121

Capítulo 5

Table 1. Apparent permeability values (P_{app}) of NFX determined from Ussing chamber experiments in mucosal-to-serosal (M-S) at 37 °C, experiments realized with duodenal portions.....	148
--	-----

LISTA DE ABREVIATURAS, SIGLAS e UNIDADES

μg	Micrograma
μL	Microlitro
μm	Micrômetro
ADN	Ácido desoxirribonucleico
ANVISA	Agência Nacional de Vigilância Sanitária
AVC	Acidente vascular cerebral
$^{\circ}\text{C}$	Grau Celsius
CD	Ciclodextrina
Da	Daltons
DSC	Calorimetria exploratória diferencial
ECA	Enzima conversora de angiotensina
FDA	Food and Drug Administration
g/mol	Grama/mol
HCTZ	Hidroclorotiazida
h	Hora
ICH	The International Conference on Harmonization of Technical Requirements for Registration of Pharmaceuticals for Human Use
ITU	Infecção do trato urinário
M	Molaridade
mAU	Mili Absorbance Units (Unidades de absorbância)
mg	Miligrama
min	Minuto
mL	Mililitro
mV	Milivolts
nm	Nanômetros
NFX	Norfloxacino
NE	Nanoemulsão
NS	Nanoesponja
OMS	Organização Mundial de Saúde
pH	Potencial hidrogeniônico
s	Segundo
SCB	Sistema de classificação biofarmacêutica
SNEDDS	Sistema de liberação autonanoemulsionável (do inglês, <i>self-nanoemulsifying drug delivery system</i>)
t_{max}	Tempo para atingir a concentração plasmática máxima
UV	Ultravioleta

SUMÁRIO

1. INTRODUÇÃO	25
1.1 OBJETIVOS.....	29
1.1.1 Objetivo geral.....	29
1.1.2 Objetivos específicos.....	29
CAPÍTULO 1 – REVISÃO BIBLIOGRÁFICA	31
1. SISTEMA DE CLASSIFICAÇÃO BIOFARMACÊUTICA	33
1.1 PERMEABILIDADE.....	35
2. HIDROCLOROTIAZIDA	37
3. NORFLOXACINO	40
4. NANOTECNOLOGIA	44
4.1 SISTEMAS AUTONAEMULSIONÁVEIS.....	45
4.2 NANOEMULSÕES.....	47
4.3 NANOESPONJAS.....	48
CAPÍTULO 2 – Sistema autonanoemulsionável de liberação de hidroclorotiazida para melhoria da dissolução e atividade diurética. Artigo submetido para periódico AAPS PharmSciTech	51
CAPÍTULO 3 – Microencapsulação de nanoemulsão revestida com quitosana para administração de hidroclorotiazida. Artigo submetido para o periódico Drug Development and Industrial Pharmacy	83
CAPÍTULO 4 - Determinação dos fatores de permeabilidade intestinal do norfloxacino em modelo de câmara de Ussing. Artigo submetido para o periódico Molecular Pharmaceutics	111
CAPÍTULO 5 - Desenvolvimento de nanoesponja de ciclodextrina contendo norfloxacino	135
DISCUSSÃO GERAL	157
CONCLUSÕES	163
REFERÊNCIAS	165
APÊNDICE A	177

1. INTRODUÇÃO

Após administração oral de fármacos, etapas como dissolução no meio aquoso gastrointestinal e permeação através das membranas celulares são fatores fundamentais para efetividade terapêutica. Um modelo de predição da absorção oral de fármacos foi estabelecido por Amidon e colaboradores e classifica os fármacos segundo suas características de solubilidade aquosa e permeabilidade intestinal em quatro categorias: classe I (alta solubilidade e alta permeabilidade), classe II (baixa solubilidade e alta permeabilidade), classe III (alta solubilidade e baixa permeabilidade) e classe IV (baixa solubilidade e baixa permeabilidade). Os fármacos classe biofarmacêutica IV poderão apresentar problemas de biodisponibilidade devido às suas características biofarmacêuticas (Amidon *et al.*, 1995; Cagno *et al.*, 2012).

A hidroclorotiazida (HCTZ) é um diurético tiazídico pertencente à classe biofarmacêutica IV, ou seja, de baixa solubilidade e baixa permeabilidade. Descoberta em 1958, foi o primeiro fármaco realmente efetivo na hipertensão arterial. Atualmente, é clinicamente muito utilizado isolado ou em associação com outros fármacos. Devido à sua limitada solubilidade aquosa, a HCTZ apresenta baixa absorção gastrointestinal e foi incluída na lista de entidades farmacêuticas descritas como “fármacos conhecidamente ou potencialmente com problemas de bioequivalência ou biodisponibilidade” (Khaled *et al.*, 2001; Rang *et al.*, 2012).

O presente trabalho de doutorado é consequência da transposição do projeto de mestrado. Este, por sua vez, iniciou-se com a avaliação de suspensões pediátricas de anti-hipertensivos manipuladas no Hospital Universitário. Baseado na avaliação físico-química detectou-se a degradação da HCTZ em suspensão. Diante de tal situação, sugeriu-se uma alteração urgente e simples na formulação de modo a manter a estabilidade do fármaco para as condições utilizadas no ambiente hospitalar (prazo de validade de 7 dias). Em decorrência foi proposta a formação de complexos de inclusão entre a HCTZ e ciclodextrinas (CD) de modo a obter melhora nas propriedades biofarmacêuticas do fármaco, principalmente a solubilidade e permeabilidade, por se tratar de um fármaco classe IV.

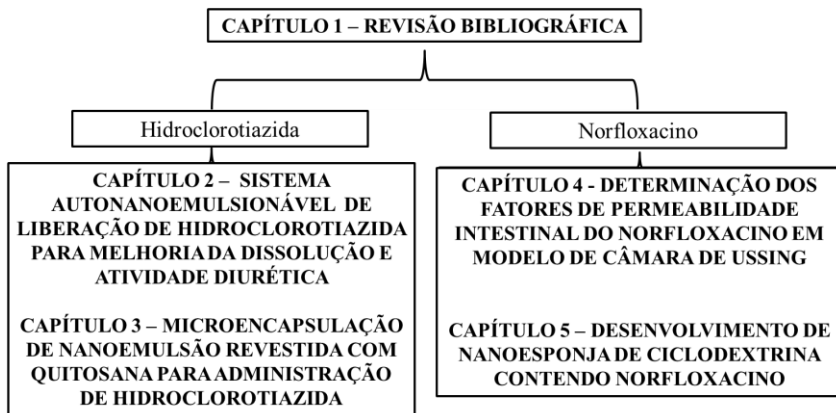
No caso da HCTZ, os resultados do mestrado demonstraram uma grande melhora na solubilidade do fármaco incluso na cavidade da β -ciclodextrina (β CD) com conseqüente melhora no perfil de dissolução do fármaco. Este complexo de inclusão aumentou a quantidade de fármaco total permeado em estudo com células Caco-2 (Apêndice A). Porém, o valor da permeabilidade não foi estatisticamente diferente do fármaco puro. A partir dos resultados obtidos, surgiram novas perspectivas de continuar com o

desenvolvimento de tecnologias que pudessem proporcionar uma melhora efetiva nas propriedades biofarmacêuticas de fármacos classe IV.

De acordo com o levantamento bibliográfico, a HCTZ tem sido alvo do desenvolvimento de algumas nanopartículas, como a de quitosana/lecitina e micelas de copolímeros (Kadam *et al.*, 2011; Chadha *et al.*, 2012). Entretanto, apenas uma literatura em se tratando de uma sistema autonanoemulsionável para a HCTZ foi descrita durante o desenvolvimento deste trabalho (Yadav *et al.*, 2014). Portanto, foi proposto neste estudo o desenvolvimento de duas tecnologias: (1) um sistema de liberação de HCTZ autonanoemulsionável acondicionadas em cápsulas de gelatina e (2) uma nanoemulsão formada por emulsificação espontânea contendo HCTZ e revestida com agente mucoadesivo, seca em *spray-dryer* e redispersa em água.

Fármacos classe SCB IV apresentam problemas significantes em relação à administração oral eficaz. No caso dos antibióticos, doses altas e subsequentes são necessárias e podem propiciar a seleção de microorganismos resistentes diminuindo a aderência do paciente ao tratamento. O norfloxacino (NFX) é um antimicrobiano classe IV, que da mesma forma que a HCTZ é objeto de estudo deste trabalho. O NFX é uma fluorquinolona de largo espectro amplamente prescrito para diversas enfermidades. Devido à sua baixa biodisponibilidade oral, altas doses são necessárias para o tratamento efetivo com este fármaco (Bolon, 2009; Breda *et al.*, 2009). No projeto de mestrado foi realizado o desenvolvimento de complexos de inclusão com o NFX, a fim de aprimorar suas propriedades e ainda a atividade antimicrobiana. O NFX é um fármaco comercializado desde 1986, porém há divergências na literatura quanto às suas propriedades físico-químicas. Houve a necessidade de um estudo para determinação dos valores de pka deste fármaco no mestrado de forma que possibilitasse o desenvolvimento dos complexos de inclusão com a β CD. Em seguida foi realizado todo desenvolvimento, caracterização e atividade antimicrobiana *in vitro* destes complexos desenvolvidos. Devido a relatos da literatura de que a baixa permeabilidade do NFX se deve a mecanismos de efluxo intestinal do fármaco, juntamente com a cooperação com um grupo de pesquisa do exterior, foi proposto neste trabalho a determinação dos fatores de permeabilidade intestinal do NFX para posteriormente desenvolver uma formulação visando a melhora de ambas as propriedades biofarmacêuticas (solubilidade e permeabilidade).

O presente trabalho tem o intuito de desenvolver estratégias por meio de sistemas nanoestruturados para a melhoria das propriedades farmacêuticas de fármacos classe IV, HCTZ e NFX. A presente tese está dividida em capítulos organizados da seguinte forma:



Capítulo 1 – Revisão bibliográfica; Capítulo 2 – Sistema autonanoemulsionável de liberação de hidroclorotiazida para melhoria da dissolução e atividade diurética; Capítulo 3 – Microencapsulação de nanoemulsão revestida com quitosana para administração de hidroclorotiazida, Capítulo 4 – Determinação dos fatores de permeabilidade intestinal do norfloxacino em modelo de câmara de Ussing e Capítulo 5 - Desenvolvimento de nanoesponja de ciclodextrina contendo norfloxacino. Uma discussão geral foi elaborada visando à contextualização no ambiente científico atual bem como o impacto que as alternativas terapêuticas poderão apresentar. Ao final como apêndice a publicação resultante do desenvolvimento dos complexos de inclusão com a HCTZ que não foram apresentados completos na dissertação: Apêndice A – Complexos de inclusão de HCTZ e β -ciclodextrina: características físico-químicas, estudos *in vitro* e *in vivo*.

1.1 OBJETIVOS

1.1.1 Objetivo geral

Desenvolvimento de sistemas nanoestruturados de fármacos classe IV, hidroclorotiazida e norfloxacino, visando a melhoria da solubilidade e permeabilidade.

1.1.2 Objetivos específicos

Para o desenvolvimento de sistemas nanoestruturados contendo hidroclorotiazida:

- Selecionar a fase oleosa de acordo com a solubilidade da hidroclorotiazida;
- Avaliar a melhor combinação entre óleo, surfactante, cosurfactante e hidroclorotiazida;
- Produzir nanoemulsão por sistema de liberação autonanoemulsionável;
- Caracterizar as nanoemulsões autonanoemulsionáveis obtidas por técnicas físico-químicas e em fluidos gastrointestinais simulados;
- Desenvolver nanoemulsão de hidroclorotiazida por formação espontânea;
- Revestir a formulação de nanoemulsão por formação espontânea com agente mucoadesivo;
- Investigar a mucoadesão da formulação revestida;
- Caracterizar as nanoemulsões por técnicas físico-químicas e morfológicas;
- Averiguar o perfil de dissolução do fármaco puro e do fármaco nas nanoemulsões em condições gastrointestinais simuladas;
- Realizar os estudos de atividade diurética *in vivo* das formulações obtidas;

Para o desenvolvimento de sistemas nanoestruturados contendo norfloxacino:

- Verificar os fatores de permeabilidade intestinal do norfloxacino por câmara de Ussing;
- Pesquisar a porção do intestino em que o norfloxacino é mais absorvido;
- Elaborar uma formulação para melhora das propriedades de solubilidade e permeabilidade encontradas para o norfloxacino;
- Produzir nanoesponja em diferentes proporções de ciclodextrina e agente reticulante;
- Determinar o teor de norfloxacino incorporado na nanoesponja;

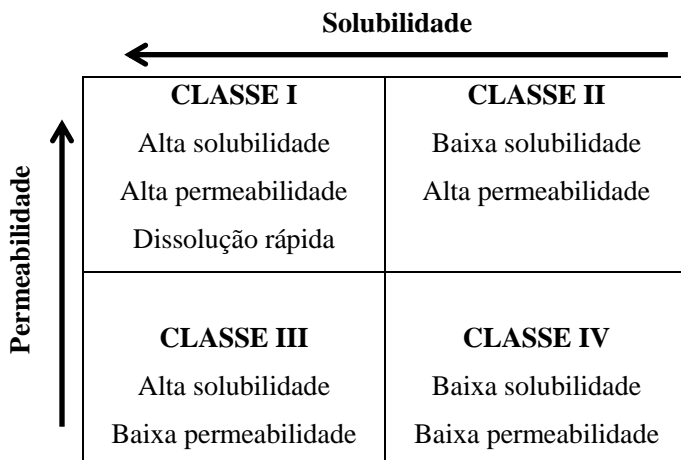
- Examinar tamanho e potencial zeta das nanoesponjas produzidas;
- Caracterizar as nanoesponjas por técnicas do estado sólido;
- Avaliar a permeabilidade intestinal da nanoesponja de norfloxacino por câmara de Ussing;
- Verificar a mucoadesão e realizar estudos de liberação da nanoesponja de norfloxacino;
- Analisar a atividade antimicrobiana *in vivo* da nanoesponja de norfloxacino em comparação com o fármaco puro por modelo de sepse induzida em ratos.

CAPÍTULO 1 – REVISÃO BIBLIOGRÁFICA

1. SISTEMA DE CLASSIFICAÇÃO BIOFARMACÊUTICA

O Sistema de Classificação Biofarmacêutica (SCB) foi proposto em 1995 por Amidon e colaboradores e baseia-se no reconhecimento da solubilidade do fármaco e sua permeabilidade gastrointestinal como parâmetros fundamentais que regulam a absorção do fármaco. Estes parâmetros constituem um alicerce científico para classificação dos fármacos em quatro classes, de acordo com sua solubilidade aquosa e permeabilidade intestinal, como representada na figura 1 (Amidon *et al.*, 1995; Ueda *et al.*, 2002).

Figura 1 – Sistema de classificação Biofarmacêutica como definido por Amidon e colaboradores (1995).



Fonte: adaptado de Smetanová (2011).

Um pré-requisito para a absorção e consequente resposta clínica da maioria dos fármacos administrados oralmente é a dissolução. Exceções, como fármacos que atuam no trato gastrointestinal (antiácidos, laxantes entre outros), não estão contempladas nesta classificação (Amidon *et al.*, 1995).

A classificação de solubilidade leva em consideração a maior dosagem de uma forma farmacêutica de liberação imediata. Um fármaco é classificado como altamente solúvel quando sua maior dosagem é solúvel em 250 mL de água ou menos, numa faixa de pH de 1,0 a 7,5. Do contrário, a substância é considerada pouco solúvel. O volume de 250 mL provém dos estudos de bioequivalência em que a forma farmacêutica é administrada com um copo

de água a voluntários humanos em jejum (Amidon *et al.*, 1995; Ueda *et al.*, 2002; Kasim *et al.*, 2004).

A extensão da quantidade de fármaco permeado através da membrana intestinal humana classificará a substância de acordo com sua permeabilidade. Esta característica pode ser avaliada por diversos modelos animais ou *in vitro*, por exemplo, modelos de perfusão *in situ* em ratos ou cultura de células. Para um fármaco ser classificado como altamente permeável, a extensão da absorção intestinal deve ser igual ou maior que 90%. Diferentemente disto, o fármaco é considerado pouco permeável (Amidon *et al.*, 1995; Smetanová *et al.*, 2011).

Um produto de liberação imediata é caracterizado com dissolução rápida quando não menos que 85% da quantidade de fármaco dissolve-se em 30 min com a utilização de aparato 2 a 50 rpm em um volume de 900 mL ou menos nos seguintes meios de dissolução: meio ácido (0,1 N HCl ou fluido gástrico simulado sem enzimas), tampão pH 4,5, tampão pH 6,8 ou fluido intestinal simulado sem enzimas. Qualquer outra condição encontrada, o produto é considerado com baixa dissolução (Avdeef *et al.*, 2000; Ueda *et al.*, 2002). Nos últimos anos, o SCB tem sido aplicado também para formas farmacêuticas orais de liberação controlada, além das formas de liberação imediata (Lennernäs e Abrahamsson, 2005; Breda *et al.*, 2009).

Apesar do avanço dos estudos de formas farmacêuticas com rotas alternativas de administração, a via oral continua representando a rota de escolha para administração dos fármacos devido a sua conveniência e baixo custo. Entretanto, para atingir concentrações terapêuticamente efetivas, o fármaco deve apresentar propriedades biofarmacêuticas satisfatórias. Após a administração de uma forma farmacêutica oral, esta deve desintegrar-se com posterior dissolução, conseqüente solubilização no meio aquoso e permeabilidade através da membrana gastrointestinal. No caso de fármacos do SCB IV, este processo de absorção é comprometido, pois suas características biofarmacêuticas representam um obstáculo significativo para absorção eficiente, o que pode acarretar em uma baixa biodisponibilidade e efeitos subterapêuticos (Lipinski, 2002; Buckley *et al.*, 2012).

O desenvolvimento de novas entidades químicas é estimado em cerca de 670 milhões de dólares. De igual importância é o fato deste processo de desenvolvimento requerer 12 anos em média para ser completado (Grass, 1997). A cada 30 mil novos compostos sintetizados, oito compostos passam por todas as fases de desenvolvimento e regulamentação e apenas um único composto é capaz de atingir o mercado (Shillingford e Vose, 2001). Neste processo, 40% das falhas devem-se a problemas de farmacocinética e 30% de falta de eficácia clínica, ou seja, os problemas de absorção estão contemplados nestas etapas e refletem em uma grande parte deste fracasso.

Neste contexto, a utilização de fármacos com propriedades bem estabelecidas, atividades e efeitos colaterais reconhecidos, como os pertencentes ao SCB IV, torna-se uma alternativa frente às dificuldades do descobrimento de novos fármacos e ao processo dispendioso. Alterações farmacotécnicas da formulação podem ser realizadas a fim de modular a liberação do fármaco de modo a melhorar as características biofarmacêuticas indesejáveis. Existem técnicas laboratoriais promissoras que acarretam em um custo muito menor em longo prazo e mais rapidamente alcançado do que a síntese de novos compostos (Florence e Attwood, 2011; Wang *et al.*, 2012).

1.1 PERMEABILIDADE

A biodisponibilidade oral de fármacos é o produto entre a fração disponível de fármaco no lúmen gastrointestinal após sua administração (fração solúvel estável), a fração do fármaco que atinge o interior do enterócito (permeabilidade de influxo), a fração que escapa do metabolismo intestinal e a fração que escapa do metabolismo do fígado. A extensão da absorção de um composto é portanto muito complexa e dependente de múltiplos fatores, como as propriedades biofarmacêuticas inerentes ao fármaco descritas anteriormente, bem como a suscetibilidade do fármaco ser substrato de enzimas e transportadores (Sjöberg *et al.*, 2013; Dressman e Reppas, 2016).

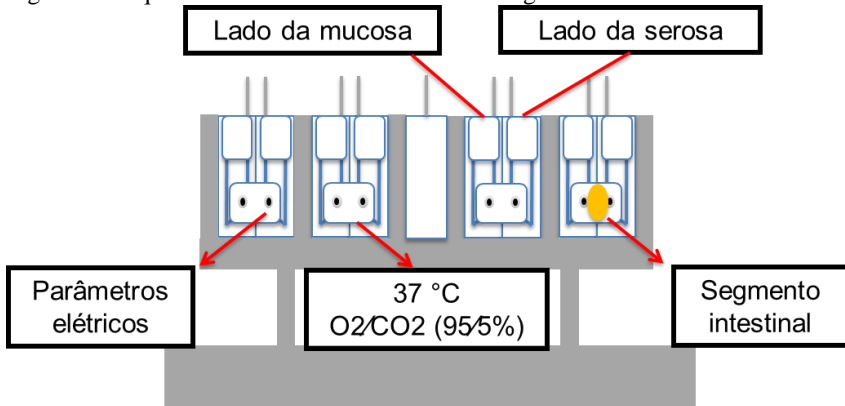
O SCB proporciona uma base científica para identificação dos fatores biofarmacêuticos limitantes na absorção de fármacos. Este sistema pode reduzir os custos e o tempo durante o processo de desenvolvimento de formas farmacêuticas e ainda diminuir exposição desnecessária de voluntários saudáveis aos testes de bioequivalência. Ademais, um melhor conhecimento do transporte do fármaco através das membranas de várias regiões do trato gastrointestinal é vital para o desenvolvimento e efetividade de novos produtos farmacêuticos (Lennernäs, 2007).

Tem sido crescente o interesse dos pesquisadores em avaliar não apenas a fração absorvida dos fármacos, mas também a contribuição do trato gastrointestinal na baixa biodisponibilidade dos fármacos. Muitos estudos recentes têm demonstrado que o transporte ativo tem um papel fundamental na permeabilidade da membrana. A absorção de fármacos pode ser estimada da permeabilidade de membrana realizada em linhagens de cultura de células como a de Caco-2. Esta determinação é simples e fornece dados de absorção substanciais, porém não prediz a absorção *in vivo* do fármaco (Sjöberg *et al.*, 2013).

O modelo de câmara de Ussing (Figura 2) é um método *ex vivo* que fornece tanto uma boa predição da permeabilidade dos fármacos como de

suas interações com os transportadores expressos na membrana dos enterócitos. Consiste em um sistema muito utilizado em que pequenas seções da mucosa intestinal são alocadas entre duas câmaras contendo solução tamponada e tanto o transporte das moléculas através do tecido como entre as câmaras pode ser medido. Este método apresenta inúmeras vantagens: uma correlação muito boa entre a permeabilidade da membrana e a porcentagem absorvida mesmo pelos compostos que têm afinidade por transportadores; uma inclinação mais gradual da porcentagem absorvida versus a permeabilidade *in vitro* em jejuno de ratos comparativamente com estudos que utilizam Caco-2, permitindo uma predição mais precisa da porcentagem absorvida, e ainda, em contraste com os ensaios com Caco-2, a habilidade de medir a absorção de compostos que estão incompletamente dissolvidos (Gotoh *et al.*, 2005).

Figura 2 - Esquema do modelo de câmara de Ussing.



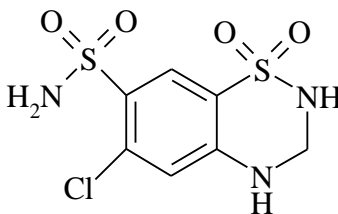
Em síntese, o modelo da câmara de Ussing permite a estimativa da porcentagem de absorção dos compostos, o que inclui o transporte ativo associado com a absorção e excreção via transportadores expressos no intestino delgado, e ainda a difusão passiva incluindo o transporte entre os espaços intercelulares e paracelulares, independentemente se o composto testado está insolúvel ou em suspensão. Acredita-se ainda que este método é muito útil como um meio para se considerar os efeitos de várias interações fármaco-fármaco na absorção oral (Gotoh *et al.*, 2005; Lennernäs, 2014).

2. HIDROCLOROTIAZIDA

A hidroclorotiazida (figura 3, HCTZ) descoberta em 1958 foi o primeiro fármaco realmente eficaz utilizado no tratamento de hipertensão arterial (Richterich, 1958). Classifica-se com baixa solubilidade e baixa permeabilidade, ou seja, pertencente à classe IV do SCB. Quimicamente, 1,1-dióxido de 6-cloro-3,4-diidro-2H-1,2,4-benzotiadiazina-7-sulfonamida, caracteriza-se como um pó cristalino branco ou quase branco, inodoro, de sabor amargo, muito pouco solúvel em água, solúvel em acetona e metanol e pouco solúvel em etanol. A faixa de fusão do fármaco é entre 266 °C e 270 °C, com decomposição (Usp, 2007; FARMACOPEIA BRASILEIRA 5ª ed, 2010). O fármaco é obtido pela combinação entre 5-cloro-2,4-disulfamilanilina e formaldeído em solução aquosa alcalina. Esta mesma reação é capaz de formar a clorotiazida, por isso é um produto conhecido como impureza da HCTZ, com atividade semelhante e propriedades biofarmacêuticas distintas. Ademais, a HCTZ apresenta instabilidade frente à luz e soluções aquosas básicas (Mollica *et al.*, 1971; Revelle *et al.*, 1997; Fang *et al.*, 2001).

Atualmente, existem 161 registros de medicamentos contendo HCTZ isolada ou em associações na Agência Nacional de Vigilância Sanitária (ANVISA, 2017). É amplamente utilizada no tratamento de edema, insuficiência cardíaca congestiva, desordens renal e hepática. Pode ser administrada isolada ou em associação para hipertensão, como por exemplo, com os inibidores da enzima conversora de angiotensina (ECA) e betabloqueadores (Rang *et al.*, 2012).

Figura 3 – Estrutura química da hidroclorotiazida.



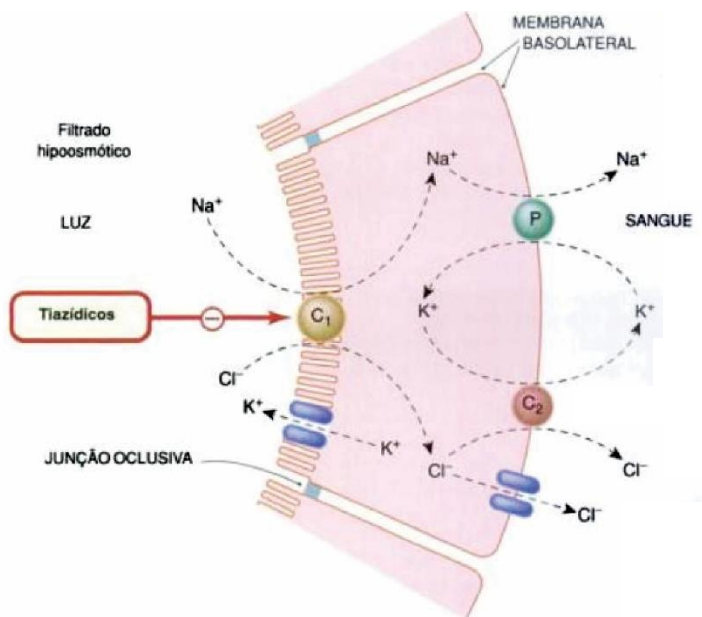
A hipertensão, ou pressão sanguínea alta, é um dos riscos primários para desenvolvimento de doenças cardiovasculares e derrame cerebral. Estas são consideradas pela Organização Mundial de Saúde (OMS) como as principais causas de mortalidade globalmente conhecidas. Trata-se de um importante desafio da saúde pública devido a sua alta frequência,

concomitante risco de doenças cardiovascular e renal, além do fato de apresentar-se de forma silenciosa, em que o paciente pode conviver por anos com a elevada pressão arterial sem ser diagnosticada (Kearney *et al.*, 2005; Chockalingam *et al.*, 2006).

Definida como elevada pressão sanguínea sem etiologia conhecida, a hipertensão primária é uma condição em ascensão e sua prevalência é entre crianças e adolescentes. Estudos estimaram uma prevalência de 3,5% nesta população, aproximadamente duas vezes maior que a estimativa prévia de 1 a 2%. Um dos maiores problemas que afetam esta população é a falta de suspensões ou outras formulações apropriadas para as crianças. Atualmente no mercado não existe nenhuma forma farmacêutica líquida de HCTZ, espironolactona ou furosemida no mercado. Diante deste cenário, a recomendação é triturar comprimidos, abrir cápsulas para misturar na alimentação da criança, ou ainda farmacêuticos são solicitados para preparar suspensões a partir destas formas farmacêuticas. Entretanto, dados de estabilidade para suspensões “extemporâneas” apresentam problemas inerentes à formulação, como estabilidade limitada e uniformidade questionável, o que repercute na problemática do seu uso (Flynn, 2002; Korolkovas *et al.*, 2006; Yoon *et al.*, 2009).

A HCTZ pertence à classe dos diuréticos tiazídicos que inibem o transporte de $\text{Na}^+ \text{Cl}^-$ no túbulo coletor distal, e o túbulo proximal pode ser considerado com um local de ação secundário. Fisiologicamente, o transporte é controlado por uma bomba de íons sódio na membrana basolateral. A energia livre do gradiente eletroquímico dos íons sódio é aproveitada pelo simporte $\text{Na}^+ \text{Cl}^-$ na membrana luminal que move o Cl^- até o epitélio celular contra seu gradiente eletroquímico. Os íons cloreto, então, saem da membrana basolateral passivamente via canal de Cl^- . Os diuréticos tiazídicos inibem o simporte $\text{Na}^+ \text{Cl}^-$ (figura 3) causando natriurese com perda destes íons. Porém, em pequena proporção, pois cerca de 90% da carga de Na^+ filtrado é reabsorvido antes de atingir o túbulo contorcido distal. Os diuréticos tiazídicos foram sintetizados com o intuito de aumentar a potência dos inibidores da anidrase carbônica, entretanto, esta ação é muito pouco observada o que leva a uma maior excreção de HCO_3^- e fosfato. Ainda, a administração aguda destes diuréticos aumenta a excreção de ácido úrico, reduzindo-se com a administração crônica. A perda de íons potássio e magnésio podem ser importantes, porém reduz a eliminação de íons cálcio, o que favorece os tiazídicos em relação aos diuréticos de alça em termos de metabolismo ósseo em longo prazo. A classe da HCTZ é bem tolerada e em ensaios clínicos demonstrou reduzir os riscos de acidente vascular cerebral (AVC) e de infarto do miocárdio associado à hipertensão (Brunton *et al.*, 2010; Sweetman, 2011; Rang *et al.*, 2012).

Figura 4 – Transporte de íons no túbulo distal, mostrando o local de ação da HCTZ, diurético tiazídico. C1 representa o sistema de cotransporte de Na^+ , K^+ e Cl^- . C2 representa o cotransporte eletroneutro de K^+/Cl^- . P representa a bomba de sódio.



Fonte: adaptado de Rang e colaboradores (2012).

As tiazidas precisam ter acesso ao lúmen tubular para exercer sua ação e fármacos como a probenecida competem pelo sítio de ação das tiazidas, ou seja, o transporte para o túbulo proximal, e podem atenuar a resposta diurética. Os tiazídicos podem ainda reduzir os efeitos dos anticoagulantes, sulfonilureias e insulina reduzindo, portanto a tolerância à glicose (Sweetman, 2011; Rang *et al.*, 2012).

A absorção da HCTZ no estômago é mínima sendo a maior parte do fármaco absorvido no duodeno e jejuno superior, com uma ampla variação na biodisponibilidade em torno de 60% e tempo de meia vida de 8 a 10h. O pico de concentração plasmático é atingido 2 h após administração oral e varia entre 120 a 500 ng/mL, dependendo da dosagem. Apresenta uma ligação preferencial às células sanguíneas vermelhas, e o equilíbrio entre estas células, o fármaco e o plasma é alcançado após 4 h da administração. A HCTZ atravessa a barreira placentária e é distribuída no leite materno. Seres humanos não são capazes de metabolizar a HCTZ e esta é eliminada

praticamente inalterada em sua totalidade (Brunton *et al.*, 2010; Sweetman, 2011; Rang *et al.*, 2012).

3. NORFLOXACINO

Infecção do trato urinário (ITU) é um termo amplo que se refere às infecções predominantemente bacterianas nas vias urinárias, seja na bexiga, próstata, sistema coletor ou rins. As ITUs estão entre as mais antigas e frequentes infecções encontradas na comunidade e na prática hospitalar (Miller e Hemphill, 2001). Nos primeiros três meses de vida, a ITU acomete mais o sexo masculino por apresentar anormalidades como a presença de válvulas na uretra posterior. Estas válvulas formam um obstáculo que se opõe a eliminação da urina e, conseqüentemente, causa a retenção urinária no segmento, fator de predisposição à infecção (González-Chamorro *et al.*, 2012).

Desta idade em diante, as infecções são mais comuns no sexo feminino devido a uma típica condição funcional, o refluxo de urina devido à incompetência da válvula vesico-uretral, o que normalmente é corrigida espontaneamente ao se atingir a puberdade. Uma vez que a infecção não é corretamente controlada, a bactéria responsável pode atingir e desenvolver-se na pélvis e no interior dos rins, o que pode resultar em múltiplos episódios de pielonefrite e evoluir para falência renal crônica (Miller e Hemphill, 2001; González-Chamorro *et al.*, 2012). Outros fatores como a uretra feminina mais curta e sua maior proximidade do ânus possibilita a colonização desta por enterobactérias (principalmente *Escherichia coli*) que são as maiores causadoras de ITU (Krieger, 2002; Wagenlehner *et al.*, 2006). Nos idosos, a instrumentação em homens, anormalidades anatômicas, e acima de tudo a condição de acamado contribuem para maior incidência de ITUs (Neu, 1992; Franco, 2005).

Estas infecções destacam-se não somente pela sua frequência, mas também pela possibilidade de complicações graves, como a insuficiência renal e a septicemia (Wagenlehner *et al.*, 2006). A escolha de antimicrobianos para o tratamento de ITU deve ser baseada no tipo de infecção, no padrão de suscetibilidade das bactérias causadoras e em possíveis contraindicações individuais do paciente. Por ser constante a prática de iniciar o tratamento empiricamente na maioria dos pacientes, o conhecimento do padrão de resistência bacteriana local é fundamental (Norrby, 1994).

O fenômeno da resistência microbiana foi descoberto nos anos 1960 a 1980 e representa a evolução contínua na luta pela sobrevivência das espécies. Estas estão relacionadas com infecções hospitalares e também

com ITUs com um potencial epidemiológico significativo. O uso prolongado de antibióticos condiciona o aumento do risco de colonização e infecção. As manifestações clínicas podem não ser mais graves, mas complicam a sua abordagem estreitando o leque de opções terapêuticas. A prescrição de doses adequadas, em intervalos corretos e otimização das condições responsáveis por permitir adequados níveis no local de infecção são igualmente variáveis determinantes na eficácia e no resultado final (Pina *et al.*, 2010; González-Chamorro *et al.*, 2012).

Neste sentido, a emergência de micro-organismos resistentes aos referidos antimicrobianos tornou-se um importante problema de saúde pública condicionando manifesto aumento de custos e, sobretudo, risco de morbimortalidade significativo (Pina *et al.*, 2010; Dalhoff, 2012).

A ANVISA lançou, em 5 de maio de 2011, a RDC nº 20 que se trata basicamente do controle de medicamentos à base de substâncias classificadas como antimicrobianos. Com esta resolução, a venda de antimicrobianos somente poderá ser efetuada mediante receita de controle especial, com a retenção da segunda via, evitando, portanto o uso indiscriminado de antibióticos e conseqüentemente o surgimento de micro-organismos resistentes (Brasil, 2011).

A descoberta do ácido nalidíxico em 1962, e sua introdução para uso clínico em 1967, marcou o início de cinco décadas de desenvolvimento e utilização de quinolonas. Entretanto, as quinolonas formaram um grupo negligenciado até o desenvolvimento das fluorquinolonas nos anos de 1970 e 1980. As fluorquinolonas representam um avanço terapêutico particularmente importante, visto que esses fármacos são dotados de ampla atividade antimicrobiana e mostram-se eficazes após administração oral no tratamento de uma grande variedade de doenças infecciosas. A relação estrutura-atividade farmacológica relata o átomo de flúor na posição 6 o que proporciona maior potência contra organismos gram-negativos e o núcleo piperazínico na posição 7 é responsável pela atividade antipseudomonas (Andersson e Macgowan, 2003; Van Bambeke *et al.*, 2005; Cheng *et al.*, 2013).

O norfloxacin (NFX, Figura 5), comercializado desde 1986, é uma fluorquinolona de largo espectro, efetivo contra micro-organismos gram-positivos e gram-negativos. O mecanismo de ação deste fármaco pode ser descrito em dois passos, em que o primeiro é a formação reversível de complexos fármaco-enzima-ADN (ação bacteriostática). Este mecanismo bloqueia a replicação do ADN bacteriano, induz a resposta bacteriana e permite a filamentação celular (Figura 6) (Van Bambeke *et al.*, 2005; Bolon, 2009; Cheng *et al.*, 2013).

Figura 5 – Estrutura química do norfloxacino.

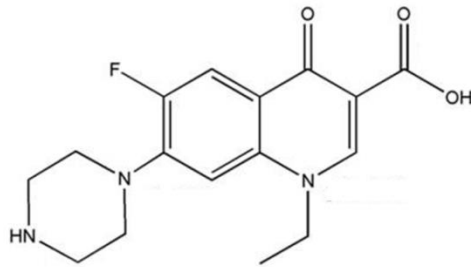
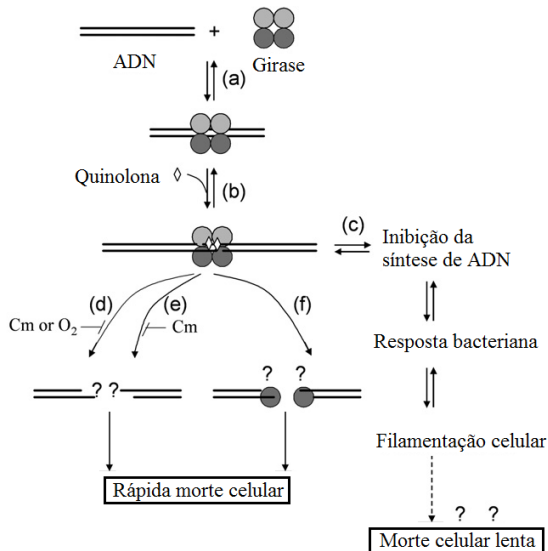


Figura 6 – Representação esquemática do mecanismo de ação das quinolonas. (a) Ligação da girase com o ADN. Formação reversível de complexos fármaco-enzima-ADN que rapidamente bloqueiam a replicação do ADN. (c) Inibição da replicação leva a indução da resposta bacteriana e filamentação celular. (d) Fragmentação letal do cromossomo que requer síntese proteica em condições aeróbias. (e) Fragmentação letal do cromossomo que requer síntese proteica, mas não condições aeróbias. (f) Fragmentação letal do cromossomo que não requer nem síntese proteica nem condições aeróbias. Pontos de interrogação indicam incertezas.



Fonte: adaptado de Cheng e colaboradores (2013).

O segundo passo letal requer altas concentrações de fármaco, e os fragmentos de ADN são liberados da restrição por duas vias, uma que requer síntese de proteína (Figura 6d-e) e outra não (Figura 6f). Cada via de morte celular depende da estrutura da quinolona. Entretanto, o conhecimento sobre a ação destas está longe de estar completamente entendido e necessita ainda ser explorado. O NFX, por exemplo, representa uma situação intermediária (Figura 6e), porém como o fármaco intercala no ADN para impedir a replicação ainda não é bem compreendido (Drlica *et al.*, 2008; Wang *et al.*, 2010; Cheng *et al.*, 2013).

O NFX é indicado terapêuticamente em humanos para o tratamento de uma variedade de infecções do trato urinário (cistite, pielite, cistopielite, pielonefrite, prostatite crônica, epididimite), bem como para o tratamento uretrite, faringite, proctite ou cervicite gonocócicas, febre tifóide e na profilaxia de infecções bacterianas em pacientes neutropênicos acometidos pelo câncer. O fármaco também é efetivo em infecções gastrointestinais, devido a sua atividade pronunciada contra patógenos responsáveis por doenças diarreicas (*Salmonella*, *Shigella*, *Campylobacter*, *Yersinia* e *E. Coli*). Recomenda-se uma posologia de 400 mg a cada 12 horas em que a duração do tratamento varia de acordo com o diagnóstico (Emmerson e Jones, 2003).

Após administração oral da dose de 400 mg, aproximadamente 30-40% é absorvida. A absorção do NFX ocorre com maior extensão no duodeno e menor no jejuno. Os alimentos podem retardar a absorção, porém a quantidade absorvida não é afetada. A absorção é rapidamente seguida por uma concentração plasmática máxima atingida (C_{max}) de aproximadamente 1,5 $\mu\text{g/mL}$ em humanos. O tempo para atingir este pico plasmático é de aproximadamente 1 a 2 horas (t_{max}). A ligação às proteínas plasmáticas é de 10 a 15%. O tempo de meia-vida ($t_{1/2}$) é de 3 a 4 horas e sua metabolização origina seis diferentes metabólitos com uma atividade antimicrobiana mínima quando comparada ao composto original. NFX é metabolizado e eliminado por excreção biliar e renal. A área sob a curva da concentração plasmática versus tempo (ASC) é de 6,4 $\mu\text{g}\cdot\text{h/mL}$ (Takács-Novák *et al.*, 1992; Al-Rashood *et al.*, 2000; Van Bambeke *et al.*, 2005; Bolon, 2009). Quimicamente, o NFX é denominado como ácido 1-etil-6-fluor-1,4-diidro-4-oxo-7-(1-piperazinil)-3-quinolino carboxílico e pertence ao grupo IV do SCB (pouco solúvel e pouco permeável). É um pó cristalino branco a amarelo claro, pouco solúvel em água, metanol, etanol, acetato de etila e acetona, facilmente solúvel em ácido acético, ligeiramente solúvel em clorofórmio e insolúvel em éter etílico. Tem faixa de fusão entre 227-228 °C, massa molecular de 319,34 g/mol e fórmula molecular

$C_{16}H_{18}FN_3O_3$ (Breda *et al.*, 2009; FARMACOPEIA BRASILEIRA 5ª ed, 2010).

O NFX é um fármaco que pode ser considerado higroscópico e fotossensível. Este sofre degradação quando em exposição à luz direta ou fluorescente, originando derivados da fotodecomposição. Ainda em exposição prolongada ao calor e solução ácida o fármaco sofre hidrólise e resulta em um análogo descarboxilado. Esta forma descarboxilada é de fundamental importância comparada com os outros produtos de degradação, uma vez que o grupo carboxílico é responsável pela atividade farmacológica do NFX. Além disso, o análogo descarboxilado tem sido identificado como precipitado em formulações injetáveis e como impureza em matérias-primas (El Khateeb *et al.*, 1998; Alnajjar *et al.*, 2007).

4. NANOTECNOLOGIA

A ampla área de estudo com uso de materiais e estruturas em nível de escala nanométrica denomina-se nanotecnologia. Nanocarreadores são materiais ou dispositivos abaixo de 1 μm feito de diferentes materiais biodegradáveis como polímeros naturais ou sintéticos, lipídeos ou fosfolipídios ou ainda compostos organometálicos (Rawat *et al.*, 2006). Estes são de crescente interesse da nanomedicina e indústrias farmacêuticas atualmente, sendo considerados como uma ferramenta que auxilia em novos tratamentos ao penetrar nas células e tecidos, visando a doença como um alvo. A nanotecnologia é utilizada para melhora das propriedades dos fármacos. Para muitas novas entidades químicas de baixa solubilidade aquosa por exemplo, a micronização não é suficiente porque o produto micronizado tem uma tendência de agregação, o que leva à uma diminuição da efetividade da área superficial para dissolução e o próximo passo normalmente tomado é o de nanonização. Técnicas sofisticadas e ferramentas têm permitido a melhor caracterização e manipulação de materiais em nanoescala de forma a elucidar o fenômeno de formação das nanopartículas gerando uma nova era de sistemas farmacêuticos nanoestruturados (McClements e Rao, 2011; Kumar e Singh, 2013).

A nanotecnologia destaca-se na pesquisa farmacêutica por fornecer oportunidades ilimitadas de liberação de fármacos com baixa biodisponibilidade. Muitos sistemas nanoestruturados têm sido explorados no âmbito de melhorias das propriedades biofarmacêuticas, como aumento da solubilidade, modulação da biodistribuição, prevenção da degradação, melhora da permeabilidade ou transporte dos fármacos, entre outros. A tecnologia em nanoescala pode ser amplamente dividida em nanocarreadores

lipídicos, poliméricos, inorgânicos, e nanopartículas ou nanosuspensões de fármacos (Anton *et al.*, 2008; Date *et al.*, 2010).

4.1 SISTEMAS AUTONANOEMULSIONÁVEIS

A percepção de que a biodisponibilidade oral de fármacos pouco solúveis ou lipofílicos pode ser aumentada quando coadministrada com uma refeição rica em gordura levou à um interesse no desenvolvimento de formulações de fármacos com baixa solubilidade aquosa em lipídeos, como um meio de aumentar a solubilização do fármaco no trato gastrointestinal. Desde então, suspensões de lipídeos, soluções e emulsões tem sido utilizadas como incremento da biodisponibilidade de fármacos pouco solúveis, e ainda, mais recentemente, o foco tem aumentando para a utilidade das formulações lipídicas autoemulsionáveis (Porter *et al.*, 2008).

As primeiras abordagens avaliadas para as formulações baseadas em lipídeos de fármacos com baixa solubilidade aquosa foram o uso de soluções simples ou suspensões de fármacos com um único lipídeo ou uma mistura de lipídeos, e mais tarde a incorporação do fármaco na fase oleosa de emulsões óleo-em-água. Em geral, lipídeos não digeríveis como o óleo mineral (por exemplo, parafina líquida) e o poliéster de sacarose (o qual permanece essencialmente não absorvido no lúmen intestinal), reduziram a absorção do fármaco por reter parte do princípio ativo coadministrado na formulação não digerida, impedindo a transferência das espécies coloidais para a fase aquosa luminal, onde acredita-se que a absorção ocorra. Para o desenvolvimento de formulações lipídicas consequentemente, lipídeos digeríveis como óleo de soja, milho, oliva e triglicerídeos de cadeia média são tipicamente preferíveis para melhora da biodisponibilidade e são usualmente atribuídos ao aumento da solubilização dos fármacos nas espécies coloidais formadas durante digestão (Pouton, 2000; 2006; Porter *et al.*, 2007).

Sistemas autonanoemulsionáveis tem sido cada vez mais empregados para o incremento da biodisponibilidade oral de fármacos pouco solúveis. Formulações autonanoemulsionáveis (do inglês SNEDDS, self-nanoemulsifying drug delivery systems) compreendem misturas isotrópicas de óleos naturais ou sintéticos com surfactantes lipofílicos ou hidrofílicos e cossolventes os quais espontaneamente emulsificam quando expostos aos fluidos gastrointestinais para formar emulsões óleo-em-água de tamanho nanométrico. Formulações autonanoemulsionáveis geralmente fornecem a vantagem de veicular maior quantidade de fármaco quando comparadas às com soluções lipídicas uma vez que a solubilidade de fármacos com coeficientes de partição intermediários (log de P entre 1 e 4) é tipicamente baixa em lipídeos naturais e muito maior em surfactantes anfílicos,

cosurfactantes e cossolventes. A rápida emulsificação destes sistemas sob agitação moderada na presença de um meio aquoso como o encontrado nos fluidos gastrointestinais, ainda gera uma grande área superficial de contato entre a formulação e os fluidos gastrointestinais o que pode gerar uma melhora na taxa e extensão da absorção resultando em maior reprodutibilidade dos perfis plasmáticos (Kawakami, 2012).

As formulações *SNEDDS* já tem contribuído para o incremento da biodisponibilidade de muitos fármacos pouco solúveis. Possivelmente o melhor exemplo de uma formulação de sucesso comercializada é a formulação Neoral® de ciclosporina. Esta formulação é composta por óleo derivado do milho como a base lipídica, Cremophor RH40 como surfactante, propilenoglicol e etanol como cossolventes e o α -tocoferol como antioxidante. Em contraste com a formulação mais antiga Sandimmun, Neoral® forma espontaneamente e termodinamicamente estável uma dispersão com tamanho de gotícula abaixo de 100 nm quando introduzida em meio aquoso. A melhora das características da dispersão de Neoral tem sido sugeridas como as responsáveis pelo aumento da absorção e ainda pela redução da variabilidade na biodisponibilidade inter e intra-pacientes (Porter *et al.*, 2008).

Entretanto, apesar de provarem-se úteis estas formulações, relativamente poucos medicamentos com base em lipídeos têm sido comercializados e exemplos incluem Neoral® (ciclosporina), Norvir® (ritonavir), Fotovase® (saquinavir) e Aгенarase® (ampenavir). A razão para a falta de aplicação destas tecnologias não são totalmente claras, porém refletem igualmente o conhecimento limitado dos parâmetros da formulação que são diretamente responsáveis pela boa performance *in vivo* encontrada e o fato de relativamente poucos estudos em humanos reportados na literatura quando comparado com às formas farmacêuticas tradicionais. Possivelmente mais importante, ao menos em nível de desenvolvimento, a falta de testes *in vitro* efetivos para predição da performance *in vivo* tem significativamente dificultado o desenvolvimento das formulações lipídicas. Como consequência, o desenvolvimento de formulações lipídicas autoemulsionáveis e a escolha dos componentes da formulação têm sido historicamente direcionados pela solubilidade do candidato à fármaco desta formulação, a facilidade de dispersão da formulação e o tamanho de partícula da emulsão resultante (Rawat *et al.*, 2006; Porter *et al.*, 2007; McClements e Rao, 2011).

Avanços considerados tem sido feitos no desenvolvimento de meios de dissolução biorelevantes visando a melhor predição da performance *in vivo* de fármacos pouco solúveis (Jantratid *et al.*, 2008).

4.2 NANOEMULSÕES

A nanoemulsão é um tipo de nanocarreador lipídico que consiste em uma dispersão heterogênea de dois líquidos imiscíveis, geralmente óleo em água, cujo diâmetro médio de gotículas varia entre 100 nm a 500 nm. Estas formam sistemas cineticamente estáveis que requerem uma quantidade de surfactante muito menor para a sua estabilização, quando comparado às microemulsões, uma importante vantagem em termos de toxicidade (Shah *et al.*, 2010).

As propriedades das nanoemulsões são dependentes da sua composição e, particularmente, do método de obtenção, podendo ser formadas por meio de uma ampla gama de misturas de óleo/água/tensoativo (Wang *et al.*, 2009). Propriedades físico-químicas, como tamanho das gotículas, potencial zeta, viscosidade e pH são fundamentais na caracterização destes sistemas, pois estas podem afetar as propriedades finais da formulação, como a absorção e biodisponibilidade de fármacos incorporados (Tagne *et al.*, 2008).

As técnicas de obtenção das nanoemulsões se dividem em técnicas que envolvem alta ou baixa energia de emulsificação. A emulsificação espontânea é uma técnica de baixa energia que é amplamente usada na obtenção destes sistemas pela simplicidade dos procedimentos envolvidos e pela versatilidade de obtenção de nanoemulsões com características apropriadas para uma dada aplicação. Esta técnica consiste basicamente em adicionar uma solução do óleo, fármaco e surfactante lipofílico em um solvente orgânico miscível em água, a uma fase aquosa contendo um surfactante hidrofílico. Uma turbulência interfacial (Efeito Marangoni) é gerada pela rápida difusão do solvente orgânico na água, resultando na formação espontânea de gotículas de óleo de tamanho submicrométrico, estabilizadas pelo tensoativo (Bouchemal *et al.*, 2004; Almeida *et al.*, 2008; Bouchemal, 2008).

Outra propriedade que tem atraído atenção dos pesquisadores é a bioadesão. Esta pode ser descrita como a ligação das macromoléculas naturais ou sintéticas às superfícies biológicas; no caso de ligação às mucosas, este fenômeno denomina-se mucoadesão. A quitosana é um polímero natural de monossacarídeo que apresenta propriedades mucoadesivas, além de exibir um efeito sobre a permeabilidade de fármacos, visto que produz a abertura transitória das junções entre as células epiteliais, promovendo a absorção. As excelentes propriedades mucoadesivas da quitosana são decorrentes da existência de interações eletrostáticas entre os grupos amina protonados deste polímero e os grupos carregados negativamente presentes nas cadeias laterais da mucina, proteína que compõe

o muco que reveste as mucosas. A junção de uma macromolécula bioadesiva como a quitosana na nanoemulsão proporciona o revestimento das gotículas oleosas e apresenta vantagens adicionais, pois além de carrear o fármaco, a nanoemulsão revestida com polímero mucoadesivo apresenta uma grande área superficial de contato, resultando em maior permeabilidade do fármaco, e, conseqüente, melhora na biodisponibilidade (Chowdary e Rao, 2004; Smart, 2005; Patil e Sawant, 2008; Andrews *et al.*, 2009).

Uma tecnologia inovadora para revestimento de nanoemulsões foi desenvolvida por Li e colaboradores (2011) e consiste em revestir as gotículas com uma macromolécula e fazer a secagem por aspersão (spray-dryer). Esta técnica de microencapsulação das nanoemulsões gera partículas denominadas “Trojan” (ou cavalo de Tróia), termo primeiramente introduzido por Tsapis e colaboradores em 2002 e refere-se às partículas largas e porosas carreadoras de nanopartículas para liberação de fármacos (Tsapis *et al.*, 2002). As partículas Trojan carreadoras da nanoemulsão preservam a integridade das nanogotículas oleosas e podem ser facilmente redispersas na fase aquosa. Esta tecnologia mantém a estabilidade do fármaco, e pode ser utilizada como uma nova estratégia para aplicações farmacêuticas, promovendo uma dispersão homogênea de fármacos pouco solúveis em água (Li *et al.*, 2011).

Em geral, as nanoemulsões, tanto as autonanoemulsionáveis como as de nanoemulsificação espontânea, devido ao diâmetro das gotículas e sua constituição, são capazes de manter a estabilidade físico-química durante longos períodos de armazenamento de forma ainda a evitar a degradação de fármacos lábeis (Nielsen *et al.*, 2007; Date *et al.*, 2010).

4.3 NANOESPONJAS

Nanoesponjas (NS) são uma nova classe de estruturas coloidais baseadas na reticulação de polímeros que constituem as nanopartículas cujas cavidades podem englobar uma ampla gama de substâncias. As NS podem ter a base de titânio, silicone, poliestireno reticulado e CD. O apelo à nova tecnologia das NS surge devido à dificuldade experiencial com formulações convencionais na administração de fármacos com baixa biodisponibilidade ou ainda para liberação estendida (Trotta *et al.*, 2012; Tejashri *et al.*, 2013).

As NS assemelham-se a estruturas tridimensionais de andaimes que possuem uma espinha dorsal longa constituída por polímeros. O polímero, em solução, combina-se com pequenas moléculas chamadas de reticulantes formando estruturas esféricas com cavidades hidrofóbicas em que os fármacos podem ser encapsulados. Este sistema tem sido proposto como um sistema de liberação de fármacos, uma vez que estes são capazes de

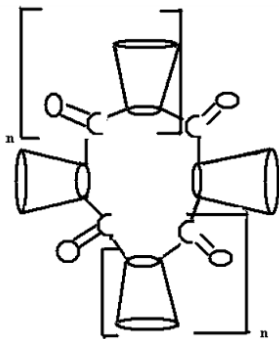
solubilizar fármacos com baixa solubilidade aquosa (classe II e IV do SCB), melhorando a biodisponibilidade por meio da modificação dos parâmetros farmacocinéticos (Trotta e Cavalli, 2009). As vantagens desse sistema de liberação de fármacos relatadas por Tejashri e colaboradores em um trabalho de revisão em 2013 foram: encapsulação de princípios ativos e redução dos efeitos colaterais, melhora da estabilidade de fármacos, liberação estendida, melhora no processamento do material uma vez que os líquidos podem ser convertidos à pós. Devido à sua natureza sólida, As NS podem ser administradas como formulações orais, parenterais, tópicas ou de inalação (Subramanian *et al.*, 2012; Tejashri *et al.*, 2013).

As NS uma vez formadas exibem uma característica atóxica, insolúveis na maioria dos solventes orgânicos e estáveis a altas temperaturas. A química simples de polímeros e agentes reticulantes não acrescenta muitos problemas na preparação desta tecnologia que pode ser facilmente transposta para escala comercial. NS são solúveis em água, porém não se dissociam quimicamente quando em soluções aquosas, misturando-se à água que é usada como um meio de transporte fluido (Cavalli *et al.*, 2006; Subramanian *et al.*, 2012).

CD são uma família de compostos formados por 5 ou mais moléculas de açúcar (α -D-glicopiranosose) ligadas por ligações glicosídicas α -1,4 gerando um oligossacarídeo cíclico, que devido à sua conformação de cadeira apresentam um formato de cone, com uma cavidade hidrofóbica e a parte externa altamente hidrofílica (Veiga *et al.*, 2006). As CD são uma entidade biodegradável que sofre degradação enzimática no corpo humano (ciclodextrina-glicosiltransferase) formando oligômeros cíclicos. As NS baseadas em CD surgiram inicialmente para descontaminação da água, porém, essas têm sido exploradas como agentes solubilizantes ou nanocarreadores para sistemas de liberação de fármacos (Subramanian *et al.*, 2012).

A β CD tem sido a CD mais escolhida entre as naturais (α , β , γ) para produção das NS por apresentar a maior habilidade e estabilidade em complexar com os agentes reticulantes. A dimensão da cavidade, baixos custos de produção e altas taxas de produtividade são algumas das vantagens oferecidas pela β CD para produção das NS. Swaminathan e colaboradores desenvolveram NS de β CD contendo itraconazol e propuseram uma estrutura de formação, representada na Figura 7 (Swaminathan *et al.*, 2007).

Figura 7 – Estrutura da nanoesponja de ciclodextrina proposta por Swaminathan (2007).



Fonte: Swaminathan *et al.*, 2007.

CAPÍTULO 2 – SISTEMA AUTONANOEMULSIONÁVEL DE LIBERAÇÃO DE HIDROCLOROTIAZIDA PARA MELHORIA DA DISSOLUÇÃO E ATIVIDADE DIURÉTICA. ARTIGO SUBMETIDO PARA PERIÓDICO *AAPS PHARMSCITECH*.

1. INTRODUÇÃO

A HCTZ é um diurético tiazídico amplamente utilizado na clínica em associação com outros fármacos para tratamento principalmente da hipertensão, sendo utilizado como um medicamento de uso contínuo. Este fármaco pertence à classe biofarmacêutica IV, ou seja, apresenta baixa solubilidade e baixa permeabilidade. Estas características físico-químicas vão influenciar na biodisponibilidade do fármaco após a sua administração oral. A solubilização nos fluidos gastrointestinais seguida da permeabilização do princípio ativo através das barreiras biológicas é essencial para atingir o local de ação. Desta forma, o incremento das propriedades biofarmacêuticas de fármacos classe IV como a HCTZ possibilitam a melhora da sua absorção oral podendo levar consequentemente à diminuição da dose (Amidon *et al.*, 1995; Yoon *et al.*, 2009; Brunton *et al.*, 2010).

Ações tecnológicas têm sido aplicadas para contornar as limitações dos fármacos e auxiliar na sua absorção oral. Com o advento dos sistemas de liberação de fármacos autonanoemulsionáveis (do inglês, *SNEDDS – self-nanoemulsifying drug delivery system*), pesquisadores têm percebido efeitos benéficos na modulação de fármacos pouco solúveis. Tais sistemas são misturas pré-concentradas ou anidras, isotrópicas, constituídas por um óleo, um surfactante e o fármaco, que quando adicionadas a uma fase aquosa sob leve agitação, formam nanoemulsões óleo-água espontaneamente. Em se tratando de formulações orais, a motilidade gastrointestinal é suficiente para formação da nanoemulsão. A adição de um cosurfactante à formulação pode auxiliar na incorporação do fármaco ou ainda facilitar a emulsificação. A grande vantagem deste sistema é a manutenção do fármaco em solução no trato gastrointestinal, omitindo a etapa fundamental de dissolução, apesar dos processos de absorção ainda não serem muito bem entendidos. Este sistema é recomendado para fármacos com baixas dosagens e propicia uma ação rápida, com comprovada melhora na biodisponibilidade oral para vários fármacos hidrofóbicos e com capacidade de transposição para escala industrial (Pouton, 1997; Gursoy e Benita, 2004; Bandyopadhyay *et al.*, 2012).

Este capítulo demonstra o desenvolvimento e a aplicação de um sistema autonanoemulsionável para a HCTZ visando a melhoria da dissolução e atividade diurética. Para tanto, estudos da formulação foram direcionados para inserção da HCTZ na fase lipídica da *SNEDDS* e sua performance nos meios gastrointestinais simulados foram avaliadas. Toda a caracterização foi realizada a fim de eleger a melhor formulação desenvolvida para avaliação *in vivo*. A farmacodinâmica foi focada na

atividade diurética da SNEDDS de HCTZ em comparação com o fármaco livre.

SELF-NANOEMULSIFIED DRUG DELIVERY SYSTEM OF HYDROCHLOROTHIAZIDE FOR INCREASING DISSOLUTION RATE AND DIURETIC ACTIVITY

Running head: SELF-NANOEMULSIFIED SYSTEM OF HYDROCHLOROTHIAZIDE

Cassiana Mendes^{*a}; Aline Buttchevitz^a, Jéssica Henriques Kruger^a; Thiago Caon^a; Patricia Oliveira Benedet^b; Elenara Lemos-Senna^c; Marcos Antônio Segatto Silva^a.

^a Post-graduation Program in Pharmaceutical Sciences, Quality Control Laboratory, Universidade Federal de Santa Catarina, J/K 207, 88040-900, Florianópolis-SC, Brazil. Phone number: +55 (48) 3721-4585; fax +55 (48) 3721-9350

^b Department of Pharmacology, Universidade Federal de Santa Catarina, 88040-900 Florianópolis-SC, Brazil

^c Laboratory of Pharmaceutical Technology, Department of Pharmaceutical Sciences, Universidade Federal de Santa Catarina, Florianópolis, SC, Brazil.

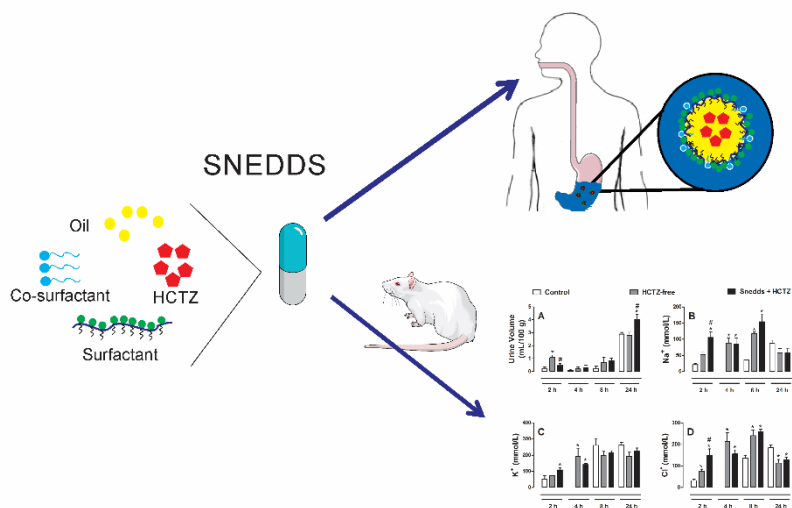
* Corresponding author: Quality Control Laboratory, Post-graduation Program in Pharmaceutical Sciences, Federal University of Santa Catarina, J/K 207, 88040-900, Florianópolis, SC, Brazil. Phone number: +55 (48) 3721-4585; fax +55 (48) 3721-9350. cassi_ana@yahoo.com.br

Keywords: biorelevant media, dissolution, diuretic activity, hydrochlorothiazide, self-nanoemulsifying drug delivery system.

ABSTRACT

Hydrochlorothiazide (HCTZ) is a class IV drug according to the Biopharmaceutical Classification System. This study aimed the development of self-nanoemulsifying drug delivery system (SNEDDS) for HCTZ as an approach to overcome the biopharmaceutical limitations. Pre-formulation screening and ternary phase diagrams were carried out to select the oil phase, the surfactant and the cosurfactant as the amount of each constituent. The optimized formulations, with reduced amount of surfactant, and composed of medium chain triglycerides, Cremophor EL and Transcutol P did not affect the pH or show drug incompatibilities. The SNEDDS were stabilized by the nanoscale globules and high negative zeta potential. All the physicochemical characterization assays were performed in biorelevant media to better predict the *in vivo* performance. The enhanced dissolution rate of the SNEDDS reflected in the *in vivo* diuretic activity, presenting a natriuresis, kaliuresis and chlориuresis at early stages and an increased volume of total urine compared with HCTZ alone. The designed SNEDDS produced an improvement in the pharmacodynamics due to high dissolution and probable inhibition of intestinal efflux protein by Cremophor EL. The use of SNEDDS demonstrated to be an efficient approach to modulate the absorption of HCTZ and drug therapeutics.

GRAPHICAL ABSTRACT



1. INTRODUCTION

Hydrochlorothiazide (HCTZ) is a drug largely used to treat hypertension, in which the decrease in the blood pressure occurs due to the reduction in the blood volume as a result of the diuresis. This drug acts by inhibiting the reabsorption of sodium and chloride ions at the early distal tubule via the Na-Cl cotransporter, resulting in an increase in the excretion of sodium, chloride, and water (1). According to the Biopharmaceutical Classification System (BCS), HCTZ belongs to the class IV (2), i.e. it has both low solubility and permeability properties. Another drawback associated to HCTZ is its poor stability in very alkaline solutions. In the pH range from 1.5 to 8.2, the chemical stability favors the HCTZ in more acidic media, and in very alkaline solutions complete hydrolysis can occur. The literature reports that the bell-shaped pH-dependent hydrolysis of HCTZ proceeds irreversibly to a ring-opened product (3-5). These characteristics make this drug a suitable candidate to formulate new drug delivery systems as an approach to improve them.

The development of self-nanoemulsifying drug delivery systems (SNEDDS) has been considered a promising approach for improving the rate and extension of the oral absorption of poorly water soluble drugs (6-8). SNEDDS are able to improve the bioavailability by enhancing the drug dissolution and drug permeability in the gastrointestinal tract (GIT). Other mechanisms implicated in the oral drug absorption include the prolongation of gastric residence time, improvement of the chemical and enzymatic stability, stimulation of the intestinal lymphatic transport pathway, and reduction of the drug efflux (9). These systems are pre-concentrated mixtures composed of oil, surfactant and drug. In an aqueous phase and under gentle agitation, an oil-water nanoemulsion is spontaneously formed. The gastrointestinal motility is enough to form a very fine droplet dispersion after an oral administration; however, the addition of cosurfactant may be required to facilitate the drug incorporation or to enable the emulsification process (10, 11). Unlike liposome and solid lipid nanoparticles, the SNEDDS form kinetically stable nanoemulsions, and require a smaller amount of surfactant compared to the microemulsions, an important advantage in terms of toxicity (9, 12, 13). Formulating drugs in SNEDDS may increase the patient drug compliance compared to oil/water emulsions since they can be filled in gelatin capsules and administered as a unit oral dosage form. The anhydrous nature of SNEDDS may also improve the stability of hydrolysable drugs as the solubilization of the drug inside of the droplets prevents its direct contact with the aqueous environment of the biological fluids (14).

The literature analysis reveals only one other study regarding SNEDDS of this drug, but biorelevant fluids were not considered during the

assays and the formulation constituents were slightly different (15). In this study, Tween 80 was replaced by Cremophor EL®, which demonstrated to be more effective for solubilizing poorly drugs in SNEDDS than Tween 80 (9, 16, 17). In addition to that, this preformulation study aimed to reduce the surfactant concentration to achieve less complication in terms of toxicity.

The development of HCTZ-loaded SNEDDS was undertaken by combining medium chain triglycerides, Cremophor EL® and Transcutol P in a lipid formulation. The formulation of HCTZ in SNEDDS could overcome the limitations in oral administration of this drug, improving its therapeutic efficacy when compared to the free drug. Firstly, preformulation and compatibility studies, physicochemical characterization, and short-term stability of HCTZ-loaded SNEDDS were carried out. The environment in which the delivery systems will meet after drug administration also is important to be considered in the development of SNEDDS (11). Therefore, the evaluation of HCTZ in biorelevant media was performed since it is more likely to be reflective of the *in vivo* formulation performance. Finally, the diuretic effectiveness of this novel proposed HCTZ-loaded self-nanoemulsifying formulation was assessed in rats.

2. MATERIALS AND METHODS

2.1 MATERIALS

HCTZ was obtained from Galena (Campinas, Brazil). Olive oil, castor oil, peanut oil, cotton oil, Tween 20 (polysorbate 20) and Tween 80 (polysorbate 80), which were used as excipients in the preformulation studies, were purchased from Sigma-Aldrich (St. Louis, USA). The other excipients tested were linseed oil acquired from Vital Âtman LTDA (Uchoa, Brazil); medium chain triglycerides (MCT) obtained from Focus Tecnologia Comercial Química (São Paulo, Brazil); Cremophor EL® purchased from BASF Chemical Company (Ludwigshafen, Germany); polyethylene glycol 400 (PEG 400) acquired from LabSynth (Diadema, Brazil); Transcutol P (diethyl glycol monoethyl ether) obtained from Selectchemie (São Paulo Brazil), propylene glycol stearate purchased from Brenntag Química (São Paulo, Brazil). All other analytical reagents were of analytical grade.

2.2 SOLUBILITY STUDIES

The HCTZ equilibrium solubility was established by adding an amount of HCTZ in excess into 5 mL of each selected excipient (oil, surfactant and cosurfactant). The mixtures were magnetically stirred for 24 h at room temperature (25 °C), and then centrifuged at 6000 rpm for 5 min. The obtained supernatant was filtered through a membrane filter displaying a pore size of 0.45 µm and diluted with methanol. HCTZ concentration was

determined using a previously validated high-performance liquid chromatography (HPLC) method (see Section 2.6.6).

2.3 SCREENING OF SURFACTANTS FOR EMULSIFYING ABILITY

The surfactants were screened regarding to their ability to emulsify the oil phase. Briefly, 20 μL of each surfactant was firstly added to 20 μL of an oil phase and stirred. After that, 25 μL of the mixture was diluted to a final volume of 25 mL with distilled water. The ease of formation of emulsions was evaluated according to the number of volumetric flask inversions required to form a uniform emulsion. After 2h, the transmittance of the samples was measured by using a UV–Visible spectrophotometer (Cary 50 Bio – Varian, Palo Alto, CA, USA) at 638 nm (12).

The emulsifying ability of different surfactant/cosurfactant mixtures was also evaluated. In these assays, 40 μL of the surfactant was firstly added to 20 μL of cosurfactant to obtain a 2:1 surfactant: cosurfactant mixture. In sequence, 60 μL of selected oil was added to the surfactant/cosurfactant mixture to obtain a final mixture composed of 1:1 oil: surfactant/cosurfactant. The final mixture was heated at 60°C in a water bath to allow the proper mixing, and 25 μL of this mixture (1:1 oil: surfactant/cosurfactant) was diluted with 25 mL of distilled water. After 2 h, the transmittance of the samples was measured as described above.

2.4 CONSTRUCTION OF TERNARY PHASE DIAGRAMS

Ternary phase diagrams were constructed to identify the self-emulsifying region. Mixtures of surfactant, cosurfactant and oil were prepared at room temperature using concentrations varying from 30% to 70%, 0% to 30% and 30% to 70%, respectively, so that the total concentration of the three constituents added was always 100%. After that, 50 mg of each mixture was diluted in 50 mL of distilled water. Only clear dispersions presenting a particle size equal or smaller than 200 nm were considered in the nanoemulsion region of phase diagrams (12, 18). Ternary phase diagrams were constructed using Sigma Plot 10 (Systat Software, San Jose, USA).

2.5 PREPARATION OF HCTZ-LOADED SNEDDS

Based on the preliminary screening of constituents and on the constructed ternary phase diagrams, two formulations were selected to load HCTZ. HCTZ (10 mg) was dissolved in 200 mg of a mixture containing MCT, Cremophor EL® and Transcutol in two proportions (40/40/20, respectively – formulation 1 or 50/40/10, respectively - formulation 2). The

mixtures were stirred by sonication in a water bath at 60 °C for 30 min until a clear dispersion was obtained.

2.6 PHYSICOCHEMICAL CHARACTERIZATION OF SNEDDS

2.6.1 DROPLET SIZE AND ZETA POTENTIAL

The mean droplet size and zeta potential were determined by dynamic light scattering (DLS) and laser-Doppler anemometry, respectively, using a Zetasizer Nano Series (Malvern Instruments, Worcestershire, UK). The samples were appropriately diluted in water, fasted state simulated gastric fluid (FaSSGF, pH 1.6) or fasted state simulated intestinal fluid (FaSSIF, pH 6.5) (19). The size measurements were performed at a scattering angle of 173°. For zeta potential analysis, the samples were placed in electrophoretic cells where a potential of ± 150 mV was applied. The zeta potential values were calculated as mean values of electrophoretic mobility by using the Smoluchowski's equation.

2.6.2 EFFECT OF DILUTION AND pH OF THE MEDIUM

The formulations were evaluated for robustness to dilution and pH of the medium. The samples were diluted 10-, 100-, and 1000-fold with water, FaSSGF (pH 1.6), and FaSSIF (pH 6.5). After 24h, the diluted SNEDDS were visually monitored for signs of drug precipitation or phase separation.

2.6.3 MORPHOLOGY

SNEDDS morphology was evaluated by transmission electron microscopy (TEM). Drops of the samples previously diluted in water (1:100) were deposited on carbon-coated copper grids and negatively stained with 1% (w/v) phosphotungstic acid solution. The samples were observed using a JEOL JEM 1011 electron microscope (Tokyo, Japan) operating at an acceleration voltage of 100 kV.

2.6.4 INFRARED SPECTROSCOPY

The compatibility between the constituents of the SNEDDS was evaluated by diffuse reflectance Fourier transform infrared spectroscopy (FTIR). HCTZ and excipients were mixed, followed by magnetic stirring for 5 min. The spectra were recorded using a FTIR Frontier (PerkinElmer, Brazil) within a scan range of 600-4,000 cm^{-1} , and an average of over 32 scans, at a spectral resolution of 4 cm^{-1} . A background spectrum was obtained for each experimental condition.

2.6.5 CLOUD POINT MEASUREMENT

The obtained SNEDDS were firstly diluted in distilled water (1:250) and placed in a water bath, with a gradual increase in temperature. The cloud point is the temperature above which could be visually a phase separation.

2.6.6 DETERMINATION OF DRUG CONTENT

For determination of the HCTZ, the SNEDDS formulations were dissolved in methanol and sonicated. The methanolic solutions were filtered through 0.45 μm membrane filter (Millipore, USA), diluted in the mobile phase, and analyzed by HPLC. The chromatographic analysis was performed in a Shimadzu liquid chromatograph (Shimadzu, Kyoto, Japan), with a LC-10A VP quaternary pump and UV detector set at 270 nm. The chromatographic system was equipped with a Phenomenex® (Torrance, CA, USA) C18 reversed-phase column (150 X 4.6 mm; 5 mm particle size) conditioned in a SPD-10AVP column oven at 40°C. The column was eluted in an isocratic mode by using phosphate buffer (25 mM, pH 3.0), acetonitrile and methanol (82:9:9 v/v) as mobile phase at a flow rate of 1.0 mL/min and an injection volume of 20 μL . The method was validated according to the International Conference on Harmonization (ICH) considering specificity, linearity, precision, accuracy, robustness, limit of detection and quantification (20). Validation parameters were within the acceptable range (data not shown).

2.6.7 EMULSIFICATION TIME

The emulsification time (time required by a preconcentrate to form a homogeneous mixture upon dilution) of SNEDDS was assessed on USP apparatus 3 (Erweka RRT 10, Germany). Each formulation (400 mg) was placed into transparent gelatin capsules and added into 200 mL of distilled water, FaSSGF pH 1.6 or FaSSIF pH 6.5 (19). The agitation speed was set at 20 dips per minute for the gastric fluid and 15 dips per minute for intestinal fluid or water. The emulsification time was observed visually as reported by Khoo and coauthors (21).

2.7 IN VITRO DISSOLUTION

Dissolution assays were performed using USP apparatus 3 Erweka RRT 10 (Germany). The dissolution was carried out in FaSSGF pH 1.6 and FaSSIF pH 6.5, both at 37°C \pm 0.5°C (19). Gelatin transparent capsules containing 10 mg of HCTZ or HCTZ-loaded SNEDDS were placed into 200 mL of dissolution medium. In the first step of the assay, the dissolution was performed in FaSSGF (20 dips/min) for 120 min. Aliquots of 5 mL of the medium were withdrawn at intervals of 5, 10, 20, 30, 40, 50, 60, 90 and 120

min. Subsequently, the dissolution medium was replaced by FaSSIF for more 180 min (15 dips/min). In addition to the previously described sampling intervals, an additional sampling was carried out at 180 min. The samples were quantified by HPLC and curves of the percentage of drug released versus time were constructed.

2.8 SHORT-TERM STABILITY

The short-term stability of the optimized formulations was evaluated during 3 months. F1 and F2 were placed in glass flasks and stored at 4°C (refrigerator temperature) and 25°C (room temperature). Droplet size, zeta potential and HCTZ content data from different time intervals were compared to those results obtained immediately after the preparation.

2.9 IN VIVO DIURETIC ACTIVITY

2.9.1 ANIMALS

Female Wistar rats (weighing 210–250 g) were housed in a temperature-controlled room (22 ± 2 °C) on 12/12 h light-dark cycle, with free access to water and food. All animal care and experimental procedures were approved by the University Institutional Ethics Committee in accordance with CONCEA (National Council for the Control of Animal Experimentation) guidelines.

2.9.2 IN VIVO DIURETIC ACTIVITY

The diuretic activity was determined according to a previously described method (22) with minor modifications. The animals were separated randomly into three different groups of 6 animals each: Group 1 (the control group) was treated with SNEDDS placebo (without HCTZ); Group 2 (the positive control) received 10 mg/kg of free HCTZ and Group 3 received 10 mg/kg of SNEDDS containing HCTZ. All formulations were administered to animals by gavage. Immediately after administration, the animals were placed individually in a metabolic cage for 24 h with free access to water and food. After treatments, urinary excretion was measured at different time intervals (2, 4, 8 and 24 h). Cumulative urine excretion was calculated in relation to body weight and expressed as mL/100 g. Electrolyte concentrations (Na^+ , K^+ , and Cl^-) of the urine samples of each rat were also measured using the ion selective method on a Dade-Behring Dimension RXL analyzer (Dade Behring, FL, USA).

2.9.3 STATISTICAL ANALYSIS

The results were expressed as mean \pm standard error of mean (SEM) of 3-6 animals per group. Statistical analysis was performed using one-way

analysis of variance (ANOVA) followed the Tukey test. A p value less than 0.05 was considered statistically significant. The statistical analysis was performed using GraphPad Prism, version 6.0 (GraphPad Software, San Diego, CA, USA).

3. RESULTS AND DISCUSSION

3.1 SNEDDS formulation studies

An optimal combination of oil, surfactant and cosurfactant is required for SNEEDS formation and thus specific pharmaceutical excipient combinations should be considered to obtain appropriate self-emulsifying performance of the system (18).

In order to obtain a maximum solubilizing capacity for the drug under investigation, it is necessary to achieve a high drug loading. In this context, HCTZ solubility was tested in different oily phases, surfactant and cosurfactant (data not shown). The solubility of HCTZ in oily phase was found to be the highest in MCT, followed by cotton oil and olive oil. MCT was selected for the next studies as it may avoid or reduce HCTZ precipitation in the gut lumen after an oral administration. Among the tested surfactants, Transcutol and propylene glycol were selected as cosurfactants for further studies.

The emulsification ability of different surfactants was evaluated by measuring the transmittance values of the dispersion obtained after dilution with water (Table 1). In this study, the higher transmittance values obtained for the mixtures of MCT and Cremophor EL as well as olive oil or cotton oil and Tween 20, indicated the better emulsifying abilities of these preparations. Subsequently, these mixtures were selected to evaluate the effect of cosurfactant on emulsifying ability.

The mixture of Cremophor EL and Transcutol P provided the faster emulsification of the MCT (Table 1), requiring only six flask inversions to produce a homogeneous emulsion. On the other hand, low transmittance values or high flask inversion number to form emulsions were required for the other oil/surfactant/cosurfactant combinations. Typically, surfactants with hydrophilic-lipophilic balance (HLB) values higher than 10 are necessary to form a uniform and fine oil/water emulsions; however, the thermodynamic stability is achieved by using a blend of low and high HLB surfactants (23).

3.2 TERNARY PHASE DIAGRAM

Based on the solubility properties and emulsifying ability data, cotton oil, olive oil and MCT were selected as oily phase, Tween 20 and Cremophor EL as surfactants, and PEG 400, propylene glycol and Transcutol

as cosurfactants to construct the ternary phase diagrams. The most appropriate mixture that could form SNEDDS displaying droplet sizes smaller than 200 nm could be selected by considering this approach. Ternary phase diagram for olive oil, Tween 20, and PEG 400 and for cotton oil, Tween 20 and propylene glycol are presented as supplementary material.

Table 1 Emulsifying ability between oils, surfactants and cosurfactants.

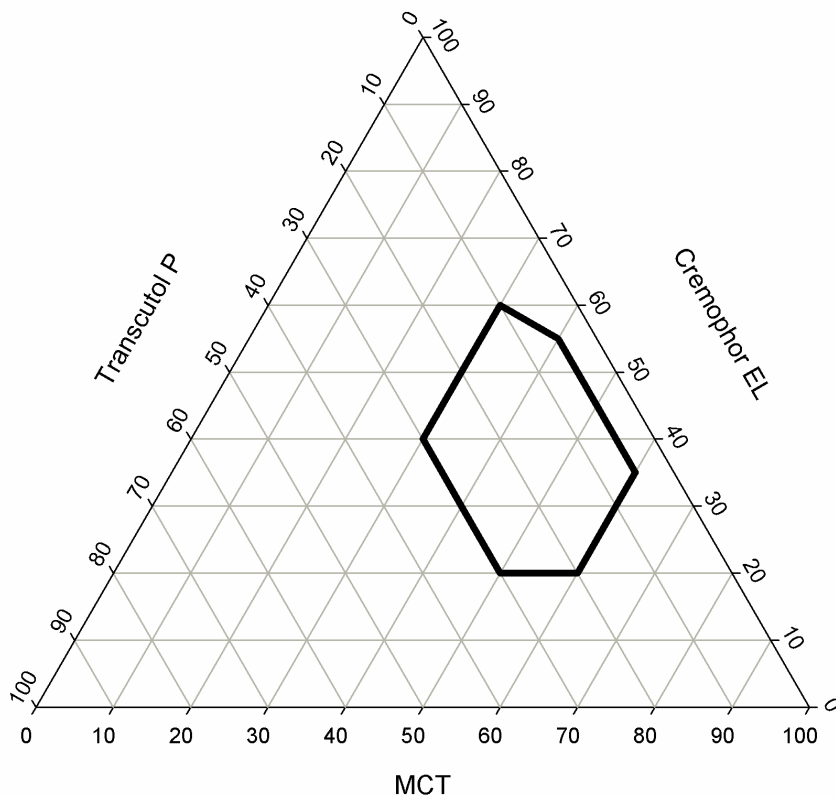
Composition			Transmittance (%)	Flask inversion number
Oil	Olive Oil	Crem EL	70.9 ± 4.3	65 ± 7
		Tween 20	90.8 ± 2.7	50 ± 5
		Tween 80	84.4 ± 5.8	60 ± 8
	Cotton Oil	Crem EL	61.5 ± 9.2	60 ± 5
		Tween 20	90.2 ± 4.5	45 ± 8
		Tween 80	80.7 ± 8.1	55 ± 4
	MCT	Crem EL	97.0 ± 1.5	25 ± 6
		Tween 20	62.2 ± 12.3	60 ± 9
		Tween 80	76.7 ± 7.2	50 ± 7
Oil/ Surfactant	Olive oil/ Tween 20	PEG 400	92.5 ± 2.8	25 ± 4
		Propylen	82.4 ± 3.5	37 ± 3
		Transc	67.5 ± 4.8	49 ± 9
	Cotton oil/ Tween 20	PEG 400	68.4 ± 9.2	53 ± 8
		Propylen	87.3 ± 5.4	19 ± 4
		Transc	73.7 ± 6.2	42 ± 10
	MCT/ Crem EL	PEG 400	80.1 ± 6.1	35 ± 8
		Propylen	66.7 ± 13.3	50 ± 9
		Transc	98.7 ± 1.1	6 ± 2

^a Data expressed as mean ± SD (n = 3). Propylen = propylene glycol; Crem EL = Cremophor EL; Transc = Transcutol.

The ternary diagram obtained for MCT, Cremophor EL, and Transcutol P (Figure 1), showed a large region corresponding to the formation of NE displaying sizes close to 130 nm and narrow size distribution (PDI < 0.101). The efficient self-nanoemulsifying property of this mixture may be attributed to the optimal combination between the Cremophor EL, a surfactant displaying a high HLB value (HLB 13) (24), and Transcutol P, which has a low HLB value (HLB 4.2) (25). Although Transcutol P is highly lipophilic, it can escape from the interface into the aqueous phase due to its amphiphilic nature, with an action as a typical

cosurfactant (26). Lipid-surfactant interactions also may have contributed to facilitating the adsorption of Cremophor EL into droplets of MCT, which would increase the stability of these systems (27).

Figure 1 – Ternary phase diagram of system A (MCT/Cremophor EL/Transcutol).



In addition to the highest values of transmittance in the emulsification studies, the combination of MCT, Cremophor EL and Transcutol demonstrated larger NE region and size droplets smaller than 200 nm. Based on this preliminary screening, toxicity issues and ease to formulate, two formulations presenting least amounts of surfactants and cosurfactants were selected for further studies. The SNEDDS were prepared using MCT:

Cremophor EL: Transcutol P weight ratios of 40:40:20 and of 50:40:10, and were named as F1 and F2, respectively.

3.3 SNEDDS CHARACTERIZATION

3.3.1 DROPLET SIZE, ZETA POTENTIAL AND DRUG CONTENT

The physicochemical and drug loading properties obtained for F1 and F2 SNEDDS formulations are demonstrated in Table 2. According to the drug content values, both formulations were able to incorporate the total drug amount added to the formulations (10 mg) and no phase separation was observed after storage at room temperature during 24 h. After dilution, both formulations (F1 and F2) exhibited oil droplets in nanometric size range (smaller than 150 nm) and narrow size distribution (Table 2), which is essential to reduce the emulsification time. Although no statistical significance was verified, the reduction of the surfactant and cosurfactant concentration from 60 to 50% (F1 to F2) resulted in a decrease of the mean droplet size. Small droplets result in the close-packed arrangement of the surfactant at the interface oil-water, which affected the thermodynamic stability of the final nanoemulsion due to the decrease in the interfacial tension of the system and the formation of a mechanical barrier to avoid coalescence. The small size allows a wide distribution in the GIT and promotes the drug permeation across the intestinal barrier (28, 29). Once the drug is administered under fasted conditions, the droplet size was measured in FaSSGF and FaSSIF. As showed in Table 2, no significant difference was observed in the droplet size of the nanoemulsions upon dilution in these biorelevant media. The small droplet size may allow a high degree of dispersibility of the nanoemulsion in the GIT and offer a large surface area so that the pancreatic lipase may hydrolyze the lipids. This increases the rate at which the drug is released and absorbed.

The zeta potential is the measure of the electric potential difference between the surface of the shear plane of particles and the electroneutral region of the continuous phase and indicates the degree of repulsion among charged particles in the dispersion. The zeta potential value indicate if the particles have enough electrical forces to repulse each other and to prevent aggregation or coalescence (30). Both F1 and F2 formulations exhibited negative surface charge and the zeta potential values were found to be similar (-32.7 and -31.3 mV). The zeta potential values were increased upon dilution of SNEDDS in FaSSGF, but were not changed in FaSSIF. These zeta potential values found after dilution in the biorelevant media clearly indicate that stable colloidal systems may be obtained.

The selected formulations were also investigated in three different media (water, FaSSGF and FaSSIF) in the same volume (1,000 fold dilution) to evaluate the pH effect on globule size (Table 2).

Table 2. Mean globule size, polydispersity index and drug content of SNEDDS diluted in distilled water, FaSSGF and FaSSIF at a ratio of 1:1000 after the preparation (time zero), 1 and 3 months at room temperature (25°C) and refrigerator temperature (4°C).

Formulation	Mean Globule Size (nm) ^a	Polispersity index ^b	Zeta potential (mV)	HCTZ content ^a (%)
F1 water	143.2 ± 35.6	0.194	- 32.7 ± 3.3	
FaSSGF	138.2 ± 27.9	0.176	- 44.1 ± 7.4	99.2 ± 3.1
FaSSIF	126.4 ± 40.1	0.187	- 25.8 ± 5.7	
F1 (25°C)				
1month	113.1 ± 27.8	0.143	-30.4 ± 3.6	96.1 ± 2.8
3months	149.6 ± 25.3	0.191	- 34.9 ± 9.6	96.9 ± 2.3
F1 (4°C)				
1month	109.6 ± 19.2	0.131	- 35.1 ± 8.1	97.2 ± 1.9
3months	137.9 ± 21.7	0.167	- 31.9 ± 5.2	95.8 ± 4.1
F2 water	169.6 ± 22.8	0.136	- 31.3 ± 2.7	
FaSSGF	155.8 ± 34.3	0.163	- 42.7 ± 4.1	95.6 ± 2.6
FaSSIF	139.4 ± 39.4	0.174	- 30.1 ± 3.9	
F2 (25°C)				
1month	178.3 ± 27.7	0.204	-36.2 ± 5.3	94.3 ± 2.9
3months	167.7 ± 40.6	0.226	-30.9 ± 4.7	91.7 ± 3.7
F2 (4°C)				
1month	150.2 ± 33.2	0.198	-33.5 ± 3.7	92.3 ± 4.2
3months	181.9 ± 25.8	0.177	-36.9 ± 7.2	89.4 ± 3.5

^a Data expressed as mean ± SD (n=3)

^b Data expressed as mean (n=3)

A fasted state was prioritized for these media because the therapeutic recommendations of HCTZ include its ingestion in a fasted state. No pH effect on mean globule size of these formulations was observed. This result is particularly relevant because SNEDDS will face large pH variation during the GIT tract after in vivo oral ingestion. A pH control is essential because it affects to the secretion and potency of digestive lipases, which act at the oil/water interface of the SNEDDS during the lipid digestion (31, 32). The bioavailability and solubilization of HCTZ in the GIT are strongly affected by lipid digestion of the SNEDDS. The small globule size observed in

different pH values could facilitate the lipid digestion and, consequently, the drug absorption.

SNEDDS could failure in the improvement of bioavailability of drugs due to drug precipitation phenomena upon dilution in the GIT (25, 33). Therefore, the robustness of SNEDDS to dilution was evaluated, testing the two optimal formulations in water, FaSSGF (pH 1.6) and FaSSIF (pH 6.5). Even after 12 h, no signs of precipitation, cloudiness or phase separation were observed for both formulations, which ensure the stability of the reconstituted emulsion. The combination of Cremophor EL and Transcutol was enough to reduce the free energy of the system and avoid coalescence or phase separation.

3.3.2 TRANSMISSION ELECTRON MICROSCOPY

Figure 2 depicts the photomicrographs of F1 (A and B) and F2 (C and D) formulations after dilution in water. Both formulations appear as dark droplets surrounded by a brighter region and are spherical in shape. Although the droplets in F2 are slightly higher in size, both formulations displayed monodisperse size distribution in a nanometric size range (this aligns with results from the dynamic light scattering method). No signs of drug precipitate or droplet coalescence were observed.

3.3.3 FOURIER TRANSFORM INFRARED SPECTROSCOPY

The FTIR analyses were carried out to investigate incompatibilities or chemical interactions between HCTZ and the selected excipients. Pure compounds and their mixtures were analyzed (infrared spectra in the supplementary material). Spectra characteristic band from 1550 cm^{-1} to 1650 cm^{-1} , corresponding to carboxylate anions, was not observed in the Cremophor EL, which is usually found in the unpurified Cremophor EL (34). The purified and unpurified Cremophor EL differ with respect to some properties; therefore, the infrared spectra and the technical information from BASF confirm that unpurified Cremophor EL was not used in this investigation, which could affect the stability studies.

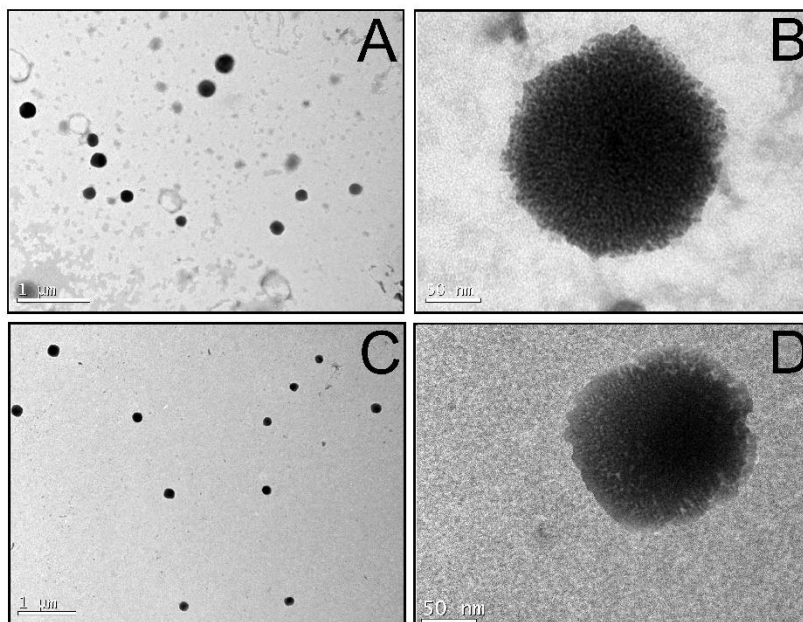
In the spectrum of the physical mixtures between HCTZ and excipients, even in the 1:1 (w/w) proportion or in the final formulations (F1 4:4:2 and F2 5:4:1), characteristic bands of HCTZ and excipients were observed, suggesting the absence of chemical incompatibilities between HCTZ and the selected constituents.

3.3.4 CLOUD POINT MEASUREMENT

The cloud point of SNEDDS is the measure of the temperature where an irreversible phase separation occurs due to the dehydration of the

components, affecting the stability of the system and, as consequence, the absorption of the drug. The cloud point observed for F1 and F2 was between 60–65°C and 70–75°C, respectively. As these temperatures are significantly higher than body temperature, no phase separation would be expected after oral administration of these systems.

Figure 2 – TEM images of the reconstituted nanoemulsion from SNEDDS F1 (A and B) and F2 (B and C).



3.3.5 *IN VITRO* DISPERSION AND EMULSIFICATION TIME

The *in vitro* dispersion assay give a more accurate description of the ability of the SNEDDS to be dispersed in gastric and intestinal media, and for digestion of lipid compounds of formulations in the presence of pancreatic and biliary fluids (35). The emulsification time was evaluated by using a USP apparatus 3. Hard gelatin capsules containing the F1 or F2 formulations were added in three different media: distilled water, FaSSGF (pH 1.6) with agitation rate of 20 dips/min, and in FaSSIF (pH 6.5) with agitation rate of 15 dips/min (as recommended due to the higher motility of the stomach compared to the small intestine). The gentle agitation from the

USP apparatus 3 may have provoked the disruption of the oil-water interface, leading to the formation of a fine droplet emulsion. The emulsification time obtained for F1 and F2 was about 30 and 45 s, respectively. No interference of tested media was observed. The slower emulsification time for the F2 was probably caused by the higher content of oily phase in this formulation.

3.4 *IN VITRO* DISSOLUTION ASSAYS

In recent years, results of appropriated dissolution assays have been used in formulation screening and to predict *in vivo* performance. As drugs in solution can permeate the gastrointestinal barriers more easily, the dissolution rate is crucial to identify bioavailability problems. Dissolution assays should be performed under conditions that resemble the physiology of human gastrointestinal tract. The official dissolution media usually used in quality control studies are not appropriate to predict *in vivo* behavior since they do not consider key parameters such as osmolarity, viscosity, ionic strength and surface tension (only typical pH conditions are evaluated). Furthermore, these dissolution media hardly simulate the pre- or postprandial conditions. Specifically, the prediction of *in vivo* behavior of formulations containing BCS class II and IV drugs should not use simple dissolution media as a first choice. Biorelevant media may be able to more accurately represent the physiological conditions faced *in vivo* compared to simplified dissolution media (36, 37).

After oral administration, SNEDDS will be firstly dispersed in the gastric fluid. Considering that HCTZ is generally administered in fasting conditions, the dissolution assays were carried out in FaSSGF (pH 1.6) and FaSSIF (pH 6.5). These biorelevant dissolution media are composed of bile salts and phospholipids (lecithin), which facilitate the wetting and solubilization of lipophilic compounds into mixed micelles. In addition to the physiologically relevant dissolution media, the type of equipment and their parameters should be carefully selected. In the current study, the USP apparatus 3 (reciprocating cylinder) was considered due to its agitation ability and the possibility of changing the composition of a medium and flow rate during the assay, which enables the establishment of a more robust *in vitro/in vivo* correlation. The USP apparatus 3 allows the product exposition to a variety of physicochemical conditions, which is crucial to SNEEDS formation and could better simulate its *in vivo* behavior. When co-ingested with fluids such as a water glass, the gastric volume of fasted conditions is approximately 200-300 mL. This volume is hardly used in the paddle or basket conventional dissolution apparatus because it would lead to loss of test reproducibility (38-40).

SNEDDS should disperse completely and spontaneously emulsify when subjected to aqueous media of GIT under mild agitation (peristaltic activity). Therefore, the apparatus 3 was used to mimic the physiological conditions of the gastrointestinal tract. For determining only the HCTZ solubilized in the dissolution medium, dialysis membranes were considered, which are designed to fit the tops and bottoms of the reciprocating cylinders. In the same way, the gastrointestinal conditions were simulated by using FaSSGF (pH 1.6) and FaSSIF (pH 6.5) at 20 dips/min and 15 dips/min, respectively.

The dissolution profiles showed that both SNEDDS formulations allowed a faster release rate of the HCTZ when compared to the free drug (Figure 3). An *in vitro* release of only 27.4% was achieved after 30 min for the HCTZ powder while 81.9% and 75.6% were achieved by F1 and F2, respectively. The higher dissolution rate was obtained in simulated gastric fluid and maintained in the intestinal simulated fluid. Changes in oil concentration between F1 and F2 did not affect the drug release rate, demonstrating that a proportion of 50% of surfactant and cosurfactant are enough to emulsify the oil and generate SNEDDS with high dissolution rate. These results suggest an increase in the HCTZ bioavailability after oral administration of SNEDDS. Moreover, considering that HCTZ belong to the BCS class IV, the improvement of drug solubility by incorporating in SNEDDS would allow a better prediction of the *in vivo* biopharmaceutical performance of the drug, contributing to both rational use of medication and patient adherence to the treatment.

3.5 SHORT TERM STABILITY

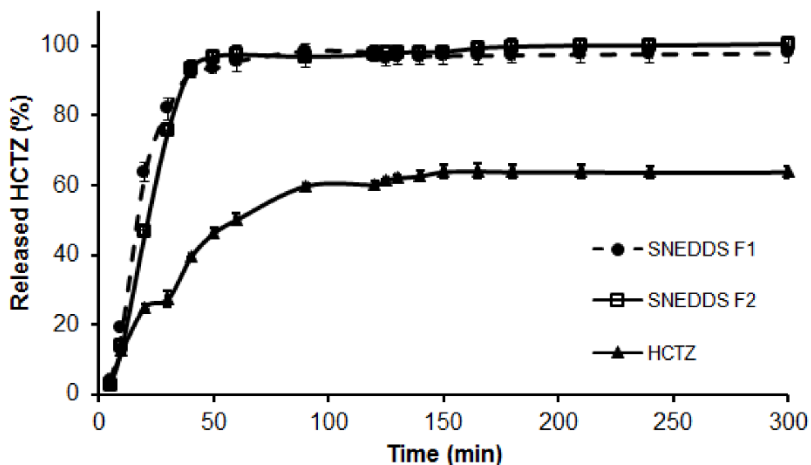
The proposed SNEDDS aims the improvement of biopharmaceutical properties of HCTZ and also protection of the drug from the alkaline hydrolysis. Once no water content was added to prepare this formulation, hydrolysis events may be avoided after the incorporation of HCTZ in the SNEDDS, which would avoid or reduce the direct contact between HCTZ and the intestinal basic aqueous medium. When pH-dependent hydrolysis is observed, HCTZ proceeds irreversibly to a ring-opened product (aminochlorobenzenedisulphonamide), which it has already been reported by our research team (41). The stability was verified by the maintenance of the drug content after dissolution step and no additional peaks were found in chromatograms (data not shown).

As demonstrated by FTIR spectra, the Cremophor EL used in this study does not present carboxylate anions, which is relevant to maintain the drug in a stable form. HCTZ degrades in an alkaline aqueous vehicle and HCTZ instability could be generated in the presence of these basic

carboxylate anions, similar to the ethanolysis of paclitaxel demonstrated by Gogaté and coworkers (34).

No differences in mean globule size, PDI, zeta potential or HCTZ content were observed after storage at room temperature (25 °C) or in the refrigerator (4 °C) (Table 2). Additionally, crystallization of the drug, precipitation phenomena or color change were not observed. Based on these results, it is possible to state that SNEDDS may be considered a suitable carrier for oral delivery of HCTZ.

Figure 3 – Dissolution profiles of HCTZ and SNEDDS F1 and F2 obtained in FASSGF (pH 1.6) during 120 min and in FASSIF (pH 6.5) for more 180 min.



3.6 *IN VIVO* DIURETIC ACTIVITY

For the *in vivo* studies, F2 was selected due to its high dissolution rate, suitable physicochemical stability and lower surfactant concentration. Figure 4 exhibits the results obtained after measuring the urinary volume and the urine electrolyte levels (Na⁺, K⁺ and Cl⁻) after 2, 4, 8, and 24 h of the treatment. The administration of HCTZ-loaded SNEDDS significantly increased the total urinary volume after 24 h of drug administration when compared to the control group as well as the free HCTZ (Fig. 4, Panel A). Dissolution studies showed that F2 is completely released in the gastrointestinal medium. As HCTZ is mostly absorbed in the upper small intestine (42), a rapid absorption of HCTZ is expected for F2 due to its rapid dissolution.

Although a more significant pharmacodynamics of urine excretion was observed in later stages, urinary excretion of Na⁺, K⁺ and Cl⁻ in

SNEDDS-HCTZ was significantly increased in early stages (2 h) compared with the control. SNEDDS containing HCTZ also resulted in an increased excretion of Na^+ and Cl^- when compared to drug-free treatment. The natriuresis, kaliuresis and chlориuresis effects of SNEDDS containing HCTZ were maintained up in the later times (Fig. 4, Panel B, C and D). A mixture of HCTZ dissolved in the aqueous media and HCTZ dissolved in the oil droplets (free oil droplets or in clusters) may justify these findings, which have already been observed by Atef (43) in its study with SEDDS of phenytoin.

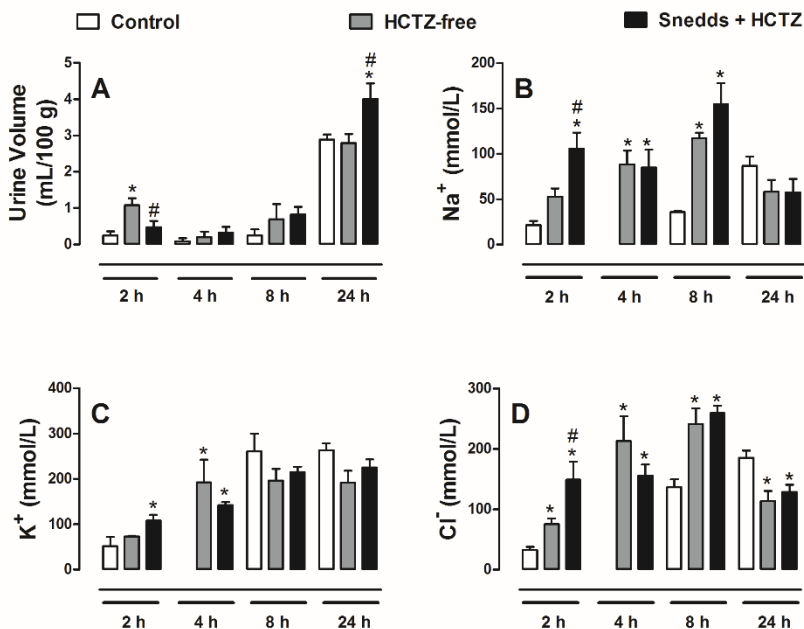
After oral administration, the SNEDDS is emulsified in the GIT and the solubilized HCTZ in the aqueous phase provide an immediate effect. The HCTZ absorbed from SNEDDS in early stages seems to be enough to produce a pharmacological effect in the ions excretion however, not enough to produce a pronounced effect on the urinary volume. The higher dissolution rate also could increase the plasma concentration of HCTZ, maintaining its levels in the therapeutic range, which would provide a sustained effect.

When comparing to the SNEDDS proposed by Yadav and coworkers (44), our study demonstrated that F2 was completely released in simulated gastric medium (50 min) while the formulation proposed by Yadav was totally released after 10 min in phosphate buffer. Despite a slower dissolution, the *in vivo* assays showed that F2 was more effective than the SNEDDS proposed by Yadav concerning the diuretic activity. The ratio between the treated group and the control group obtained in this study and Yadav's study was used for comparison purposes once the measurement units are different. The ratio of diuretic volume between the treated group and control group after 24 h was approximately 1.58 for the literature formulation and 1.75 for F2. The difference is even higher when the time intervals of 4 and 8 h are considered (1.4 and 2.4 for Yadav, respectively, and 5 in both time intervals for F2). In summary, F2 had a more promissory pharmacodynamics than the SNEDDS system studied by Yadav, besides presenting the low percentage of surfactants.

The presence of Cremophor EL also may justify the high pharmacodynamic activity of F2. HCTZ is a substrate of BCRP, an important drug efflux transporter identified in the intestine (36, 45). Beery and coworkers (2012) have already demonstrated that BCRP plays a role in limiting the bioavailability of chlorothiazide (37). Therefore, an excipient that inhibits the intestinal efflux caused by BCRP could improve the intestinal permeability and consequently the absorption of HCTZ. Cremophor EL has already been described as an inhibitor of BCRP (46), which could improve the bioavailability and consequently the pharmacodynamical activity.

Based on these *in vivo* results, it is possible to state that the selection of a suitable surfactant is relevant to increase and extend the pharmacological effect of HCTZ as well as produce an appropriate self-emulsifying performance at lower concentrations.

Figure 4 – Effects of acute oral administration of SNEDDS containing HCTZ on urine output (Panel A) and electrolyte excretion (Panel B, C, D). The graphs show the urinary volume (A), concentration of Na⁺, K⁺ and Cl⁻ (B, C and D, respectively) in samples collected 2, 4, 8 and 24 h after the treatment. The results show the mean ± S.E.M of 3-6 animals per group. Statistical analyses were performed by means of one-way analysis of variance (ANOVA) followed by Tukey post-test. * P < 0.05; when compared with the control group and # P < 0.05 significantly different from corresponding SNEDDS-HCTZ group.



4. CONCLUSIONS

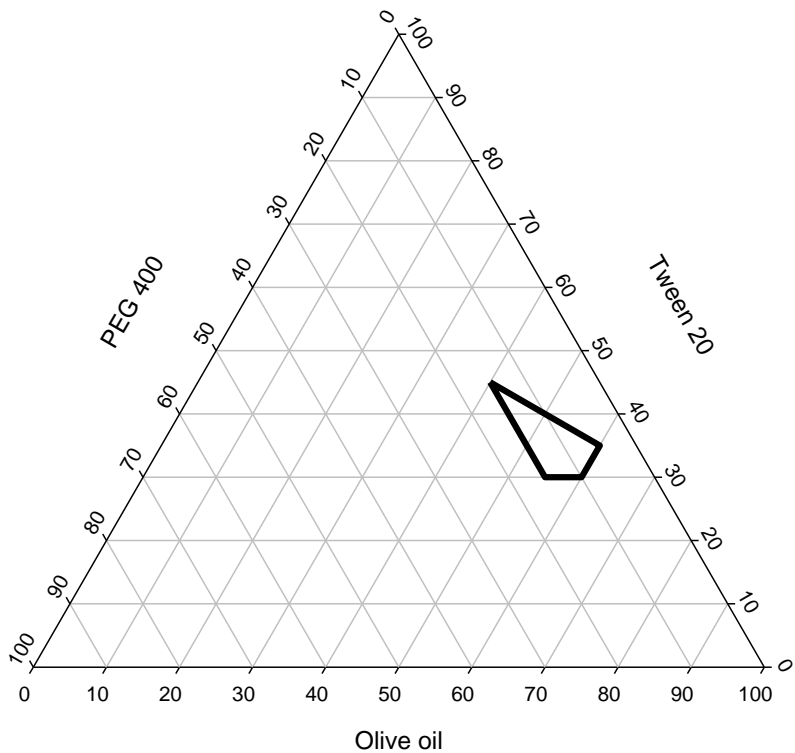
In this study, SNEDDS were prepared as an alternative to the oral traditional administration of HCTZ aiming to overcome their biopharmaceutical limitations. A preliminary screening of constituents was assessed and a simple and stable HCTZ nanoemulsion was obtained. The selected formulation, which was composed of MCT, Cremophor EL and Transcutol

P provided rapid nanoemulsification in water or gastrointestinal fluids and its globule size was not changed at different pH values. The blend of surfactant and cosurfactant of this formulation was sufficient to ensure its stability. The optimal SNEDDS also presented higher dissolution rates than HCTZ free. For the diuretic activity, an increase in total volume of urine at later stages and ions excretion at early stages was observed when compared with the control (pure HCTZ). The selected formulation presented an appropriate performance in both *in vitro* and *in vivo* assays. The improvement in the pharmacodynamics may be associated with high dissolution rates, improvement of absorption and inhibition of BCRP by Cremophor EL. In summary, it is possible to state that the design of suitable SNEDDS can be beneficial in improving biopharmaceutical properties which impact on the diuretic activity.

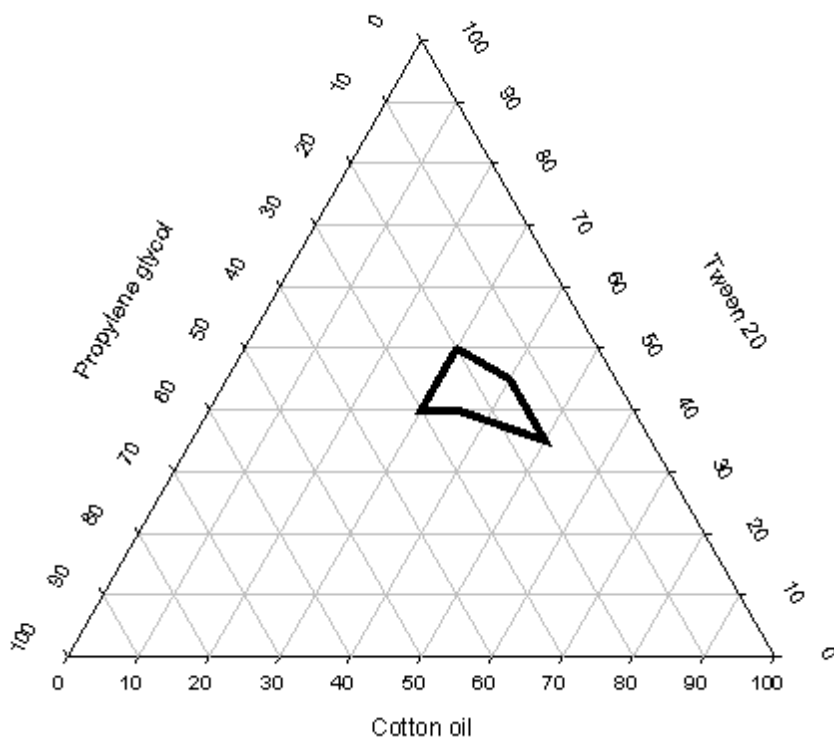
ACKNOWLEDGMENTS

The authors would like to thank LCME/UFSC for technical support during microscopy analysis, Flora Lucena Sant'ana for her skillful assistance with the *in vivo* studies and Dr. José Eduardo da Silva Santos, who kindly allowed the use of the metabolic cages. This study was supported by the National Counsel of Technological and Scientific Development (CNPq) and Coordination for Enhancement of Higher Education Personnel (CAPES).

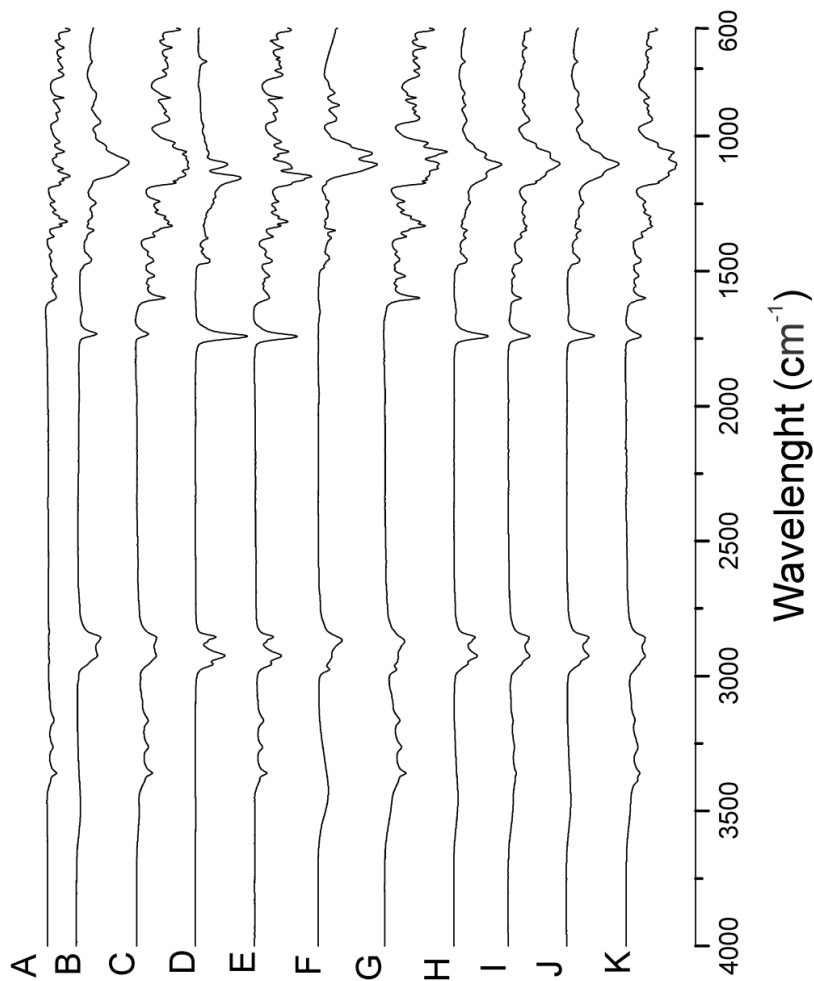
SUPPLEMENTARY MATERIAL



Ternary phase diagram for olive oil, Tween 20, and PEG 400.



Ternary phase diagram for cotton oil, Tween 20 and propylene glycol.



FTIR spectra obtained for drug, excipient and their physical mixtures. (A) HCTZ, (B) Cremophor EL, (C) HCTZ and Cremophor EL 1:1 w/w, (D) MCT, (E) HCTZ and MCT 1:1 w/w, (F) Transcutol P, (G) HCTZ and Transcutol P 1:1 w/w, (H) MCT:Cremophor EL: Transcutol 4:4:2, (I) MCT:Cremophor EL: Transcutol P (4:4:2) 1:1 w/w with HCTZ, (J) MCT:Cremophor EL: Transcutol P (5:4:1) and (K) MCT:Cremophor EL: Transcutol P (5:4:1) 1:1 w/w with HCTZ.

REFERENCES

1. Rang HP, Ritter JM, Dale MM, editors. *Farmacologia*. Rio de Janeiro: Elsevier; 2012.
2. Yu LX, Amidon GL, Polli JE, Zhao H, Mehta MU, Conner DP, et al. Biopharmaceutics classification system: the scientific basis for biowaiver extensions. *Pharm Res*. 2002;19(7):921-5.
3. Fang X, Bibart RT, Mayr S, Yin W, Harmon PA, McCafferty JF, et al. Purification and identification of an impurity in bulk hydrochlorothiazide. *J Pharm Sci*. 2001;90(11):1800-9.
4. Revelle LK, Musser SM, Rowe BJ, Feldman IC. Identification of chlorothiazide and hydrochlorothiazide UV-A photolytic decomposition products. *J Pharm Sci*. 1997;86(5):631-4.
5. Mollica JA, Rehm CR, Smith JB, Govan HK. Hydrolysis of benzothiadiazines. *J Pharma Sci*. 1971;60(9):1380-4.
6. Basalious EB, Shawky N, Badr-Eldin SM. SNEDDS containing bioenhancers for improvement of dissolution and oral absorption of lacidipine. I: Development and optimization. *International Journal of Pharmaceutics*. 2010;391(1–2):203-11.
7. Villar AMS, Naveros BC, Campmany ACC, Trenchs MA, Rocabert CB, Bellowa LH. Design and optimization of self-nanoemulsifying drug delivery systems (SNEDDS) for enhanced dissolution of gemfibrozil. *International Journal of Pharmaceutics*. 2012;431(1–2):161-75.
8. Zhao T, Maniglio D, Chen J, Chen B, Motta A, Migliaresi C. Design and optimization of self-nanoemulsifying formulations for lipophilic drugs. *Nanotechnology*. 2015;26(12):125102.
9. Date AA, Desai N, Dixit R, Nagarsenker M. Self-nanoemulsifying drug delivery systems: formulation insights, applications and advances. *Nanomedicine*. 2010;5(10):1595-616.
10. Porter CJ, Trevaskis NL, Charman WN. Lipids and lipid-based formulations: optimizing the oral delivery of lipophilic drugs. *Nature Reviews Drug Discovery*. 2007;6(3):231-48.
11. Müllertz A, Ogbonna A, Ren S, Rades T. New perspectives on lipid and surfactant based drug delivery systems for oral delivery of poorly soluble drugs. *Journal of pharmacy and pharmacology*. 2010;62(11):1622-36.
12. Date AA, Nagarsenker M. Design and evaluation of self-nanoemulsifying drug delivery systems (SNEDDS) for cefpodoxime proxetil. *International journal of pharmaceutics*. 2007;329(1-2):166-72.
13. Muller RH, Mader K, Gohla S. Solid lipid nanoparticles (SLN) for controlled drug delivery-a review of the state of the art. *European journal of pharmaceutics and biopharmaceutics*. 2000;50(1):161-77.

14. Cagno Md, Stein PC, Styskala J, Hlaváč J, Skalko-Basnet N, Bauer-Brandl A. Overcoming instability and low solubility of new cytostatic compounds: A comparison of two approaches. *Eur J Pharm Biopharm.* 2012;80(3):657-62.
15. Patil S, Sandberg A, Heckert E, Self W, Seal S. Protein adsorption and cellular uptake of cerium oxide nanoparticles as a function of zeta potential. *Biomaterials.* 2007;28(31):4600-7.
16. Goyal U, Gupta A, Rana AC, Aggarwal G. Self micro emulsifying drug delivery system: A method for enhancement of bioavailability. *International journal of pharmaceutical sciences and research.* 2012;3(1):66-79.
17. Gursoy RN, Benita S. Self-emulsifying drug delivery systems (SEDDS) for improved oral delivery of lipophilic drugs. *Biomedicine & Pharmacotherapy.* 2004;58(3):173-82.
18. Pouton CW. Lipid formulations for oral administration of drugs: non-emulsifying, self-emulsifying and 'self-microemulsifying' drug delivery systems. *European Journal of Pharmaceutical Sciences.* 2000;11:S93-S8.
19. Jantratid E, Janssen N, Reppas C, Dressman JB. Dissolution media simulating conditions in the proximal human gastrointestinal tract: an update. *Pharmaceutical research.* 2008;25(7):1663-76.
20. ICH. Validation of Analytical Procedures: Text and Methodology Q2 (R1). Harmonization ICo, editor. Geneva2005.
21. Khoo S-M, Humberstone AJ, Porter CJ, Edwards GA, Charman WN. Formulation design and bioavailability assessment of lipidic self-emulsifying formulations of halofantrine. *International Journal of Pharmaceutics.* 1998;167(1):155-64.
22. Kau S, Keddie J, Andrews D. A method for screening diuretic agents in the rat. *J Pharmacol Methods.* 1984;11(1):67-75.
23. Kommuru T, Gurley B, Khan M, Reddy I. Self-emulsifying drug delivery systems (SEDDS) of coenzyme Q 10: formulation development and bioavailability assessment. *International journal of pharmaceutics.* 2001;212(2):233-46.
24. Taha EI, Al-Saidan S, Samy AM, Khan MA. Preparation and in vitro characterization of self-nanoemulsified drug delivery system (SNEDDS) of all-trans-retinol acetate. *Int J Pharm.* 2004;285(1):109-19.
25. Nepal PR, Han H-K, Choi H-K. Preparation and in vitro–in vivo evaluation of Witepsol® H35 based self-nanoemulsifying drug delivery systems (SNEDDS) of coenzyme Q 10. *European Journal of Pharmaceutical Sciences.* 2010;39(4):224-32.
26. Zargar-Shoshtari S, Wen J, Alany RG. Formulation and physicochemical characterization of imwitor 308 based self

- microemulsifying drug delivery systems. *Chemical and Pharmaceutical Bulletin*. 2010;58(10):1332-8.
27. Nazzal S, Khan MA. Response surface methodology for the optimization of ubiquinone self-nanoemulsified drug delivery system. *AAPS PharmSciTech*. 2002;3(1):23-31.
28. Wang L, Tabor R, Eastoe J, Li X, Heenan RK, Dong J. Formation and stability of nanoemulsions with mixed ionic–nonionic surfactants. *Physical Chemistry Chemical Physics*. 2009;11(42):9772-8.
29. Balakumar K, Raghavan CV, Abdu S. Self nanoemulsifying drug delivery system (SNEDDS) of Rosuvastatin calcium: design, formulation, bioavailability and pharmacokinetic evaluation. *Colloids and Surfaces B: Biointerfaces*. 2013;112:337-43.
30. Parmar N, Singla N, Amin S, Kohli K. Study of cosurfactant effect on nanoemulsifying area and development of lercanidipine loaded (SNEDDS) self nanoemulsifying drug delivery system. *Colloids and Surfaces B: Biointerfaces*. 2011;86(2):327-38.
31. Chakraborty S, Shukla D, Mishra B, Singh S. Lipid—an emerging platform for oral delivery of drugs with poor bioavailability. *European Journal of Pharmaceutics and Biopharmaceutics*. 2009;73(1):1-15.
32. Ljusberg-Wahren H, Nielsen FS, Brogård M, Troedsson E, Müllertz A. Enzymatic characterization of lipid-based drug delivery systems. *Int J Pharm*. 2005;298(2):328-32.
33. Narang AS, Delmarre D, Gao D. Stable drug encapsulation in micelles and microemulsions. *International journal of pharmaceutics*. 2007;345(1):9-25.
34. Sultana N, SAEED ARAYNE M, Waheed A. IN-vitro interaction studies of verapamil with fluoroquinolones using first order derivative uv spectrophotometry and RP-HPLC. *J Chil Chem Soc*. 2011;56(4):848-55.
35. Porter CJ, Pouton CW, Cuine JF, Charman WN. Enhancing intestinal drug solubilisation using lipid-based delivery systems. *Advanced Drug Delivery Reviews*. 2008;60(6):673-91.
36. Hasegawa M, Kusuhara H, Adachi M, Schuetz JD, Takeuchi K, Sugiyama Y. Multidrug resistance–associated protein 4 is involved in the urinary excretion of hydrochlorothiazide and furosemide. *J Am Soc Nephrol*. 2007;18(1):37-45.
37. Beery E, Rajnai Z, Abonyi T, Makai I, Bansaghi S, ERDŐ F, et al. ABCG2 Modulates Chlorothiazide Permeability In Vitro—characterization of Its Interactions. *Drug metabolism and pharmacokinetics*. 2012;27(3):349-53.
38. Cascone S, De Santis F, Lamberti G, Titomanlio G. The influence of dissolution conditions on the drug ADME phenomena. *Eur J Pharm Biopharm*. 2011;79(2):382-91.

39. Joshi A, Pund S, Nivsarkar M, Vasu K, Shishoo C. Dissolution test for site-specific release isoniazid pellets in USP apparatus 3 (reciprocating cylinder): optimization using response surface methodology. *Eur J Pharm Biopharm.* 2008;69(2):769-75.
40. Lakshmi CS, Badarinath A. An updated review of dissolution apparatus for conventional and novel dosage forms. *International Journal of Pharma Research & review.* 2013;2(7):42-53.
41. Mendes C, Costa AP, Oliveira PR, Tagliari MP, Silva MAS. Physicochemical and microbiological stability studies of extemporaneous antihypertensive pediatric suspensions for hospital use. *Pharm Dev Technol.* 2013;18(4):813-20.
42. Brunton L, Chabner B, Knollman B. Goodman and Gilman's the pharmacological basis of therapeutics. 12^a ed ed: McGraw Hill Professional; 2010.
43. Atef E, Belmonte AA. Formulation and in vitro and in vivo characterization of a phenytoin self-emulsifying drug delivery system (SEDDS). *European journal of pharmaceutical sciences.* 2008;35(4):257-63.
44. Yadav PS, Yadav E, Verma A, Amin S. Development, Characterization, and Pharmacodynamic Evaluation of Hydrochlorothiazide Loaded Self-Nanoemulsifying Drug Delivery Systems. *The Scientific World Journal.* 2014;2014.
45. Estudante M, Morais JG, Soveral G, Benet LZ. Intestinal drug transporters: an overview. *Adv Drug Delivery Rev.* 2013;65(10):1340-56.
46. Yamagata T, Kusuhara H, Morishita M, Takayama K, Benameur H, Sugiyama Y. Effect of excipients on breast cancer resistance protein substrate uptake activity. *Journal of Controlled Release.* 2007;124(1):1-5.

**CAPÍTULO 3 – MICROENCAPSULAÇÃO DE NANOEMULSÃO
REVESTIDA COM QUITOSANA PARA ADMINISTRAÇÃO DE
HIDROCLOROTIAZIDA. ARTIGO SUBMETIDO PARA O
PERIÓDICO *DRUG DEVELOPMENT AND INDUSTRIAL
PHARMACY***

INTRODUÇÃO

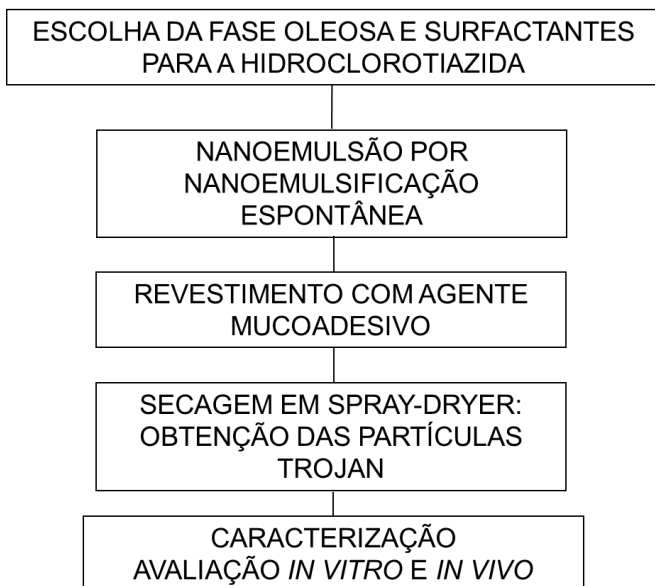
A nanotecnologia é uma área de destaque na pesquisa farmacêutica por fornecer oportunidades ilimitadas de liberação de fármacos com baixa biodisponibilidade. Muitos sistemas nanoestruturados têm sido explorados no âmbito de melhorias das propriedades biofarmacêuticas, como aumento da solubilidade, modulação da biodistribuição, prevenção da degradação, melhora da permeabilidade ou transporte dos fármacos, entre outros (Anton *et al.*, 2008).

As nanoemulsões (NE) são um grupo de sistemas bifásicos que têm demonstrado um futuro promissor para utilização em cosméticos, diagnóstico, terapia com fármacos e biotecnologia. NE podem ser definidas como emulsões óleo-em-água que apresentam um diâmetro médio de tamanho de gotículas variando de 50 a 1000 nm. Em geral, a média do tamanho de gotículas observado está entre 100 e 500 nm. Estas são facilmente produzidas em larga escala pela mistura de uma fase oleosa imiscível em água com uma fase aquosa mediante um processo de extrusão mecânico disponível mundialmente. As NE são sistemas cineticamente estáveis e apresentam grande potencial para carrear fármacos, principalmente os de baixa solubilidade aquosa (Shah *et al.*, 2010; Bruxel *et al.*, 2012).

Li e colaboradores (2011) desenvolveram uma tecnologia inovadora que consiste na secagem das NE por aspersão, ou *spray-dryer*, gerando uma partícula denominada Trojan. *Spray-drying* é uma técnica muito utilizada na indústria farmacêutica e alimentar que consiste na produção de partículas secas por atomização de um líquido (solução, suspensão, emulsão, etc.) gerando micropartículas relativamente monodispersas com alta porcentagem de encapsulação. Neste caso, a nanoemulsão é suspensa em uma solução aquosa contendo um material de parede, e em seguida, a atomização da suspensão final resulta na produção de micropartículas. As micropartículas, devido à seu grande tamanho, não tem a capacidade de se difundir amplamente pelos tecidos como as nanopartículas. Estas por sua vez, são de difícil manipulação na forma seca e podem ter a tendência de agregação. Nestas circunstâncias, um sistema híbrido que combine as vantagens terapêuticas de um sistema nanométrico e a facilidade de manipulação das micropartículas surge como um sistema interessante de liberação de fármacos. Este sistema híbrido capaz de veicular a nanoemulsão na forma de micropartículas sólidas, as partículas Trojan, preservam a integridade das nanogotículas oleosas e podem ser facilmente redispersas na fase aquosa (Li *et al.*, 2011).

Neste capítulo, foi desenvolvido uma nanoemulsão para HCTZ com uma tecnologia diferente do capítulo anterior. A nanoemulsão proposta desta

vez por emulsificação espontânea foi aliada com um revestimento mucoadesivo. A junção de uma macromolécula bioadesiva como a quitosana na nanoemulsão proporciona o revestimento das gotículas oleosas e apresenta vantagens adicionais, pois além de carrear o fármaco, a nanoemulsão revestida com polímero mucoadesivo apresenta uma grande área superficial de contato, resultando em maior permeabilidade do fármaco, e, conseqüente, melhora na biodisponibilidade (Chowdary e Rao, 2004; Smart, 2005; Patil e Sawant, 2008; Andrews *et al.*, 2009). Esta nanoemulsão revestida será então seca por aspersão para a microencapsulação das nanoemulsões gerando então as partículas “Trojan”, conforme esquema apresentado abaixo. Este capítulo propõe então uma tecnologia inovadora como sistema de liberação da HCTZ e a atividade diurética *in vivo* foi investigada visando avaliar o impacto do desenvolvimento tecnológico na farmacodinâmica.



MICROENCAPSULATION OF NOVEL CHITOSAN-COATED NANOEMULSION FOR HYDROCHLOROTHIAZIDE DELIVERY

Cassiana Mendes^{*a}; Aline Buttchevitz^a, Jéssica Henriques Kruger^a;
Thiago Caon^a; Patricia de Oliveira Benedet^b; Elenara Maria Teixeira
Lemos-Senna^c; Marcos Antônio Segatto Silva^a.

^a Post graduation Program in Pharmaceutical Sciences, Quality
Control Laboratory, Universidade Federal de Santa Catarina, J/K 207,
88040-900, Florianópolis-SC, Brazil. Phone number: +55 (48) 3721-4585;
fax +55 (48) 3721-9350

^b Department of Pharmacology, Universidade Federal de Santa
Catarina, 88.040-900 Florianópolis-SC, Brazil

^c Pharmaceutical Technology Laboratory, Department of
Pharmaceutical Sciences, Federal University of Santa Catarina,
Florianópolis, SC, Brazil.

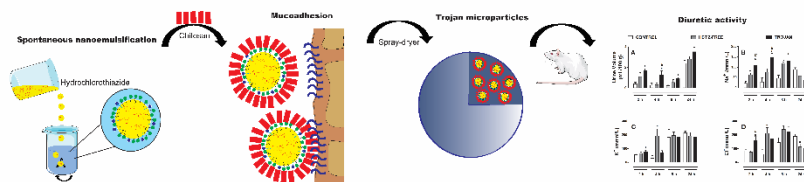
* Corresponding author: Laboratory of Quality Control, Department
of Pharmaceutical Sciences, Federal University of Santa Catarina, J/K 207,
88040-900, Florianópolis, SC, Brazil. Phone number: +55 (48) 3721-4585;
fax +55 (48) 3721-9350. cassi_ana@yahoo.com.br

ABSTRACT

In view of biopharmaceutical limitations of hydrochlorothiazide (HCTZ), Trojan-type mucoadhesive systems were proposed, aiming improve HCTZ pharmacological properties by modulating its release. Nanoemulsions were firstly formed spontaneously by combining medium chain triglycerides, Lipoid® S75 and Pluronic® F68 and high encapsulation efficiency was observed. The mucoadhesive properties were provided by chitosan and microencapsulation of nanoemulsions in spray-dryer was successfully achieved by using Aerosil® as wall material. The rapid redispersion of nanoemulsion in simulated fluids led to a fast and complete release of HCTZ in gastric medium. The pharmacodynamic of HCTZ was improved as biopharmaceutical properties, extending the diuretic activity. Once a simple and low-energy method contributed to obtain stable mucoadhesive nanoemulsions, advantages in terms of production could also be achieved, allowing easy scaling up. This novel mucoadhesive Trojan particulate system of HCTZ showed to be a promising approach to overcome limitations in terms of absorption and consequently improve the therapeutic efficacy.

Keywords: diuretic activity; hydrochlorothiazide; mucoadhesion; nanoemulsion; Trojan system.

GRAPHICAL ABSTRACT



1. BACKGROUND

Over the past few decades, many efforts have been done for developing efficient drug delivery systems when a limited bioavailability is observed. Nanotechnology is a prominent field in the pharmaceutical research for providing unlimited opportunities to release drugs belonging to class II-IV of the Biopharmaceutical Classification System (BCS). Several nanostructured systems have been exploited aiming to improve the biopharmaceutical properties, which also may be used to modulate biodistribution and reduce degradation events [1-5].

Nanoemulsions (NE) represent an advance in therapies of low aqueous solubility drugs and it has been demonstrated very efficient to improve oral bioavailability [1, 6]. The spontaneous nanoemulsification is a low cost technique that employs low energy and once the ideal components are selected, these systems are of easy preparation, manipulation and transposed to industrial scale [7-9].

An innovative technology, which “entraps” nano-oil droplets of NE in a polymer core generating microparticles, has been recently developed by Li and coworkers (2011) [10]. These microparticles are so-called Trojan particles, which could preserve the nano-oil droplets integrity being easily redispersed in aqueous phase, facilitating their handling and use in drug therapy [10]. Bioadhesion is another property that has been exploited to intimate the contact between the biological membrane and the drug, increasing its absorption. Chitosan is the most studied polysaccharide in relation to mucoadhesion properties and also has the ability to open the tight junctions between the intestinal cells, improving the drug absorption [11-14].

Hydrochlorothiazide (HCTZ) is a thiazide-type diuretic belonging to BCS class IV, which is used to treat hypertension. In addition to its low solubility and permeability, HCTZ presents chemical instability since it is susceptible to pH-dependent hydrolysis. Although various approaches have been developed to overcome these limitations over the years [15, 16], the association of Trojan microparticles with mucoadhesion has not yet been exploited. In this context, microencapsulation of chitosan-coated nanoemulsions by using spray-dryer is a promising and innovative approach to explore, pointing towards the production of one system to deliver HCTZ. This study aims the microencapsulation of novel chitosan-coated nanoemulsion produced by spontaneous nanoemulsification for the maintenance of the nanometric oil-droplets loaded in a mucoadhesive polymer to improve HCTZ bioavailability.

2. MATERIALS AND METHODS

2.1 Materials

HCTZ raw material was obtained from Galena (Campinas, Brazil). Olive oil, castor oil and cotton oil, used as excipients in the NE development, were purchased from Sigma Aldrich (St. Louis, USA). The other excipients tested were medium chain triglycerides (MCT) which were acquired from Focus Tecnologia Comercial Química LTDA (São Paulo, Brazil); Lipoid® S75 was obtained from Lipoid GmbH (Germany), Pluronic® F68 from BASF (Germany), Tween 20 (polysorbate 20) and chitosan (medium molar mass CSM 190,000 - 310,000) acquired from Sigma Aldrich (St. Louis, USA). As wall materials, polyvinilic alcohol was obtained from Merck (Germany), maltodextrin from Corn Products, (São Paulo, Brazil), Aerosil® (silicon dioxide) from Colorcon (Cotia, Brazil). Mucin for mucoadhesion experiments was purchased from Sigma Aldrich (St. Louis, USA). All other analytical reagents were of analytical grade.

2.2 Oil solubility studies

The HCTZ equilibrium solubility was established by adding an amount of HCTZ in excess into 5 mL of the different oils (castor oil, olive oil, cotton oil, MCT). The mixtures were magnetically stirred for 24 h at room temperature (25 °C), and after they were centrifuged at 6000 rpm for 5 min. The obtained supernatant was filtered through a membrane filter displaying a pore size of 0.45 µm and diluted with methanol. HCTZ concentration was determined using a previously validated high performance liquid chromatography (HPLC) method (Section 2.8).

2.3 Preparation of nanoemulsions

NE were prepared according to Bouchemal and coworkers, called spontaneous emulsification. HCTZ (10 mg) was dissolved in acetone as the selected oil (200 mg) and the lipophilic surfactant (Lipoid S75), resulting in organic phase (20 mL). The aqueous phase was formed by ultrapure water and the selected hydrophilic surfactant (Pluronic® F68, Tween 20, total volume of 40 mL). Then, the organic phase was injected in the aqueous phase under magnetic stirring and the organic solvent was removed by evaporation under reduced pressure [17]. After NE preparation, the NE was coated with chitosan, as mucoadhesive agent. Chitosan coating was realized by the dispersion of the Chitosan (0 – 0.4% v/v) in an aqueous solution of citric acid 1% (w/v).

The influence of different oils (castor oil, olive oil, cotton oil, MCT), lipophilic and hydrophilic surfactants (Lipoid S75, Pluronic® F68, Tween 20), as their concentrations, in the emulsion size were evaluated.

2.4 Nanoemulsion characterization

2.4.1 Droplet size and zeta potential

The mean droplet size and zeta potential were determined by dynamic light scattering (DLS) and laser-Doppler anemometry, respectively, using a Zetasizer Nano Series (Malvern Instruments, Worcestershire, UK). The NE samples, before and after spray-drying process, were appropriated diluted in distilled water. The size analyses were performed at a scattering angle of 173°. For zeta potential analysis, the samples were placed in electrophoretic cells where a potential of ± 150 mV was applied. The zeta potential values were calculated as mean electrophoretic mobility values by using Smoluchowski's equation.

2.4.2 Entrapment efficiency and HCTZ content

The entrapment efficiency (%) was estimated after the determination of HCTZ total content in NE and in the supernatant obtained after ultrafiltration/centrifugation procedure of the NE using Amicon Centrifugal Filter Devices with Ultracel-100 membrane (100 kDa, Millipore Corp., USA). The entrapment efficiency (%) was expressed as the difference between the HCTZ total content founded in the NE and the HCTZ content founded in the supernatant. The samples concentration was determined by high performance liquid chromatography (HPLC).

The chromatographic analysis was performed in a Shimadzu liquid chromatograph (Shimadzu, Kyoto, Japan) consisting of a LC-10A VP quaternary pump and UV detector set at 270 nm. The chromatographic system was equipped with a Phenomenex® (Torrance, CA, USA) C18 reversed-phase column (150 X 4.6 mm; 5 mm particle size) conditioned in a SPD-10AVP column oven at 40 °C. The column eluted in isocratic mode using a mobile phase consisting of phosphate buffer (25 mM, pH 3.0), acetonitrile and methanol (82:9:9 v/v) at a flow rate of 1.0 mL/min and injection volume of 20 μ L. All methodology was validated according to the International Conference on Harmonization (ICH) by evaluating specificity, linearity, precision, accuracy, robustness, limit of detection and quantification [18]. Validation parameters all were within the acceptable range (unpublished data).

2.5 Microencapsulation of nanoemulsion

The coated NE was mixed with the wall material (maltodextrin, Aerosil®, polyvinyl alcohol) at different proportions and the resultant liquid suspensions was spray-dried in a Mini Spray Dryer (Buchi B-290, Germany) under the following conditions: inlet temperature 160 °C, outlet temperature 120 °C, air flow rate 30 mL/min and atomizing air pressure 1.5 bar.

2.6 Interactions between coated NE and mucin

Mucin from bovine submaxillary glands was diluted in phosphate buffer (pH 6.8) at different concentrations (125 and 250 µg/mL). Coated NE was added to mucin dispersion at different concentrations (0 - 5%), mixed under magnetic stirring for 10 minutes and the interaction effect was evaluated by DLS using a Zetasizer Nano Series as already described.

2.7 NE microencapsulated characterization

2.7.1 Morphology analysis

The morphology of the dry NE was evaluated by scanning electron microscopy (SEM). The photomicrographs of the samples were obtained using a Philips scanning electron microscope, model XL30 (United States). Samples were mounted onto metal stubs using double-side adhesive tape, vacuum-coated with gold (350 Å) in a Polaron E 5000 and directly analyzed by SEM. Particle size was measured by the Size Meter software (version 1.1).

2.7.2 Infrared spectroscopy

The dry NE samples obtained were evaluated by diffuse reflectance Fourier transform infrared spectroscopy (FTIR). The spectra were recorded using a FTIR Frontier (PerkinElmer, Brazil) within a scan range of 600 - 4,000 cm⁻¹, and an average of over 32 scans, at a spectral resolution of 4 cm⁻¹. A background spectrum was obtained for each experimental condition.

2.7.3 Differential scanning calorimetry (DSC)

DSC curves of dry NE samples were obtained on a Shimadzu DSC-60 cell (Kyoto, Japan) using aluminum crucibles with around 2.0 mg of sample. The temperature ranged from 30 to 300 °C, with a heating rate of 10 °C/min, dynamic N₂ atmosphere and flow rate of 50 mL/min.

2.8 In vitro dissolution studies

Dissolution assays were performed using USP apparatus 3 Erweka RRT 10 (Germany). The dissolution was carried out in FaSSGF at pH 1.6 and FaSSIF at pH 6.5, both at 37 °C ± 0.5 °C [19]. Gelatin transparent capsules containing 10 mg of HCTZ or equivalent of NE microencapsulated

were placed into 200 mL of dissolution medium. In the first step of the experiment, the dissolution was performed in FaSSGF (20 dip/min), during 120 min. Aliquots of 5 mL of the medium were withdrawn at intervals of 5, 10, 20, 30, 40, 50, 60, 90 and 120 min. Next, the dissolution medium was changed to FaSSIF, and the dissolution assay was performed during 180 min (15 dip/min). The samples were analyzed by HPLC and curves of percent of HCTZ dissolved versus time were constructed.

2.9 *In vivo* diuretic activity

2.9.1 Animal Welfare and Ethical Statements

The animal protocols used in this study were approved by the University Institutional Ethics Committee (PP00790) in accordance with CONCEA (National Council for the Control of Animal Experimentation) Guidelines. This study was carried out 18 female Wistar rats (weighing 210–250 g). The animals were housed in a temperature ($22 \pm 2^\circ\text{C}$) and light (12 h light/dark cycles) controlled room, with free access to water and food.

2.9.2 Evaluation of diuretic activity

The diuretic activity was determined as previously described [20] with minor modifications. The rats were randomly allocated into the following groups: Group 1 (the control group) was given Trojan formulation; Group 2 (the positive control) received 10 mg/kg of free hydrochlorothiazide and Group 3 received 10 mg/kg of Trojan of hydrochlorothiazide. All formulations were administered to animals by gavage using gelatin capsules (size 9) and a dosing syringe for capsule delivery (Torpac®, Fairfield, NJ). After administration, the animals were placed individually in a metabolic cage for 24 hours, with free access to water and food. Urinary excretion was evaluated at different time points after treatment (2, 4, 8 and 24 h). Cumulative urine excretion was calculated in relation to body weight and expressed as mL/100 g. Electrolyte concentrations (Na^+ , K^+ , and Cl^-) of the urine samples of each rat were also measured, using the ion selective method on a Dade-Behring Dimension RXL analyzer.

2.9.3 Statistical analysis

The results are expressed as mean \pm standard error of mean (S.E.M) of 3-6 animals per group. Statistical analyses were performed using one-way analysis of variance (ANOVA) followed by Tukey's test. P values less than 0.05 were considered statistically significant. The graphs were drawn and the statistical analyses were performed using GraphPad Prism version 6.0 for Windows (GraphPad Software, San Diego, CA, USA).

3. RESULTS

3.1 Nanoemulsion production and optimization

Firstly, the solubility of HCTZ in oils used to prepare NE was evaluated (data not shown). HCTZ was more soluble in MCT, cotton oil, castor oil and olive oil, respectively. These oils were selected to compose the organic phase together with HCTZ and Lipoid® S75 (lipophilic surfactant – 1, 2 or 4 mg/mL), both dissolved in acetone. The aqueous phase was composed by the hydrophilic surfactant (0.5- 1% w/v Tween 20 and 0.25 - 0.5% w/v Pluronic® F68) qsp with ultrapure water to 40 mL. Figure 1 presents the hydrodynamic diameter of all the formulations evaluated.

Formulations containing castor oil, Lipoid® S75 and Pluronic® F68 showed smaller size when the concentration of Lipoid® S75 is increased and the concentration of Pluronic® F68 is decreased. For this surfactant combination, the formulation with smaller size presented 215.4 nm and PDI value of 0.119. The HCTZ total content was also evaluated, which was maintained close to 95%. When the hydrophilic surfactant of castor oil formulation was change to Tween 20 (HLB 16.7), it resulted in a formulation with the smaller HLB and particle size (212.8 nm).

In the case of cotton oil, formulations containing 4 mg/mL of Lipoid® S75 and 0.25% of Pluronic® F68 presented smaller HLB value (15.4) as well as mean diameter size (254.8 nm, PDI 0.363). When Tween was used, there is no better nanoemulsify effect with this oil. In addition to that, lower content of HCTZ was founded (mean of 70%). For the olive oil, NE presenting large size and distribution of particles was observed (PDI > 0.3). This oil was not effective to maintain the HCTZ content.

Transparent NE may be obtained by using MCT as carrier oil containing fine droplets. Narrow distribution size was achieved by combining Lipoid® S75 at high concentrations and Pluronic® F68 or Tween 20. When Lipoid® S75 was used at 4 mg/mL, both hydrophilic surfactants were able to produce NE with reduced mean size (around 200 nm). Therefore, the MCT-based formulation containing, respectively, 4 mg/mL and 0.5% of Lipoid® S75 and Pluronic® F68 was selected due to higher total content of HCTZ (97%), lower size and polydispersity (208.3 nm, PDI 0.092).

3.2 Chitosan coating

Different chitosan concentration was added after the NE preparation aiming the coating and the results are expressed in Table 1.

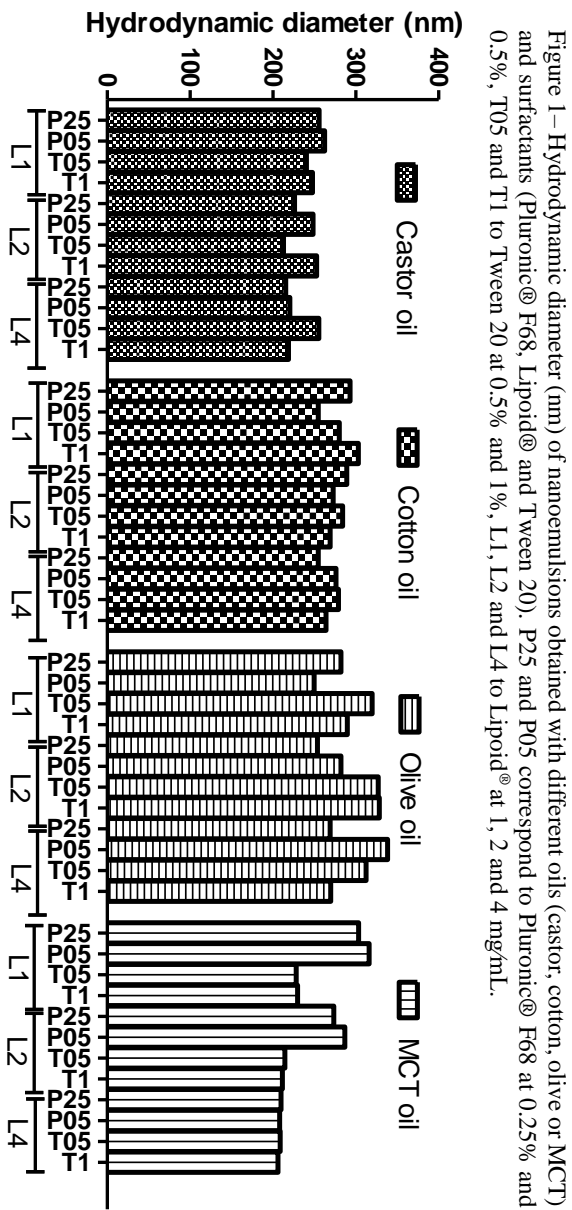


Table 1. Hydrodynamic diameter and polydispersity index (PDI) of HCTZ-loaded NE after chitosan coating.

Chitosan added (%)	Hydrodynamic diameter (nm)	PDI	Zeta potential (mV)	HCTZ total content	HCTZ loaded
0	228.5	0.086	-32.2	100.3	95.4
0.01	234.8	0.065	16.9	99.2	93.5
0.02	242.4	0.157	17.9	98.3	90.6
0.03	236.9	0.127	17.2	98.7	90.3

The hydrodynamic radius was minimally increased after the chitosan coating, forming a thin coating layer. No influence of chitosan concentrations was observed in the hydrodynamic diameter. The zeta potential of uncoated NE revealed a high negative value. Different concentrations of chitosan were added to coat the oil-droplets of NE and 0.01% of this polymer was enough to successfully coat and change the particle charge. High concentrations of chitosan did not change the hydrodynamic diameter neither the zeta potential. Both parameters tend to a plateau after the addition of chitosan, suggesting a strong interaction between chitosan and NE. Therefore, the chitosan concentration of 0.01% was selected to coat the HCTZ-loaded NE and this formulation was selected to continue the study.

3.3 Microencapsulation of nanoemulsion

The spray-drying technique was used to produce dried microparticles of coated NE. Several wall materials able to entrap the oily droplets were tested. A dispersion of the NE in the aqueous phase containing the wall material 2.5 wt.% was considered during the processing in spray-dryer. An extend analysis from the literature was made in order to evaluate the characteristics of wall materials usually applied. As wall material, maltodextrin, Aerosil® and polyvinyl alcohol were selected. The concentration of wall material was defined by considering solubility aspects and therapeutic concentration [21, 22].

Once a very low yield was obtained for polyvinyl alcohol, this wall material was discarded. The Table 2 presents the size distribution of the coated NE and the wall material at different proportions before and after processing by spray-drying. Maltodextrin also demonstrated a low yield, and thus only one proportion of this polymer was used.

When NE before and after spray-drying were compared an increase in the oil droplet size with a wider distribution was observed. The type of wall materials did not present significant effect on the particle size after

redispersion. Take into account all the results presented, the formulations F1, F2 and F3 were selected for the next steps.

Table 2. Nanoemulsion size distribution, after preparation (raw nanoemulsion), mixed with wall material before spray-drying (NE + WM before spray-drying), and mixed with wall material after spray-drying and resuspended in the same volume of water.

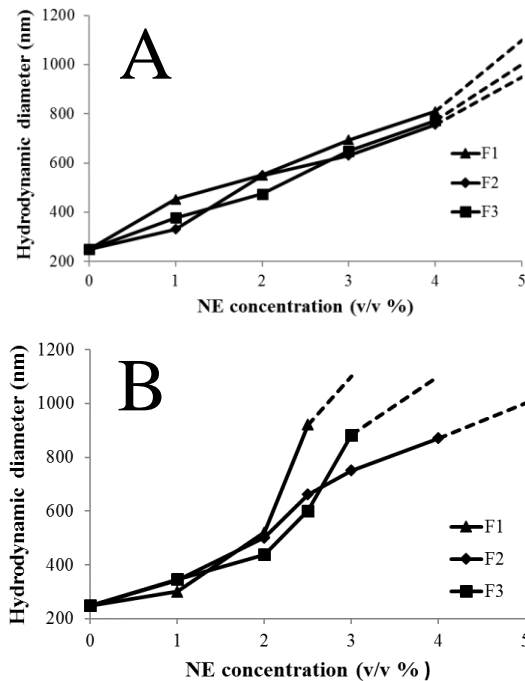
Wall Material	Yield (%)	Raw nanoemulsion		NE + WM before spray-drying		NE + WM after spray-drying	
		D (nm)	PDI	D (nm)	PDI	D (nm)	PDI
F1 - Aerosil [®]	93	228.5	0.086	230.1	0.092	266.2	0.227
F2 - MAL:AER 1:1 (w/w)	72			236.6	0.105	273.3	0.248
F3 - MAL:AER 1:2 (w/w)	83			233.2	0.061	267.8	0.229
F4 - MAL:AER 1:4 (w/w)	70			231.1	0.094	295.3	0.281
F5 - Maltodextrin	45			234.5	0.137	271.9	0.294

MAL: Maltodextrin; AER: Aerosil[®].

3.4 Interactions between coated NE and mucin

The mucoadhesion was evaluated between the coated NE and mucin. The hydrodynamic diameter formed between increasing concentrations of the three coated NE (F1, F2 and F3) and two different mucin concentrations is presented in Figure 2. The mucin colloidal dispersion alone presented a main hydrodynamic radius of 250 nm. The addition of the chitosan-coated NE on mucin dispersion at 125 and 250 $\mu\text{g/mL}$ increased the hydrodynamic diameter to 800 and 900 nm, respectively. The systems undergo a progressive precipitation due to the aggregates formation at 125 $\mu\text{g/mL}$ of mucin (Figure 2A) and NE concentrations higher than 4% (V/V). The formulations were better discriminated at 250 $\mu\text{g/mL}$ of mucin (Figure 2B). F1 aggregates at lower concentrations, followed by F3 and F2, respectively. Overall, F1 showed stronger mucoadhesion properties compared to other formulations.

Figure 2– Hydrodynamic diameter variation (nm) of the mucin colloidal system at 125 $\mu\text{g/mL}$ (A) or 250 $\mu\text{g/mL}$ (B) as a function of added chitosan coated NE (% , v/v).



3.6 Solid analysis

3.6.1 Morphology analysis

For scanning electron microscopy (SEM) analyses, wall materials were firstly spray-dried individually in order to verify the influence of the polymer or its mixture in shape, size and polydispersity. To prepare microparticles containing NE, HCTZ-NE was dispersed in an aqueous solution of wall material to a final concentration of 2% of HCTZ (w/w drug:wall material) and 2.5 wt.% of wall material (wV wall material:aqueous medium). Photomicrographs of pure wall materials and the resultant microparticles of coated-NE entrapped in the wall material are shown in Figure 3.

Aerosil® pure at 2.5 wt.% used to prepare F1 displayed large size dispersity and medium particle diameter of 18 μm , while F1 demonstrated a medium size of 7 μm with more regular spherical geometry. NE droplets filled the entire core, generating a massive spherical microparticle. Although a very well defined structure was not observed by the physical combination of Aerosil® and maltodextrin (Figure 3C and 3E), the mixture of two different polymers is clear. The diameter of the wall material mixtures was higher than Aerosil® alone, presenting a size of 26 μm and large polydispersity. F2 and F3 (Figure 3D, F) revealed two different microparticle populations, which presented a mean diameter of 12 and 26 μm , respectively.

3.6.2 Differential scanning calorimetry (DSC)

Binary mixtures of excipients or microparticles containing NE were assayed by DSC and the results are expressed in Figure 4. HCTZ curve (A) presented an endothermic event at 265.2 °C ($\Delta H=124.37$ J/g), which may be attributed to melting of the drug. Aerosil® did not display any thermal event in the temperature range evaluated (B), corroborating with its non-crystalline nature. In the physical mixture with HCTZ (C), only the endothermic event of HCTZ was observed. The DSC curve of maltodextrin (D) revealed the degradation that begins after 220 °C without melting [23]. Thermal events in the physical mixtures of HCTZ and maltodextrin (E) due to the polymer decomposition were not identified and a possible interaction between these two constituents should be verified by other technique. For all formulations (F-K), DSC curves did not change from unloaded microencapsulated NE formulation to HCTZ-loaded, evidencing the absence of crystalline HCTZ at least at the particle surface level.

Figure 3– Photomicrographs of the powders of spray-dried pure wall materials (scale bar 100 μm) and NE microencapsulated with the respective wall material (scale bar 30 μm): (A) Aerosil[®], (B) F1 (microencapsulated NE Aerosil[®]), (C) Maltodextrin: Aerosil[®] 1:1 w, (D) F2 (microencapsulated NE Maltodextrin: Aerosil[®] 1:1 w/w), (E) Maltodextrin: Aerosil[®] 1:2 w/w, (F) F3 (microencapsulated NE Maltodextrin: Aerosil[®] 1:2 w/w).

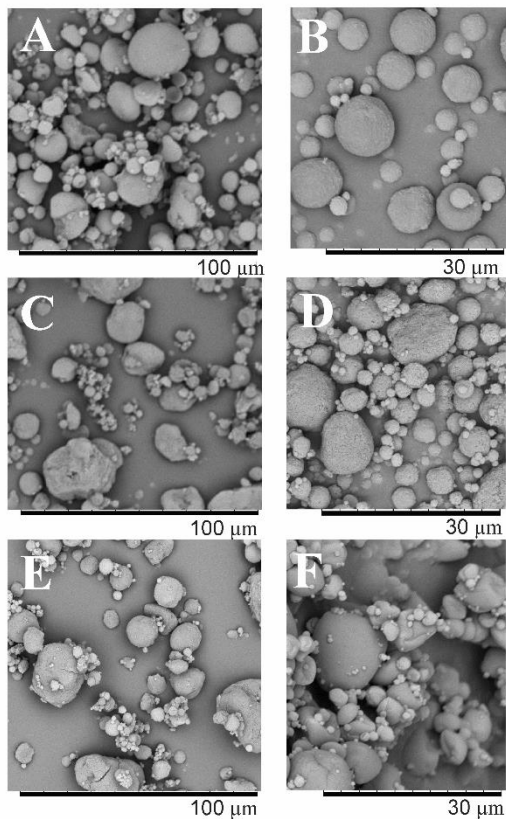
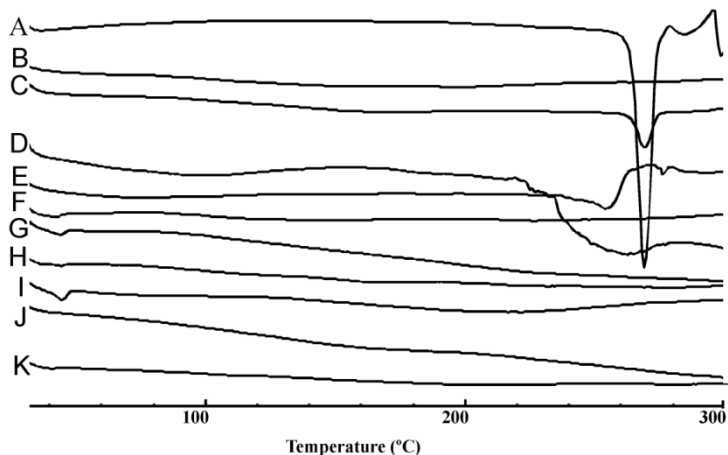


Figure 4 – DSC curves obtained to HCTZ (A), Aerosil® (B), HCTZ:Aerosil® (1:1 w/w) (C), maltodextrin (D), HCTZ:maltodextrin (1:1 w/w) (E), F1 HCTZ-loaded (F) F1 unloaded (G), F2 HCTZ-loaded (H), F2 unloaded (I), F3 HCTZ-loaded (J), F3 HCTZ unloaded (K).

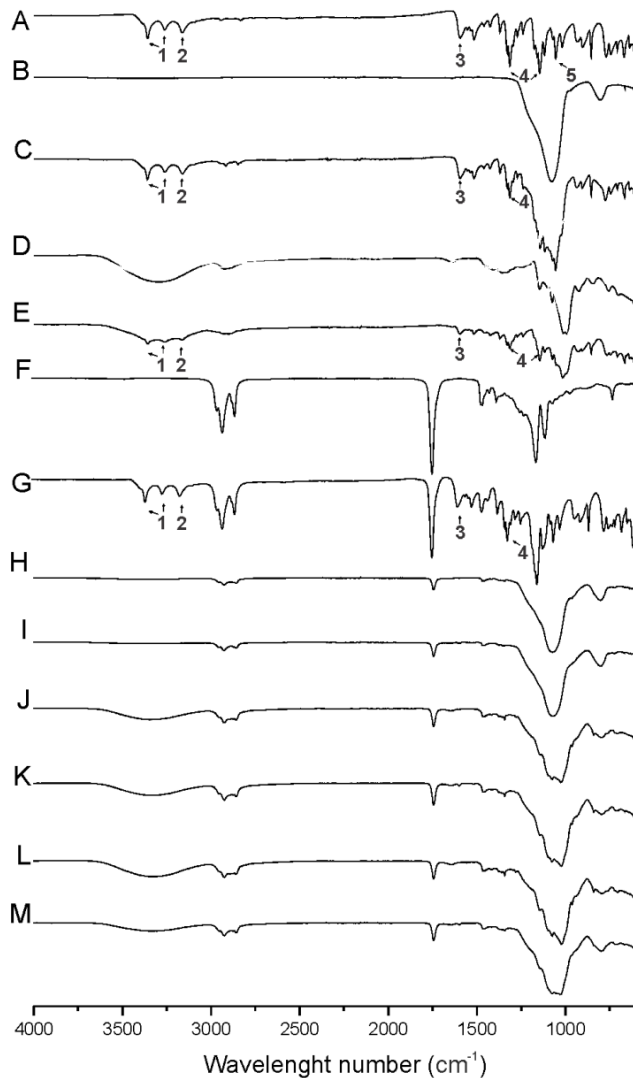


3.6.3 Infrared spectroscopy

The Figure 5 presents infrared spectrum data of HCTZ or excipients alone, their mixtures and NE formulations. HCTZ displayed characteristic bands denoted by Arabic numbers (Figure 5A), that could be also identified in the spectra of physical mixtures with excipients.

The characteristic band at $1,741\text{ cm}^{-1}$ due to the presence of carbonyl groups and the asymmetric and symmetric methylene vibrations at $2,924$ and $2,950\text{ cm}^{-1}$ presented in MCT can be observed for all formulations (Figure 5H-M). Aerosil® (SiO_2) as amorphous structure reveals stretching vibrations at 800 and $1,100\text{ cm}^{-1}$ (Figure 5B), which were also easily observed in the F1 (Figure 5H, I) given that this polymer was used alone as wall material in this formulation. For F2 and F3 (Figure 5J-M) characteristic bands of Aerosil® as well as OH and C-O stretching vibrations ($3,400$ and $980 - 1200\text{ cm}^{-1}$, respectively) of maltodextrin were identified.

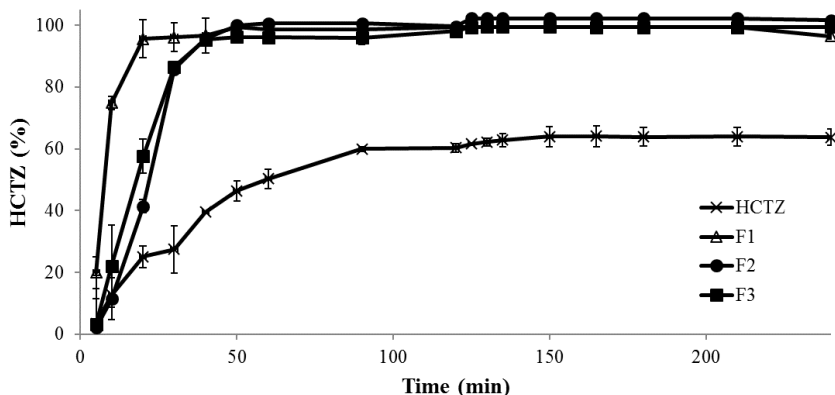
Figure 5 – FTIR spectrum of HCTZ (A), Aerosil® (B), HCTZ:Aerosil® (1:1 w/w) (C), maltodextrin (D), HCTZ:maltodextrin (1:1 w/w) (E), MCT (F), HCTZ:MCT (1:1 w/w) (G), F1 unloaded (H), F1 HCTZ-loaded (I), F2 unloaded (J), F2 HCTZ-loaded (K), F3 HCTZ unloaded (L), F3 HCTZ-loaded (M).



3.7 In vitro release profile

Figure 6 shows the dissolution profile of F1, F2 and F3. Formulations were completely released in gastric medium before 40 min, while assays performed to free drug released only 40% at the same time. F1 provided a faster drug release (100% after 30 min). In view of performance of F1 in the dissolution assay, the mucoadhesive property and yield, this formulation was selected for pharmacodynamic evaluation.

Figure 6 - Dissolution profile of HCTZ (A) and NE microencapsulated systems: F1 (B) F2 (C) and F3 (D) obtained in FASSGF (pH 1.6) during 120 min and in FASSIF (pH 6.5) for more 180 min.

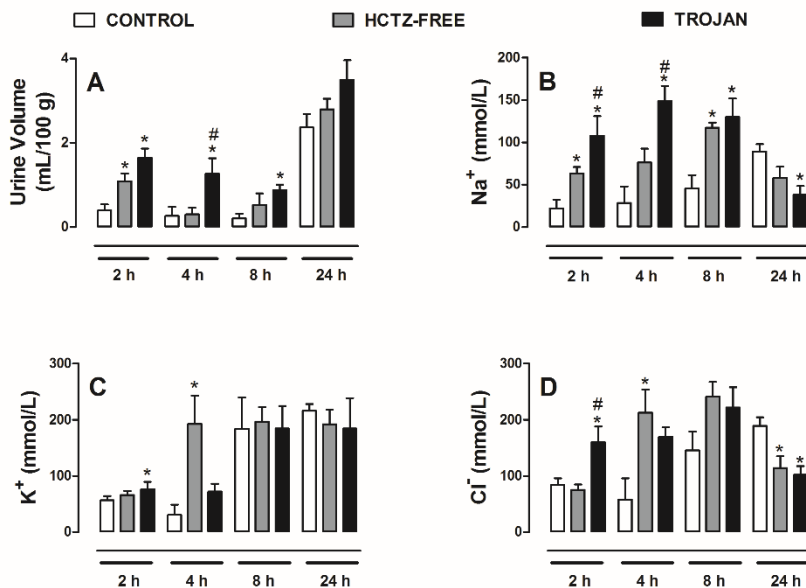


3.8 In vivo diuretic activity

The diuretic activity of free drug was compared to that of Trojan system. Urinary volume was analyzed 2, 4, 8 and 24 h after treatment and Na^+ , K^+ and Cl^- were quantified (Figure 7).

Rats treated with Trojan microparticles demonstrated a significant increase in urinary diuresis at all times. Urinary excretion of Trojan system was higher than free HCTZ group until 8h after treatment. Moreover, results also showed that the diuretic activity induced by Trojan was kept for a long time period (Figure 7, Panel A). Trojan also led to an increased natriuresis and chlориuresis when compared to HCTZ-free group (Figure 7, Panel B, and D). This formulation increased the urinary excretion of Na^+ at all times, K^+ and Cl^- (Figure 7, Panel B, C, D) at 2 and 4 h after treatment, respectively.

Figure 7– Effects of acute oral treatment of Trojan on urine output (Panel A) and electrolyte excretion (Panel B, C, D). The graphs show the urinary volume (A), concentration of Na⁺ K⁺ Cl⁻ (B, C and D, respectively) in urine samples collected 2, 4, 8 and 24 h after the treatment. The results show the mean \pm S.E.M of 3-6 animals per group. One-way analysis of variance (ANOVA) followed by Tukey post-test was used for statistical analysis. * $P < 0.05$; when compared with the control group and # $P < 0.05$ significantly different from corresponding Trojan-HCTZ group.



4. DISCUSSION

4.1 Nanoemulsion formulation and optimization

Solubility in the oil is crucial to maintenance of the drug in the oil phase. Oils able to increase the solubilization of HCTZ were selected to compose the organic phase together with HCTZ and Lipoid® S75 both dissolved in acetone. This solvent was selected because HCTZ is soluble and the experimental solubility founded was 0.7 mg/mL. The hydrophilic surfactants, as Tween 20 or Pluronic® F68, presenting non-ionic nature are characterized by low toxicity and irritation potential compared to ionic surfactants after an oral administration [24].

Formulations containing castor oil, Lipoid® S75 (HLB 7) [17, 20, 25] and Tween 20 (HLB 16.7), the HLB of the final mixture decreased in comparison to Pluronic® F68 (HLB 29), which is closer to the value desirable to this oil (HLB of 14) [26]. This fact resulted in a formulation with

the smaller HLB and particle size (212.8 nm), which may be associated with an efficient emulsification of oil droplets.

In the case of cotton oil, low HLB value is required (HLB 10). As expected, formulations containing 4 mg/mL of Lipoid® S75 and 0.25% of Pluronic® F68 presented smaller HLB value (15.4) as well as mean diameter size. On the other hand, the HLB generated by this combination was not enough for the complete nanoemulsification, which explain the polydispersity.

For the olive oil, it was not effective to maintain the HCTZ content, which could be associated with solubility of HCTZ in olive oil. The large oil droplets obtained with this oil could be attributed to emulsion instability caused by Ostwald ripening and/or the phenomena of coalescence [26].

The type of oily carrier is critical for the spontaneous formation of fine oil droplets as well as the surfactant combination. When Lipoid® S75 was used at 4 mg/mL with MCT, both hydrophilic surfactants were able to produce NE with reduced mean size probably due to the proximity between the HLB values (HLB 11). Higher surfactant concentrations at the oil-water boundary could produce a reduction in the interfacial tension and consecutively an interface able to generate fine oil droplets spontaneously.

Aiming to improve the biopharmaceutical properties of HCTZ, the optimized NE developed was coated with mucoadhesive polymer to extend the contact with the mucosa. Chitosan is a biocompatible and biodegradable polymer that interacts with the intestinal membrane by electrostatic interactions. The chitosan bioadhesion is very-well reported in the literature as positive charges available in chitosan able to interact with the negatively charged mucosal surface [27-29]. This mucoadhesion could extend the contact between the NE with the intestinal mucous, facilitating the absorption.

The high negative value of zeta potential of uncoated NE ensures the stability of the NE formed due to the electrostatic repulsion of colloidal particles. The negative charges could be attributed to the phosphatidic acid present in the anionic-type surfactant (Lipoid® S75 - soybean lecithin). The adsorption of chitosan molecules in the external layer of the NE is probably related to hydrogen bonds between ether of polaxamer and amino groups of chitosan. The interaction between polaxamer and chitosan has already been reported in other studies [23, 27, 29].

4.2 Trojan microparticles

After the addition of water to the Trojan microparticles, the wall material rapidly solubilizes and occurs the redispersion of the oil droplets from the entrapped NE. The increased particle size after the spray-drying

process could be explained by oil droplet coalescence or even by the turbulence and heat during the spray-drying process, as already described by Li and coworkers [10]. This study showed that the NE could be efficiently microencapsulated and conserves the nanosize after redispersion of the dried powder in water.

Epithelial cells of the gastrointestinal tract present residues of proteins and active ion pumps that generate negative charges in the surface. Mucoadhesion is mediated by electrostatic interactions of the positively charged chitosan amino bounds and negatively charged mucin on the mucosal surface [30]. The difference in wall material probably leads to a redispersion more rapid of F1, enabling that the mucoadhesive NE from F1 aggregates faster in contact with mucin in comparison to other formulations.

In the SEM analyses, smaller microparticles were obtained when Aerosil® was used separately as coating material. The hypothesis to explain this fact is the capability of the nanoemulsion to entrap in the water/air interface and consequently reduces the interfacial tension giving rise to smaller particles, as proposed by Li and co-authors in the first Trojan study [10].

The DSC and IR analysis demonstrated that HCTZ showed to be compatible with tested excipients, which allows their use for NE microencapsulation. These techniques suggest that HCTZ is loaded in the microencapsulated NE system due to the absence of HCTZ thermal event or characteristic bands, which is in agreement with the entrapment efficiency.

Dissolution studies were performed in USP apparatus 3 by using simulated gastric and intestinal fluid (FASSGF and FASSIF) to mimic the physiological conditions once no dissolution profiles for Trojan systems were found in the literature.

Shape and size of microencapsulated NE due to the wall material explain the differences in dissolution profiles of the formulations. As observed in SEM analysis, F1 presented small microparticles with more regular shape, which would contribute to improve wettability, providing a rapid solubilization of wall material and consequently release of HCTZ from NE by lipid digestion. HCTZ released from NE could precipitate or dissolve into the simulated gastric medium and resolubilize as micelles by emulsification in biliary salts presented in FASSGF [31]. For oral lipid-based systems, the uses of simulated media are essential to predict human digestion processes after oral administration. Once F1 provided the faster drug release, this formulation was selected for pharmacodynamic evaluation.

The *in vivo* performance of Trojan microparticles is a consequence of the fast solubilization of the wall material, NE redispersion and the rapid

release profile observed in dissolution when simulated fluids were used. Once HCTZ is completely release in the gastric medium and absorbed in small intestine, pharmacodynamic effects are expected at early stages. The mucoadhesive characteristic probably increase the contact time between NE and intestinal epithelial cells, extending the absorption of the HCTZ. Furthermore, the Pluronic® F68 used in the NE formulation could inhibit the activity of intestinal efflux transporter such as BCRP (breast cancer resistance protein), responsible for HCTZ efflux [28, 32]. This efflux inhibition could increase the drug absorption and consequently the therapeutic efficiency. The *in vivo* diuretic activity suggests that a single dose of this formulation enhances pharmacological effect of HCTZ and it will be probably related with increased bioavailability of HCTZ.

Overall, the microencapsulation of NE was successfully achieved and a rapid redispersion was obtained after contact with dissolution medium. The Trojan microparticles presented high entrapment efficiency, release and mucoadhesive properties that justify the increase in pharmacodynamic activity of HCTZ. This system could in fact be used as NE carrier leading easy manipulation and administration at required concentration to therapeutic dose. Furthermore, the developed formulation with improved pharmacodynamic effect represents a promising carrier to circumvent the HCTZ bioavailability limitations.

ACKNOWLEDGMENTS

The authors would like to thank LCME/UFSC for technical support during microscopy analysis, Flora Lucena Sant'ana for her skillful assistance with the *in vivo* studies and Dr. José Eduardo da Silva Santos, who kindly allowed the use of the metabolic cages. This study was supported by the National Counsel of Technological and Scientific Development (CNPq) and Coordination for Enhancement of Higher Education Personnel (CAPES).

REFERENCES

- [1] A.A. Date, N. Desai, R. Dixit, M. Nagarsenker, Self-nanoemulsifying drug delivery systems: formulation insights, applications and advances, *Nanomedicine*, 5 (2010) 1595-1616.
- [2] N. Anton, J.-P. Benoit, P. Saulnier, Design and production of nanoparticles formulated from nano-emulsion templates—a review, *Journal of Controlled Release*, 128 (2008) 185-199.
- [3] M.M. Issa, M. Köping-Höggard, P. Artursson, Chitosan and the mucosal delivery of biotechnology drugs, *Drug Discovery Today: Technologies*, 2 (2005) 1-6.

- [4] C. Prego, M. Garcia, D. Torres, M. Alonso, Transmucosal macromolecular drug delivery, *Journal of Controlled Release*, 101 (2005) 151-162.
- [5] C. Prego, D. Torres, M. Alonso, Chitosan nanocapsules as carriers for oral peptide delivery: effect of chitosan molecular weight and type of salt on the *in vitro* behaviour and *in vivo* effectiveness, *Journal of nanoscience and nanotechnology*, 6 (2006) 9-10.
- [6] F.S. Nielsen, E. Gibault, H. Ljusberg-Wahren, L. Arleth, J.S. Pedersen, A. Müllertz, Characterization of prototype self-nanoemulsifying formulations of lipophilic compounds, *Journal of pharmaceutical sciences*, 96 (2007) 876-892.
- [7] J.-Y. Hong, J.-K. Kim, Y.-K. Song, J.-S. Park, C.-K. Kim, A new self-emulsifying formulation of itraconazole with improved dissolution and oral absorption, *Journal of Controlled Release*, 110 (2006) 332-338.
- [8] R.N. Gursoy, S. Benita, Self-emulsifying drug delivery systems (SEDDS) for improved oral delivery of lipophilic drugs, *Biomedicine & Pharmacotherapy*, 58 (2004) 173-182.
- [9] Y. Zhao, C. Wang, A.H. Chow, K. Ren, T. Gong, Z. Zhang, Y. Zheng, Self-nanoemulsifying drug delivery system (SNEDDS) for oral delivery of Zedoary essential oil: formulation and bioavailability studies, *International journal of pharmaceutics*, 383 (2010) 170-177.
- [10] X. Li, N. Anton, T.M.C. Ta, M. Zhao, N. Messaddeq, T.F. Vandamme, Microencapsulation of nanoemulsions: novel Trojan particles for bioactive lipid molecule delivery, *International journal of nanomedicine*, 6 (2011) 1313 - 1325.
- [11] J.D. Smart, The basics and underlying mechanisms of mucoadhesion, *Advanced Drug Delivery Reviews*, 57 (2005) 1556-1568.
- [12] K.P.R. Chowdary, Y. Srinivasa Rao, Mucoadhesive microspheres for controlled drug delivery, *Biological and pharmaceutical Bulletin*, 27 (2004) 1717-1724.
- [13] S.B. Patil, K.K. Sawant, Mucoadhesive microspheres: a promising tool in drug delivery, *Current drug delivery*, 5 (2008) 312-318.
- [14] G.P. Andrews, T.P. Lavery, D.S. Jones, Mucoadhesive polymeric platforms for controlled drug delivery, *European Journal of Pharmaceutics and Biopharmaceutics*, 71 (2009) 505-518.
- [15] Y. Kadam, U. Yerramilli, A. Bahadur, P. Bahadur, Micelles from PEO–PPO–PEO block copolymers as nanocontainers for solubilization of a poorly water soluble drug hydrochlorothiazide, *Colloids and Surfaces B: Biointerfaces*, 83 (2011) 49-57.
- [16] R. Chadha, S. Bhandari, D. Kataria, S. Gupta, D. Singh Jain, Exploring the potential of lecithin/chitosan nanoparticles in enhancement of

antihypertensive efficacy of hydrochlorothiazide, *Journal of microencapsulation*, 29 (2012) 805-812.

[17] K. Bouchemal, S. Brianc¸on, E. Perrier, H. Fessi, Nano-emulsion formulation using spontaneous emulsification: solvent, oil and surfactant optimisation, *International journal of pharmaceutics*, 280 (2004) 241-251.

[18] ICH, *Validation of Analytical Procedures: Text and Methodology Q2 (R1)*, Geneva, 2005.

[19] E. Jantratid, N. Janssen, C. Reppas, J.B. Dressman, Dissolution media simulating conditions in the proximal human gastrointestinal tract: an update, *Pharmaceutical research*, 25 (2008) 1663-1676.

[20] S. Kau, J. Keddie, D. Andrews, A method for screening diuretic agents in the rat, *Journal of pharmacological methods*, 11 (1984) 67-75.

[21] L.H. Reddy, J.L. Arias, J. Nicolas, P. Couvreur, Magnetic nanoparticles: design and characterization, toxicity and biocompatibility, pharmaceutical and biomedical applications, *Chemical reviews*, 112 (2012) 5818-5878.

[22] J.L. Arias, M.A. Ruiz, V. Gallardo, Á.V. Delgado, Tegafur loading and release properties of magnetite/poly (alkylcyanoacrylate)(core/shell) nanoparticles, *Journal of Controlled Release*, 125 (2008) 50-58.

[23] L. Mazzarino, C. Travelet, S. Ortega-Murillo, I. Otsuka, I. Pignot-Paintrand, E. Lemos-Senna, R. Borsali, Elaboration of chitosan-coated nanoparticles loaded with curcumin for mucoadhesive applications, *Journal of colloid and interface science*, 370 (2012) 58-66.

[24] D.J. McClements, J. Rao, Food-grade nanoemulsions: formulation, fabrication, properties, performance, biological fate, and potential toxicity, *Critical reviews in food science and nutrition*, 51 (2011) 285-330.

[25] J.F. Figueiro, T. Andreani, M.A. Egea, M.L. Garcia, S.B. Souto, A.M. Silva, E.B. Souto, Design of cationic lipid nanoparticles for ocular delivery: Development, characterization and cytotoxicity, *Int J Pharm*, 461 (2014) 64-73.

[26] Y. Chang, D.J. McClements, Optimization of orange oil nanoemulsion formation by isothermal low-energy methods: influence of the oil phase, surfactant, and temperature, *Journal of agricultural and food chemistry*, 62 (2014) 2306-2312.

[27] P. Calvo, J.L. Vila-Jato, M.a.J. Alonso, Evaluation of cationic polymer-coated nanocapsules as ocular drug carriers, *International Journal of Pharmaceutics*, 153 (1997) 41-50.

[28] D.Y. Alakhova, A.V. Kabanov, Pluronic and MDR reversal: an update, *Molecular pharmaceutics*, 11 (2014) 2566-2578.

[29] E. Sashina, A. Vnuchkin, N. Novoselov, A study of the thermodynamics of chitosan interaction with polyvinyl alcohol and polyethylene oxide by

differential scanning calorimetry, Russian journal of applied chemistry, 79 (2006) 1643-1646.

[30] I. Bravo-Osuna, C. Vauthier, A. Farabollini, G.F. Palmieri, G. Ponchel, Mucoadhesion mechanism of chitosan and thiolated chitosan-poly (isobutyl cyanoacrylate) core-shell nanoparticles, Biomaterials, 28 (2007) 2233-2243.

[31] S. Chakraborty, D. Shukla, B. Mishra, S. Singh, Lipid—an emerging platform for oral delivery of drugs with poor bioavailability, European Journal of Pharmaceutics and Biopharmaceutics, 73 (2009) 1-15.

[32] V. Grabovac, A. Bernkop-Schnürch, Improvement of the intestinal membrane permeability of low molecular weight heparin by complexation with stem bromelain, International journal of pharmaceutics, 326 (2006) 153-159.

CAPÍTULO 4 - DETERMINAÇÃO DOS FATORES DE PERMEABILIDADE INTESTINAL DO NORFLOXACINO EM MODELO DE CÂMARA DE USSING. ARTIGO SUBMETIDO PARA O PERIÓDICO *MOLECULAR PHARMACEUTICS*

INTRODUÇÃO

A administração oral de fármacos é a via de administração mais comum devido à sua simplicidade, conveniência e baixo custo. A absorção oral de fármacos vai depender de dois fatores principais, a solubilidade do fármaco e sua permeabilidade gastrointestinal. Transportadores de influxo e de efluxo localizado na membrana dos enterócitos desempenham papel fundamental na permeabilidade intestinal de fármacos. A biodisponibilidade será a resposta de ambos transportadores, juntamente com a difusão passiva, o transporte paracelular e o metabolismo. Desde a descoberta da glicoproteína-P em 1976 (P-gp), os transportadores intestinais têm sido amplamente estudados devido à sua influência na farmacocinética e nas interações fármaco-fármaco (Shugarts e Benet, 2009; Estudante *et al.*, 2013).

As quinolonas constituem uma das classes de antimicrobianos mais prescritas no mundo devido à sua alta atividade antibacteriana de amplo espectro de ação utilizadas para uma grande variedade de doenças infecciosas. O ácido nalidíxico é o membro fundador desta classe, isolado primeiramente em 1962, e em 1980 a porção fluorina foi adicionada às quinolonas originando as fluorquinolonas, um avanço terapêutico com ampla atividade antimicrobiana após administração oral (Aldred *et al.*, 2014). O NFX é uma fluorquinolona pertencente à classe biofarmacêutica IV, ou seja, de baixa solubilidade e baixa permeabilidade. Após administração oral da dose de 400 mg, aproximadamente 30 a 40% é absorvida. Devido à baixa biodisponibilidade oral, altas doses são necessárias para o tratamento com este fármaco (Bolon, 2009; Breda *et al.*, 2009; Cheng *et al.*, 2013).

Os transportadores dependentes de adenosina trifosfato (ATP) localizados na membrana dos enterócitos podem facilitar a absorção dos fármacos ou ainda impedir sua absorção por meio do efluxo intestinal. As fluorquinolonas têm sido descritas como um grupo capaz de sofrer efluxo intestinal dos fármacos, o que ajuda a explicar a baixa biodisponibilidade destes compostos. Dados da literatura sugerem que estes medicamentos podem sofrer eliminação transintestinal por meio de um transportador ABC, a P-glicoproteína, que pode estar envolvida na secreção transepitelial do ciprofloxacino e do ofloxacino. Existem ainda relatos na literatura que sugerem também o efluxo ativo intestinal do NFX por meio de transportadores de ânions orgânicos (Cao *et al.*, 1992; Rabbaa *et al.*, 1996; Alvarez *et al.*, 2008).

Neste contexto, este capítulo apresenta o estudo de determinação dos fatores de permeabilidade intestinal do NFX. De acordo com o recente levantamento bibliográfico, não existem trabalhos com este enfoque na literatura e são apenas sugeridos os mecanismos de efluxo que o NFX pode

sofrer. Este estudo foi realizado durante estágio sanduíche na Université Paris-Sud sob a supervisão do professor Dr. Gilles Ponchel. A equipe da França é referência em estudos de melhoria da passagem de moléculas ativas através de barreiras biológicas, principalmente a gastrointestinal. O grupo de pesquisa possui ampla experiência na utilização de câmaras de Ussing, utilizadas para avaliação da permeabilidade intestinal. O grupo visa aprofundar o conhecimento no funcionamento destas barreiras como chave para a concepção racional de novos sistemas de administração de fármacos mais eficazes e capazes de diminuir os efeitos indesejáveis. Com a avaliação dos mecanismos de permeabilidade do NFX, será possível delinear uma formulação estrategicamente planejada e direcionada para os problemas biofarmacêuticos do NFX.

INTESTINAL PERMEABILITY DETERMINANTS OF NORFLOXACIN
IN USSING CHAMBER MODEL

*Cassiana Mendes^{*a,b}; Gabriela C. Meirelles^a; Marcos A. S. Silva^b, Gilles
Ponchel^a*

^a CNRS UMR 8612, Université de Paris Sud XI, Faculté de Pharmacie, 5
rue J.B. Clément, 92296 Châtenay-Malabry, France

^b Post graduation Program in Pharmaceutical Sciences, Quality Control
Laboratory, Universidade Federal de Santa Catarina, J/K 207, 88040-900,
Florianópolis-SC, Brazil. Phone number: +55 (48) 3721-4585; fax +55 (48)
3721-9350

KEYWORDS

Efflux, intestinal permeability, norfloxacin, transporter, uptake, Ussing chamber.

ABSTRACT

Recently, many efforts are taken to identify the intestinal uptake and efflux transporters since they are responsible for the absorption of many drugs as their interactions. Norfloxacin (NFX) is a fluoroquinolone that presents low solubility and low permeability, and as a consequence, low bioavailability. In this context, the aim of this study is evaluate for the first time the intestinal permeability mechanisms of NFX by Ussing chamber model. The low permeation of NFX at low temperature, where the efflux pumps are not active, reveals that NFX permeation is transporter-dependent. The permeation study at different level of intestine demonstrated that NFX passage is in the crescent order: ileum > jejunum > duodenum > colon, probably attributed to transporters that are expressed differently along the intestinal tract. NFX intestinal flow was evaluated in the presence of many inhibitors and substrates to identify the uptake and efflux transporters implicate in NFX permeability mechanism. It could be observed that BCRP and MRPs are involved in the NFX efflux and PEPT1, PMAT and OCT in the NFX uptake transport. Furthermore, this work revealed that NFX has itself an affinity for OCTN and OATP, demonstrating that NFX could inhibit these transporters and influence the absorption of other drugs. The updated description of NFX intestinal permeability factors could contribute to the development of rational pharmaceutical formulations that could circumvent the efflux problems and consequently improve NFX biopharmaceutical properties and avoid drug-drug interactions.

INTRODUCTION

Oral route is the most simple, safe and convenient route of administration. The absorption of drugs that are taken orally will depend of its bioavailability. Over the past few years, much research has been focused in the importance of intestinal drug transporters as one of the determinants of pharmacokinetics. Uptake and efflux transporters identified in the intestine plays a critical role in the membrane permeability and may influence the oral absorption of drug together with passive diffusion, paracellular transport and intestinal metabolism. ATP-dependent transporters localized in the enterocytes determine oral bioavailability, intestinal efflux and drug-drug interactions.¹⁻⁵

In this context, a method that could mimetics the *in vivo* conditions most closely will be useful to predict the absorption rate of drugs. Ussing chamber is an *ex vivo* method, recommended by Food and Drug Administration (FDA), that provides good prediction of permeability, metabolism and transporters interaction.^{6, 7} This technique could evaluate

different regions of gastrointestinal tract using integral tissues from rats, for instance, considering the effect of drug-drug interactions. Usually, parallel artificial membrane permeability (PAMPA) and cultural cell lines like Caco2 are used to permeability studies; however these systems lack the morphological and physiological features of intestine, mainly permeability involving transporter-mediated process.^{8,9}

Norfloxacin (NFX) is a fluoroquinolone antibiotic with a broad activity spectrum, which presents low solubility and low permeability, belonging to class IV of Biopharmaceutical Classification System.^{10,11} The usual dose is 400mg (12/12h) and only about 30-40% is absorbed. There are reports in the literature that the low bioavailability of fluoroquinolones could be attributed to intestinal efflux.^{12,13} Therefore, the aim of this study is evaluate the intestinal permeability mechanisms of NFX by Ussing chamber model. According to the recent literature review, there is no study that explains the determinants of intestinal permeability of NFX. Ussing chamber model was used to obtain useful information regarding the contribution of all the relevant intestinal drug uptake and efflux transporters in NFX absorption.

EXPERIMENTAL SECTION

Materials

Budesonide, Cyclosporine, Lisinopril, Levofloxacin, MK-571, Norfloxacin, Novobiocin, Quinidine, Pyruvate, Rhodamine 123 and Verapamil were obtained from Sigma Aldrich (St. Louis, USA). All other analytical reagents were of analytical grade.

Animals

This study was carried out with male Wistar rats weighing 210–250 g (Janvier Lab, Paris, France). The animals were housed in a temperature ($22 \pm 2^\circ\text{C}$) and light- (12 h light/dark cycles) controlled room, with free access to water and food, submitted to fasted state 12h before the experiment. The studies were approved by ethical committee of University of Paris-Sud in accordance with European legislation on animal experiments.

Ussing chamber experiments

Different intestinal segments of sacrificed rats were excised, washed with cold physiological saline solution and visually examined to discard sections containing Payer's patches. The tissue was mounted in the Ussing chambers (intestinal surface of 1 cm²) bathed with Ringer's Krebs Bicarbonate solution at pH 7.4, with mucosal side facing the donor compartment and serosal side facing the receptor compartment. The system was maintained at 37 °C and continuously oxygenated with O₂/CO₂ (95/5%).

NFX solution (150µM) was placed in the donor chamber and 500 µL were recovered from donor side and replaced with the same volume of fresh medium each 30 min until 180 min. Samples of donor side were also recovered to verify any change in NFX concentration. In the experiments with inhibitors, the system (donor and receptor chamber) was equilibrated only with inhibitor solution, after 30 min the medium of the donor chamber was replaced by NFX solution containing inhibitor and the experiment was carried out by 180 min. Transporters inhibitors were used to investigate which transporter is involved with the passage or inhibition of NFX. Budesonide (100 µM), Cyclosporine (10 µM), Novobiocin (5 µM), Lisinopril (100 µM), Levofloxacin (100 µM), MK-571 (50 µM), Quinidine (100 µM), Rhodamine 123 (100 µM) and Verapamil (100 µM) were used as inhibitors and Pyruvate (10 000 µM) as substrate competitor. All samples were analyzed by high performance liquid chromatography (HPLC) validated method as described below. Tissue viability was assessed during the experiments by continuously recording the transmucosal potential difference. If tissue damage was suspected, the experiment was discarded. The experiment was also realized at 4 °C to evaluate NFX permeation where efflux pumps are not active. The apparent permeability coefficient (Papp) was calculated using:

$$P_{app} = dQ/dt \times 1/AC_0 \text{ Eq. (1)}$$

where dQ/dt is the flux of NFX from the mucosal to the serosal side of the mucosa, C_0 is the initial concentration of NFX in the donor compartment and A is the area of the membrane. The values of P_{app} were calculated between 30 and 180 min after addition of NFX in all experiments, in order to standardize the calculations.¹⁴

High performance liquid chromatography

The chromatographic analysis of NFX was performed in a Waters 515 pump, a Waters 717 plus autosampler (Milford, MA, USA) and UV detector Waters 486 set at 270 nm. The chromatographic system was equipped with a Phenomenex® (Torrance, CA, USA) C18 reversed-phase column (150 X 4.6 mm; 5 mm particle size) conditioned at 40 °C. The column eluted in isocratic mode using a mobile phase consisting of phosphate buffer (0.04 M, pH 3.0) and acetonitrile (84:16 v/v) at a flow rate of 1.0 mL/min and injection volume of 20 µL.¹⁵

To analyze verapamil samples, the mobile phase was constituted of acetonitrile water (45:55 v/v) and the pH was adjusted to 2.8 with phosphoric acid (85%) at a flow rate of 1.2 mL/min and injection volume of 20 µL. The chromatographic system was constituted of CLC-ODS (6.0 x 150 mm) Shim-

Pack reverse phased at room temperature and the chromatograms were recorded at 230 nm.¹⁶

Statistical analysis

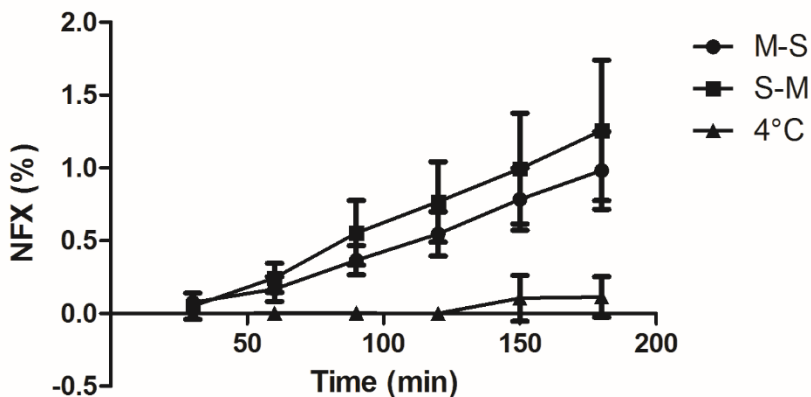
Results are expressed as mean \pm standard deviation of three replicates. The graphs were drawn and the statistical analysis was performed using GraphPad Prism, version 6.0 for Windows (GraphPad Software, San Diego, CA, USA).

RESULTS

NFX intestinal passage study

The Ussing chamber experiment was realized with NFX at 4 °C mucosal-to-serosal, at 37 °C mucosal-to-serosal and serosal-to-mucosal and the results are expressed as percentage of NFX that permeate in Figure 1. The permeability values are expressed in Table 1.

Figure 1 – NFX quantity (%) that permeates during 180 minutes at 37 °C mucosal-to-serosal and serosal-to-mucosal and at 4 °C.



Efflux and uptake investigation

The intestinal NFX flow encountered in the presence of inhibitor transporters used in the efflux investigation are presented in Table 2.

NFX is a zwitterionic drug presenting four pka values, as already described experimentally by the group.^{17, 18} All the ionic species that could be formed, highlighting the NFX specie presents in the pH 7.4 of the medium, are shown in Figure 3.

Table 1. Apparent permeability values (P_{app}) of NFX determined from Ussing chamber experiments in mucosal-to-serosal (M-S) and serosal-to-mucosal (S-M) at 37 °C, and mucosal-to-serosal at 4 °C, both experiments realized with duodenal portions.

Condition	P_{app} ($\times 10^{-6}$ cm/s)
M-S	1.07 ± 0.18
S-M	1.32 ± 0.46
4 °C	0.20 ± 0.19

NFX permeation at different portions of rat intestine was evaluated. The results are expressed in Figure 2.

Figure 2 – NFX intestinal passage (%) at different portions of rat intestine: duodenum, jejunum, ileum and colon.

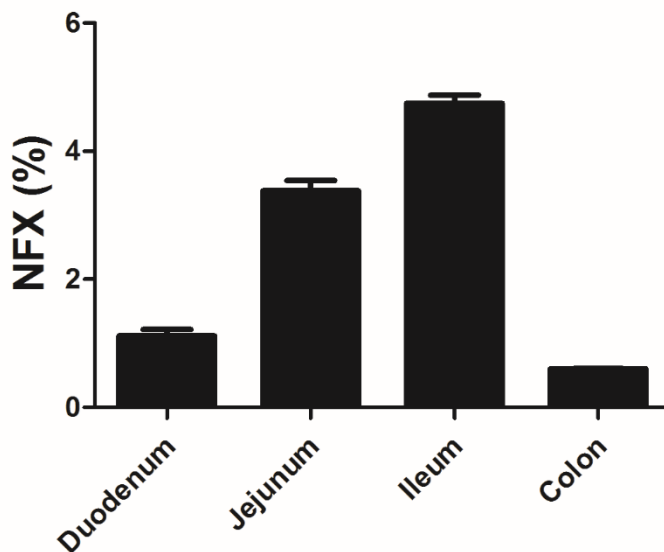


Table 2. Flow obtained to NFX alone or in presence of transporter inhibitor at duodenum (duod), jejunum (jej), ileum or colon.

Transporter studied	Condition	Flow (x10⁻¹² nmol/cm²/s)
Pg-p	NFX duod	1.84 ± 0.16
	NFX + VRP duod	1.88 ± 0.27
	NFX jej	6.88 ± 2.53
	NFX + VRP jej	4.96 ± 2.29
BCRP	NFX+ NVB duod	3.70 ± 0.20
MRP1/MRP2	NFX + MK571 duod	3.47 ± 0.59
PEPT-1	NFX ileum	8.22 ± 0.57
	NFX + LIS ileum	5.24 ± 0.68
OCT1/OCT2/PMAT	NFX + QUIN ileum	2.04 ± 0.99
	NFX + ROD ileum	2.42 ± 1.57
OCTN1/OCTN2	NFX + LEVO duod	4.93 ± 0.87
OATP2B1/ OATP1A2	NFX + BUD duod	5.11 ± 1.38
MCT1	NFX colon	2.12 ± 1.11
	NFX + PYR	2.55 ± 0.83

NFX: norfloxacin, VRP: verapamil, CYC: cyclosporine, NVB: novobiocin, LIS: lisinopril, QUIN: quinidine, LEVO: levofloxacin, BUD: budesonide, PYR: pyruvate.

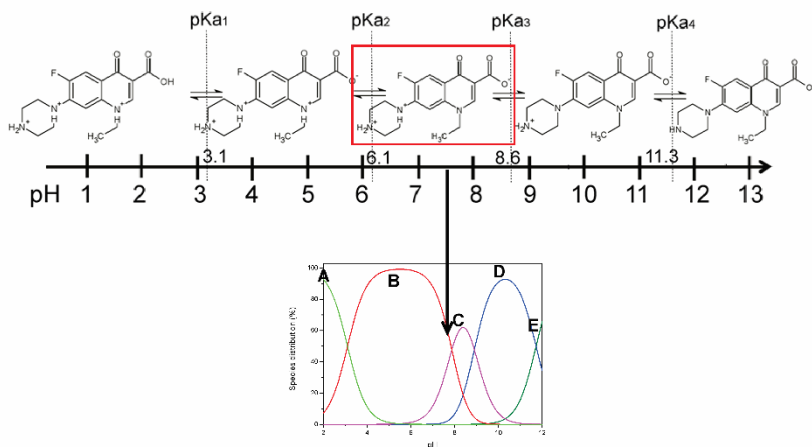
DISCUSSION

In the first Ussing chamber experiment, the results present the already known low permeability of NFX and consequently low permeate quantity (less than 1%). The permeability of NFX mucosal-to-serosal (Papp 1.07 ± 0.18 x10⁻⁶ cm/s) could be considered very low, once is lower to < 10⁻⁴, as determined by BCS class IV. When the experiment was carried out at 4 °C, it could be seen that very low content of NFX that permeates, approximately zero, resulting in apparent permeability value statistically different between 4 °C and 37 °C. This low permeation at low temperature, where the efflux pumps are not active reveals that NFX permeation is transporter-dependent.

NFX passage at different intestinal segments was evaluated in order to verify if there is difference between them. It could be seen in Figure 2 that NFX passage is in the decrescent order: ileum > jejunum > duodenum > colon. Older literature describes higher absorption of fluoroquinolones in

duodenum, different from that was observed experimentally.²⁰ This difference between different segments is probably attributed to transporters that are expressed differently along the intestinal tract. One important study, developed by Englund and coworkers, shows regional levels of drug transporters along the human intestine and other important literature used in this work was the correlation between human and rat intestine.^{21, 22} A vast numbers of drugs have the transport facilitate or hamper by drug intestinal transporters.

Figure 3– NFX and its species distributions according to pH value. The pH of 7.4 is highlighted because is the pH of the medium used in the Ussing chamber experiments. (Based on Mendes et al., 2015)¹⁷



Because of this difference of NFX passage between the intestinal segments and also due to the lack of information about the transporters that are involved in the NFX absorption together with the literature that attributes the intestinal efflux of NFX responsible for the low permeability, transporters inhibitors were used to investigate which transporter is involved in the passage or inhibition of NFX. First of all, the NFX passage in the presence of the transporter inhibitor was determined in duodenum. When the transporter is more expressed in some specific region of the intestine, the experiment was realized also in this segment.

In the efflux investigation, P-glycoprotein (P-gp) or multidrug resistance gene 1, breast cancer resistance protein (BCRP) and multidrug resistance-associated protein 1/2 (MRP1/MRP2) expressed on the apical membrane of human and rodents were investigated for influence in NFX

absorption. P-gp is the first ATP-dependent efflux transporter described and plays an important role in limiting entry of a broad range of therapeutic drugs.²³ Verapamil (VRP) was used in this study as P-gp inhibitor.²⁴ In spite of the variety of structurally compounds that this protein can recognize, there is no statistical difference in the NFX flow in presence of VRP at duodenum (Table 2). The test was reevaluated in jejunum segment because P-gp expression is increased at this portion and it could be inferred that P-gp is not involved in NFX efflux.²¹

BCRP is another multidrug resistance protein with a highly diverse range of substrate. Contrasting to P-gp, BCRP expression does not vary along the length of the intestine.³ This efflux transporter influence was evaluated using novobiocin as BCRP inhibitor.²⁴ The presence of novobiocin increases NFX flow of 1.84×10^{-12} up to around 3×10^{-12} nmol/cm²/s in duodenum. This result reveals the NFX efflux by this transporter, as already observed by Merino and coworkers using polarized cell lines and discussed by Alvarez group in the review about fluoroquinolone efflux.^{12, 13}

Concerning MRP family, MRPs 1 to 5 have been identified to plays a role in drug transport. MRP1, MRP3 and MRP5 are in the basolateral side; therefore, they act as absorptive transporters. Differently, MRP1 and MRP4 are localized in the apical / luminal membrane of enterocytes together with BCRP and P-gp forming a barrier to drug absorption.²⁵ When Cao and coworkers examined the correlation between human and rat transporters, they found both human and rat genechip for correlation analysis of MRP3 and MRP2.²² Secretion of leukotriene (LTC₄) is a physiological function of MRPs, for that reason, MK571, a leukotriene analog, was used as MRPs inhibitor.²⁶ However, MK571 is not appropriate to MRP1, 3 and 5 inhibitions due to the lack of cellular penetration properties.^{25, 27} Therefore, this inhibitor was used to block MRP2 that is located in the apical side acting as efflux transporter. Table 2 shows that the flow was increased in the presence of MK571, revealing that NFX could be a substrate to MRP2 efflux as already observed to grepafloxacin.²⁸ As demonstrated in Figure 3, NFX at the pH of the medium used is at the zwitterionic form and MRP family of transporters usually transports anionic and zwitterionic compounds.²⁹ Here, we propose only the possibility of NFX being a substrate, because MK571 is not specific in MRP2 inhibition as it extensively affects organic anion uptake system as well. In the uptake transporter study, we will discuss the importance of organic anion transporters in NFX absorption. On the other hand, there is an overlap in substrate specificity already described between BCRP and MRP2 that can lead to a synergic effect of these transporters in limiting NFX penetration.³ Literature about intestinal relation between MRP2 and drug

bioavailability is still quite limited;³⁰ therefore, more specific inhibitors will have to be discovered and more studies are needed to confirm this influence.

The key uptake transporters that present influence in drug disposition were investigated: peptide protein (PEPT-1), organic cation carnitine transporters (OCTN1/OCTN2), organic cation transporter (OCT1/OCT2), plasma membrane monoamine transporter (PMAT), organic anion transporter polypeptide OATP2B1/OATP1A2 and monocarboxylate transporter (MCT1). The structural requirements for binding with these transporters are different between them. However, all of them were considered as possible NFX transporters due to its structure and pka values. It is fundamental observe the physicochemical properties of drugs in relation to micro pH environment.²⁹ At the pH of the medium used in the Ussing chamber experiment (pH 7.4), NFX present both cationic and anionic charges (Figure 3).^{17, 18}

PEPT-1 is the intestinal peptide transporter expressed in apical membrane responsible to transports small peptides as several pharmacologically active compounds that are peptide-like structure. Lisinopril is an angiotensin converting enzyme that has been demonstrated to inhibit PEPT-1 intestinal transporter, and as so, was used in this study.³¹ This evaluation was realized in ileum due to higher expression of PEPT-1 in presence or absence of its inhibitor.²¹ From table 2, it could be observed that NFX flow reduced when Lisinopril was pre-incubated with the intestine segment, blocking PEPT-1 transporter and consequently eliminating the NFX transport by this peptide transporter. This suggests the involvement of this uptake transporter in the NFX absorption, since NFX present the minimum structure requirement to bind PEPT-1 that is the free carboxylic acid moiety and an amine bond (Figure 3 – NFX structure).^{31, 32} Peptide transporters are important in many drugs bioavailability, and this work reveals its influence in NFX absorption too.

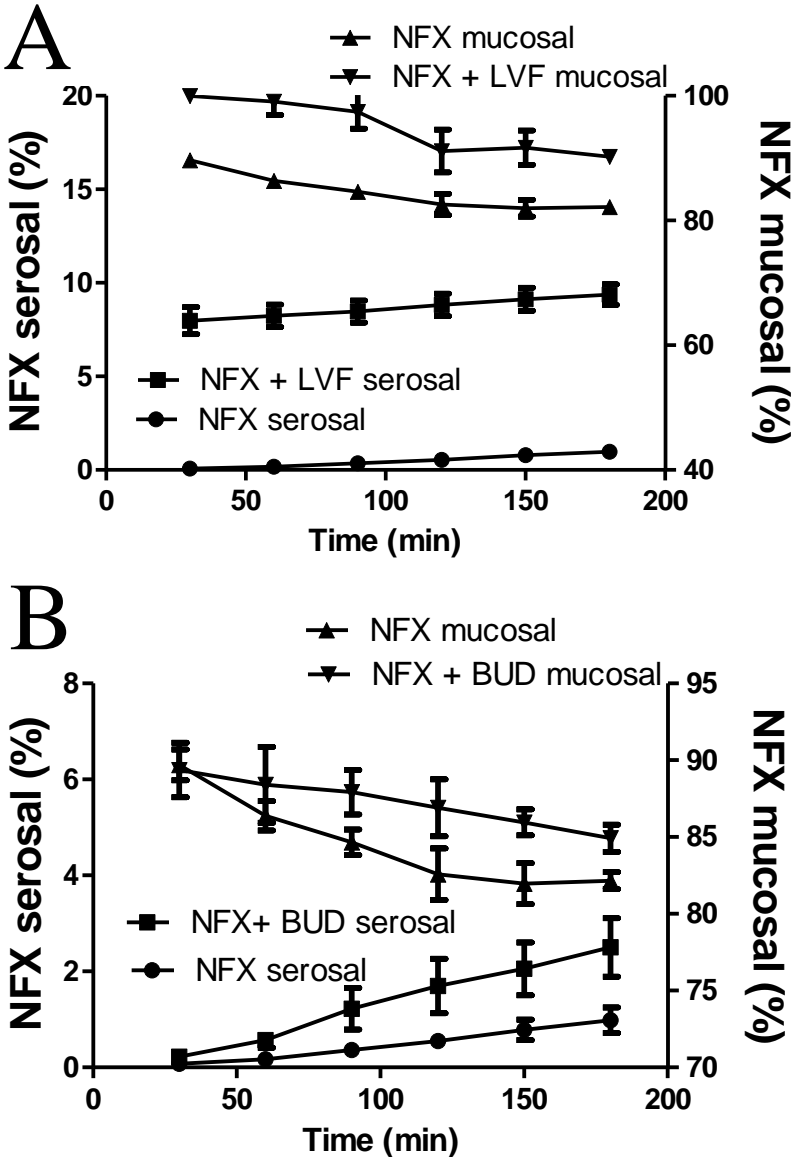
The SLC22 family is a superfamily of transporters that comprises electrogenic cation transporters OCT1-3 and organic cation carnitine transporters (OCTN1/OCTN2). OCT1 and OCT2 are transporters localized in the intestinal tissue; however, there is an inconsistency in the literature concerning their location at the apical or basolateral membrane. Indeed, according to the most recent publications about OCT1 expression, there are substantial evidences that demonstrate the apical localization of OCT1 in Caco-2 cells, mouse and human enterocytes.^{33, 29} Therefore, the apical membrane was considered to evaluate the results of intestinal transport of NFX. Many pharmaceuticals have been identified as OCTs substrate, and NFX was evaluated due to its cation portion. Another novel organic cation transporter identified is the monoamine transporter (PMAT), and its substrate

and inhibitor specificity overlaps with that of OCTs. Moreover, substrates handled by OCTs are often transported by PMAT also.³⁴ Therefore, PMAT and OCTs influence in NFX absorption were evaluated together. Quinidine is a known inhibitor of these transporters, and was evaluated with NFX in rat ileum. There is no much literature about correlation between human and rat concerning OCTs, therefore, ileum segment was selected due to the study of Choudhuri group that demonstrates the presence of OCT1 in rat ileum.³⁵ To confirm the involvement of OCTs and PMAT in NFX transport, rhodamine 123, recently described as high-affinity inhibitor of OCT1 and 2 was also evaluated. It is noteworthy the reduction of NFX flow in the presence of both inhibitors, revealing the contribution of OCT1 and PMAT in NFX transport.

Other relevant organic cation transporters, OCTNs are expressed in the apical membrane of enterocytes. OCTN2 is the most important transporter of L-carnitine, but also transports many cationic drugs like spironolactone, tetraethylammonium, pyrilamine and others. Literature reveals that zwitterionic drugs like cephaloridine, levofloxacin and grepafloxacin are inhibitors of OCTN in Caco-2 cells. There is already stated that cephaloridine inhibits transport and causes carnitine deficiency.^{36, 37} In this context, levofloxacin was used in the experiment that evaluated the influence of OCTN2 in NFX transport. The fasted state which rats were submitted previously to intestine excision is reported to increase the concentration of OCTN2 in the small intestine of these animals.³⁸ When levofloxacin was present in NFX transport study, the flow was highly increased. A possible explanation to this result could be that NFX acts as an affinity itself for this transporter and, therefore, due to inhibitor competition when in presence of this inhibitor, the amount of free NFX able to permeate was increased. This hypothesis was verified by NFX quantification into the donor chamber in the presence and absence of inhibitor (Figure 4). It was revealed the amount of free NFX in the presence of inhibitor was increased, confirming our hypothesis that NFX could act as OCTN inhibitor.

Verapamil is an OCTN substrate, and to verify the inhibition of this transporter by NFX, permeation studies of verapamil in Ussing chamber was realized. In the same way, the tissue was equilibrated with NFX solution during 30 min before the experiment. The quantification by HPLC of verapamil revealed a decrease of the total quantity of verapamil that permeates in 180 min in presence of NFX, changing the verapamil flow value of $2.22 \pm 0.47 \times 10^{-12}$ nmol/cm²/s to $0.73 \pm 0.39 \times 10^{-12}$ nmol/cm²/s, alone and in presence of NFX respectively, confirming the ability of OCTN inhibition that NFX exerts.

Figure 4 – Total quantity of NFX (NFX) in mucosal and serosal side of Ussing chamber experiment in the presence of levofloxacin (LVF, Panel A) or budesonide (BUD, Panel B).

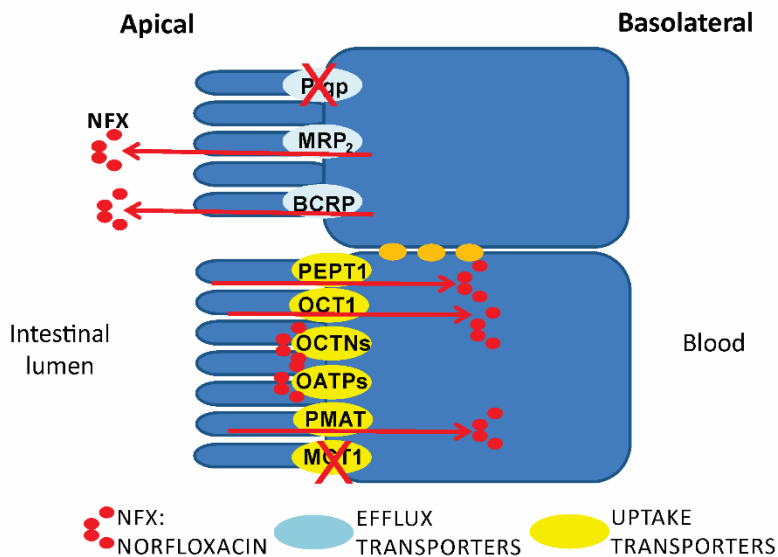


Organic anion-transporting polypeptide family (SLCO) represent a superfamily of important protein transporters that mediate the sodium-independent transport of a wide range of organic compounds including drugs and determining their absorption, distribution and effect. The mechanism of this transport is based on anion exchange by coupling the efflux of endogenous intracellular uptake of substrate like bicarbonate with the cellular uptake of substrate. 39 Garver and coworkers (2008) already studied the influence of OATPs in drug absorption in rats. 40 OATP1A2 and OATP2B1 are the representatives of OATP located in the apical membrane of enterocytes and, therefore, these transporters were investigated with budesonide their inhibitor. 41,42 In the same way as OCTNs, when budesonide is present, NFX flow is increased. Again, the hypothesis is that NFX could show an affinity to this transporter, so NFX concentration at the mucosal donor was evaluated. Figure 4B demonstrates that in presence of inhibitor there is more NFX free and able to permeate, increasing NFX flow and confirming the hypothesis that NFX could act also as OATP inhibitor. Literature presents a study that demonstrates the affinity of other fluoroquinolone by OATP transporter, however, ciprofloxacin bind to OATP1A2 to be transported, instead of NFX that probably blocks this transporter. 43

Proton-linked monocarboxylate transporters (MCTs) are a family of transporters that catalyze the movement of monocarboxylic acids across the membrane as lactate and pyruvate. MCT1 is a member of this family known to influence the drug transport in enterocytes and it is expressed in the apical side of the small and large intestine. In the MCT1 influence investigation, pyruvate that is a substrate of MCT1 was used due to the lack of inhibitors of this transporter. The flow of NFX in presence of pyruvate was statistically the same of NFX alone, in other words, the presence of pyruvate did not influenced the NFX transport, revealing that MCT1 has no relation in NFX permeability mechanism.

In summary, this study provides the influence that uptake and efflux transporters exercise in NFX intestinal transport using inhibitors and substrates in one method that could simulate the *in vivo* permeability mechanism. It could be observed in Figure 5 that BCRP and MRPs are implicated in the NFX efflux and PEPT1, PMAT and OCT in the NFX uptake transport. Furthermore, this work revealed for the first time in the literature that NFX has itself an affinity for OCTN and OATP, demonstrating that NFX could inhibit these transporters and influence the absorption of other drugs.

Figure 5 – Schematic summary representation of main efflux (blue) and uptake (yellow) intestinal transporters and their involvement in NFX intestinal permeability. P-glycoprotein (P-gp), breast cancer resistance protein (BCRP), multidrug resistance-associated protein (MRP1/MRP2), peptide protein (PEPT-1), organic cation transporter (OCT1/OCT2), organic cation carnitine transporters (OCTN1/OCTN2), plasma membrane monoamine transporter (PMAT), organic anion transporter polypeptide (OATP2B1/OATP1A2), monocarboxylate transporter (MCT1).



CONCLUSION

This study was able to identify the uptake and efflux transporters implicate in NFX permeability mechanism. In view of the scarcity of the literature, we believe that this updated description of NFX intestinal permeability factors could contribute to the development of rational pharmaceutical formulations that could circumvent the efflux problems and consequently improve NFX biopharmaceutical properties, becoming a technological and pharmacoeconomics alternative to presently available formulations.

AUTHOR INFORMATION

Corresponding Author

* Corresponding author: Laboratory of Quality Control, Department of Pharmaceutical Sciences, Federal University of Santa Catarina, J/K 207,

88040-900, Florianópolis, SC, Brazil. Phone number: +55 (48) 3721-4585; fax +55 (48) 3721-9350. cassi_ana@yahoo.com.br

Author Contributions

The manuscript was written through contributions of all authors. All authors have given approval to the final version of the manuscript.

ACKNOWLEDGMENT

The authors would like to thank Animex of Châtenay-Malabry for technical support during *in vivo* manipulation. This study was supported by Coordination for Enhancement of Higher Education Personnel (CAPES).

ABBREVIATIONS

NFX, norfloxacin. BCS, Biopharmaceutical Classification System. P-gp, P-glycoprotein. HPLC, high performance liquid chromatography. BCRP, breast cancer resistance protein. MRP1/MRP2, multidrug resistance-associated protein. PEPT-1, Peptide protein. OCT1/OCT2, organic cation transporter. OCTN1/OCTN2, organic cation carnitine transporters. PMAT, plasma membrane monoamine transporter. OATP2B1/OATP1A2, organic anion transporter polypeptide. MCT1, monocarboxylate transporter.

REFERENCES

1. Kim, R. B. Transporters and Drug Discovery: Why, When, and How. *Molecular Pharmaceutics* 2006, 3, (1), 26-32.
2. Lennernäs, H. Human *in Vivo* Regional Intestinal Permeability: Importance for Pharmaceutical Drug Development. *Molecular Pharmaceutics* 2014, 11, (1), 12-23.
3. Estudante, M.; Morais, J. G.; Soveral, G.; Benet, L. Z. Intestinal drug transporters: an overview. *Adv Drug Delivery Rev* 2013, 65, (10), 1340-1356.
4. Rozehnal, V.; Nakai, D.; Hoepner, U.; Fischer, T.; Kamiyama, E.; Takahashi, M.; Yasuda, S.; Mueller, J. Human small intestinal and colonic tissue mounted in the Ussing chamber as a tool for characterizing the intestinal absorption of drugs. *European Journal of Pharmaceutical Sciences* 2012, 46, (5), 367-373.
5. Lennernäs, H. Animal data: the contributions of the Ussing Chamber and perfusion systems to predicting human oral drug delivery *in vivo*. *Advanced drug delivery reviews* 2007, 59, (11), 1103-1120.
6. Food; Administration, D., Guidance for industry: waiver of *in vivo* bioavailability and bioequivalence studies for immediate-release solid oral

dosage forms based on a biopharmaceutics classification system. In Food and Drug Administration, Rockville, MD, 2000.

7. Sjöberg, Å.; Lutz, M.; Tannergren, C.; Wingolf, C.; Borde, A.; Ungell, A.-L. Comprehensive study on regional human intestinal permeability and prediction of fraction absorbed of drugs using the Ussing chamber technique. *European Journal of Pharmaceutical Sciences* 2013, 48, (1), 166-180.

8. Gotoh, Y.; Kamada, N.; Momose, D. The advantages of the Ussing chamber in drug absorption studies. *Journal of biomolecular screening* 2005, 10, (5), 517-523.

9. Kerns, E. H.; Di, L.; Petusky, S.; Farris, M.; Ley, R.; Jupp, P. Combined application of parallel artificial membrane permeability assay and Caco-2 permeability assays in drug discovery. *Journal of pharmaceutical sciences* 2004, 93, (6), 1440-1453.

10. Amidon, G. L.; Lennernas, H.; Shah, V. P.; Crison, J. R. A theoretical basis for a biopharmaceutic drug classification: the correlation of *in vitro* drug product dissolution and *in vivo* bioavailability. *Pharm Res* 1995, 12, (3), 413-20.

11. Breda, S. A.; Jimenez-Kairuz, A. F.; Manzo, R. H.; Olivera, M. E. Solubility behavior and biopharmaceutical classification of novel high-solubility ciprofloxacin and norfloxacin pharmaceutical derivatives. *International journal of pharmaceutics* 2009, 371, (1), 106-113.

12. Merino, G.; Álvarez, A. I.; Pulido, M. M.; Molina, A. J.; Schinkel, A. H.; Prieto, J. G. Breast cancer resistance protein (BCRP/ABCG2) transports fluoroquinolone antibiotics and affects their oral availability, pharmacokinetics, and milk secretion. *Drug Metabolism and Disposition* 2006, 34, (4), 690-695.

13. Alvarez, A. I.; Pérez, M.; Prieto, J. G.; Molina, A. J.; Real, R.; Merino, G. Fluoroquinolone efflux mediated by ABC transporters. *J Pharm Sci* 2008, 97, (9), 3483-3493.

14. Bravo-Osuna, I.; Vauthier, C.; Chacun, H.; Ponchel, G. Specific permeability modulation of intestinal paracellular pathway by chitosan-poly(isobutylcyanoacrylate) core-shell nanoparticles. *European Journal of Pharmaceutics and Biopharmaceutics* 2008, 69, (2), 436-444.

15. Oliveira, P. R.; Bernardi, L. S.; Mendes, C.; Cardoso, S. G.; Sangoi, M. S.; Silva, M. A. Liquid chromatographic determination of norfloxacin in extended-release tablets. *Journal of chromatographic science* 2009, 47, (9), 739-744.

16. Sultana, N.; SAEED ARAYNE, M.; Waheed, A. IN-vitro interaction studies of verapamil with fluoroquinolones using first order

derivative uv spectrophotometry and RP-HPLC. *J. Chil. Chem. Soc.* 2011, 56, (4), 848-855.

17. Mendes, C.; Buttchevitz, A.; Barison, A.; Ocampos, F. M. M.; Bernardi, L. S.; Oliveira, P. R.; Silva, M. A. S. Investigation of β -cyclodextrin–norfloxacin inclusion complexes. Part 2. Inclusion mode and stability studies. *Expert review of anti-infective therapy* 2015, 13, (1), 131-140.

18. Mendes, C.; Buttchevitz, A.; Kruger, J. H.; Bernardi, L. S.; Oliveira, P. R.; Silva, M. A. S. Quantitative Analysis of Norfloxacin in β -Cyclodextrin Inclusion Complexes—Development and Validation of a Stability-indicating HPLC Method. *Analytical Sciences* 2015, 31, (10), 1083-1089.

19. Kato, K.; Shirasaka, Y.; Kuraoka, E.; Kikuchi, A.; Iguchi, M.; Suzuki, H.; Shibasaki, S.; Kurosawa, T.; Tamai, I. Intestinal Absorption Mechanism of Tebipenem Pivoxil, a Novel Oral Carbapenem: Involvement of Human OATP Family in Apical Membrane Transport. *Molecular Pharmaceutics* 2010, 7, (5), 1747-1756.

20. Nix, D. E.; Schentag, J. J. The quinolones: an overview and comparative appraisal of their pharmacokinetics and pharmacodynamics. *The Journal of Clinical Pharmacology* 1988, 28, (2), 169-178.

21. Englund, G.; Rorsman, F.; Rönnblom, A.; Karlbom, U.; Lazorova, L.; Gråsjö, J.; Kindmark, A.; Artursson, P. Regional levels of drug transporters along the human intestinal tract: co-expression of ABC and SLC transporters and comparison with Caco-2 cells. *European Journal of Pharmaceutical Sciences* 2006, 29, (3), 269-277.

22. Cao, X.; Gibbs, S. T.; Fang, L.; Miller, H. A.; Landowski, C. P.; Shin, H.-C.; Lennernas, H.; Zhong, Y.; Amidon, G. L.; Lawrence, X. Y. Why is it challenging to predict intestinal drug absorption and oral bioavailability in human using rat model. *Pharmaceutical research* 2006, 23, (8), 1675-1686.

23. Giacomini, K. M.; Huang, S.-M.; Tweedie, D. J.; Benet, L. Z.; Brouwer, K. L.; Chu, X.; Dahlin, A.; Evers, R.; Fischer, V.; Hillgren, K. M. Membrane transporters in drug development. *Nature reviews Drug discovery* 2010, 9, (3), 215-236.

24. Duan, L.; Yan, Y.; Sun, Y.; Zhao, B.; Hu, W.; Li, G. Contribution of TRPV1 and multidrug resistance proteins in the permeation of capsaicin across different intestinal regions. *International Journal of Pharmaceutics* 2013, 445, (1–2), 134-140.

25. Yu, X.-Q.; Xue, C. C.; Wang, G.; Zhou, S.-F. Multidrug resistance associated proteins as determining factors of pharmacokinetics and pharmacodynamics of drugs. *Current drug metabolism* 2007, 8, (8), 787-802.

26. Xu, H.; Kulkarni, K. H.; Singh, R.; Yang, Z.; Wang, S. W. J.; Tam, V. H.; Hu, M. Disposition of Naringenin via Glucuronidation Pathway Is Affected by Compensating Efflux Transporters of Hydrophilic Glucuronides. *Molecular Pharmaceutics* 2009, 6, (6), 1703-1715.
27. Liu, Y. H.; Di, Y. M.; Zhou, Z. W.; Mo, S. L.; Zhou, S. F. Multidrug resistance-associated proteins and implications in drug development. *Clinical and Experimental Pharmacology and Physiology* 2010, 37, (1), 115-120.
28. Naruhashi, K.; Tamai, I.; Inoue, N.; Muraoka, H.; Sai, Y.; Suzuki, N.; Tsuji, A. Involvement of multidrug resistance-associated protein 2 in intestinal secretion of grepafloxacin in rats. *Antimicrobial agents and chemotherapy* 2002, 46, (2), 344-349.
29. Proctor, W. R.; Ming, X.; Bourdet, D.; Han, T. K.; Everett, R. S.; Thakker, D. R. Why Does the Intestine Lack Basolateral Efflux Transporters for Cationic Compounds? A Provocative Hypothesis. *Journal of pharmaceutical sciences* 2016, 105, (2), 484-496.
30. Takano, M.; Yumoto, R.; Murakami, T. Expression and function of efflux drug transporters in the intestine. *Pharmacology & therapeutics* 2006, 109, (1), 137-161.
31. Guo, X.; Meng, Q.; Liu, Q.; Wang, C.; Mao, Q.; Sun, H.; Peng, J.; Kaku, T.; Liu, K. Peptide cotransporter 1 in intestine and organic anion transporters in kidney are targets of interaction between JBP485 and lisinopril in rats. *Drug metabolism and pharmacokinetics* 2012, 27, (2), 232-241.
32. Terada, T.; Sawada, K.; Irie, M.; Saito, H.; Hashimoto, Y.; Inui, K.-i. Structural requirements for determining the substrate affinity of peptide transporters PEPT1 and PEPT2. *Pflügers Archiv* 2000, 440, (5), 679-684.
33. Han, T. K.; Everett, R. S.; Proctor, W. R.; Ng, C. M.; Costales, C. L.; Brouwer, K. L.; Thakker, D. R. Organic cation transporter 1 (OCT1/mOct1) is localized in the apical membrane of Caco-2 cell monolayers and enterocytes. *Molecular pharmacology* 2013, 84, (2), 182-189.
34. Engel, K.; Wang, J. Interaction of organic cations with a newly identified plasma membrane monoamine transporter. *Molecular pharmacology* 2005, 68, (5), 1397-1407.
35. Choudhuri, S.; Cherrington, N. J.; Li, N.; Klaassen, C. D. Constitutive expression of various xenobiotic and endobiotic transporter mRNAs in the choroid plexus of rats. *Drug Metabolism and Disposition* 2003, 31, (11), 1337-1345.
36. Tune, B. M.; Hsu, C.-Y. Toxicity of cephaloridine to carnitine transport and fatty acid metabolism in rabbit renal cortical mitochondria:

structure-activity relationships. *Journal of Pharmacology and Experimental Therapeutics* 1994, 270, (3), 873-880.

37. Hirano, T.; Yasuda, S.; Osaka, Y.; Kobayashi, M.; Itagaki, S.; Iseki, K. Mechanism of the inhibitory effect of zwitterionic drugs (levofloxacin and grepafloxacin) on carnitine transporter (OCTN2) in Caco-2 cells. *Biochimica et Biophysica Acta (BBA)-Biomembranes* 2006, 1758, (11), 1743-1750.

38. Ringseis, R.; Wege, N.; Wen, G.; Rauer, C.; Hirche, F.; Kluge, H.; Eder, K. Carnitine synthesis and uptake into cells are stimulated by fasting in pigs as a model of nonproliferating species. *The Journal of nutritional biochemistry* 2009, 20, (11), 840-847.

39. Hagenbuch, B.; Gui, C. Xenobiotic transporters of the human organic anion transporting polypeptides (OATP) family. *Xenobiotica* 2008, 38, (7-8), 778-801.

40. Garver, E.; Hugger, E. D.; Shearn, S. P.; Rao, A.; Dawson, P. A.; Davis, C. B.; Han, C. Involvement of intestinal uptake transporters in the absorption of azithromycin and clarithromycin in the rat. *Drug Metabolism and Disposition* 2008, 36, (12), 2492-2498.

41. Glaeser, H.; Bailey, D.; Dresser, G.; Gregor, J.; Schwarz, U.; McGrath, J.; Jolicoeur, E.; Lee, W.; Leake, B.; Tirona, R. Intestinal drug transporter expression and the impact of grapefruit juice in humans. *Clinical Pharmacology & Therapeutics* 2007, 81, (3), 362-370.

42. König, J.; Glaeser, H.; Keiser, M.; Mandery, K.; Klotz, U.; Fromm, M. F. Role of organic anion-transporting polypeptides for cellular mesalazine (5-aminosalicylic acid) uptake. *Drug Metabolism and Disposition* 2011, 39, (6), 1097-1102.

43. Maeda, T.; Takahashi, K.; Ohtsu, N.; Oguma, T.; Ohnishi, T.; Atsumi, R.; Tamai, I. Identification of influx transporter for the quinolone antibacterial agent levofloxacin. *Molecular pharmaceutics* 2007, 4, (1), 85-94.

**CAPÍTULO 5 – DESENVOLVIMENTO DE NANOESPONJA DE
CICLODEXTRINA CONTENDO NORFLOXACINO**

1. INTRODUÇÃO

Avanços em nanotecnologia têm demonstrado aplicação dos sistemas de reticulação supramolecular a partir de blocos monoméricos simples para hospedagem das moléculas de fármacos. As CDs são amplamente conhecidas por sua típica estrutura toroidal com a cavidade interna hidrofóbica e sua superfície exterior hidrofílica, apresentando a oportunidade de moléculas de fármacos interagirem e complexarem. A formação de um complexo tem a capacidade de melhorar as propriedades físico-químicas dos fármacos inclusos na cavidade da CD, uma oportunidade para sistemas de liberação de fármacos extensivamente explorada. Entretanto, a CD mais comumente utilizada, a β CD apresenta baixa solubilidade aquosa que limita sua habilidade de complexação (Del Valle, 2004; Challa *et al.*, 2005; Loftsson e Brewster, 2012).

Um novo sistema de liberação de fármacos, as nanoesponjas (NS) baseadas em CD, foram desenvolvidas por pesquisadores a cerca de uma década para driblar os possíveis problemas de liberação de fármacos. NS leva esse nome devido à sua propriedade de formar uma estrutura como a de uma esponja e pela sua alta capacidade de encapsular pequenas moléculas na sua matriz. O termo “nanoesponja” foi primeiramente introduzido por DeQuan Li e Min Ma no ano de 2000, quando a β CD foi reticulada com diisocianatos orgânicos para purificação da água (Li e Ma, 2000). Estes pesquisadores demonstraram que os contaminantes da água foram completamente removidos pelo tratamento com as NS. Entretanto, foram Trotta e colaboradores (2006) que publicaram o “*proof of concept*” com resultados utilizando fármacos modelo. Este trabalho foi seguido de muitas publicações de pesquisa na área das NS como sistemas de liberação de fármacos de autores como Trotta, Cavalli, Vavia, Swaminathan, Torne, Ansari e coautores. Um relatório da União Europeia destacou o uso das NS baseadas em CD como um sistema inovador promissor para aplicação de sistemas de liberação de fármacos (Li e Ma, 2000; Cavalli *et al.*, 2006; Swaminathan *et al.*, 2007).

Até o momento, muitos trabalhos têm explorado o desenvolvimento das NS para diversas aplicações, entretanto, salvo melhor crença, não existe ainda na literatura um trabalho de desenvolvimento de NS baseada em CD com estudos *in vitro* e *in vivo*. Portanto, devido ao conhecimento prévio do grupo da problemática do NFX de solubilidade, e dos mecanismos de permeabilidade (efluxo intestinal e “sequestro” do fármaco pelos transportadores de fluxo) este capítulo aborda o desenvolvimento de NS de CD contendo NFX.

CYCLODEXTRIN BASED NANOSPONGE OF NORFLOXACIN:
INTESTINAL PERMEATION ENHANCEMENT AND IMPROVED
ANTIBACTERIAL ACTIVITY

Cassiana Mendes^{a,b}; Gabriela C. Meirelles^a; Clarissa Germano Barp^c;
Jamil Assreuy^c; Marcos A. S. Silva^b, Gilles Ponchel^a*

^a CNRS UMR 8612, Université de Paris Sud XI, Faculté de Pharmacie, 5
rue J.B. Clément, 92296 Châtenay-Malabry, France

^b Post graduation Program in Pharmaceutical Sciences, Quality Control
Laboratory, Universidade Federal de Santa Catarina, J/K 207, 88040-900,
Florianópolis-SC, Brazil. Phone number: +55 (48) 3721-4585; fax +55 (48)
3721-9350

^c Post graduation Program in Pharmacology, Pharmacology of Nitric Oxide
Laboratory, Universidade Federal de Santa Catarina, Biological Sciences
Centre, Block D/CCB, 88040-900, Florianópolis, SC, Brazil.

KEYWORDS

Cyclodextrin; intestinal permeability; mucoadhesion; nanosponge;
norfloxacin; Ussing chamber.

ABSTRACT

Nanosponges are a novel class of hyperbranched cyclodextrin-based that emerged in the last decade exhibiting remarkable potential as drug host system in improving biopharmaceutical properties. Norfloxacin is an antibiotic agent used in the treatment of urinary tract infections that belongs to class IV of biopharmaceutical classification system (BCS). Besides low solubility and permeability, previous work of our group highlighted the intestinal permeability as an additional barrier that needs to be circumvented for effective drug absorption. This work aims the development of cyclodextrin-based nanosponge of norfloxacin to improve its physicochemical characteristics. β -cyclodextrin was used as base and diphenyl carbonate as crosslinker agent at different proportions to produce nanosponge that were evaluated by *in vitro* and *in vivo* techniques. CD:crosslinker 1:2 MM was chosen due to its higher encapsulation efficiency (80%) revealing a mean diameter size of 40 nm with zeta potential of -19 mV. Infrared and thermal analysis techniques evidenced the nanosponge formation and the norfloxacin-loaded nanosponges demonstrated higher passage of NFX in comparison to NFX drug alone by Ussing chamber methods. The nanosponge formulation also revealed a mucoadhesive property that could increase the norfloxacin absorption which improves its antibiotic activity evaluated by *in vivo* sepsis induction. NS might be suitable carrier of NFX to maximize and facilitate oral absorption being as a potential alternative to the existing NFX drug formulations.

INTRODUCTION

Cyclodextrins (CDs) are well known cyclic structures with a torus shape that could include hydrophobic molecules into their inner cavity and improve physicochemical characteristic of many drugs. However, inclusion complexes with CD were already extensively exploited and the results are complexes that can easy dissociate with aqueous solubility limited. Nanosponges (NS) technology arises as CD-based host system more efficient in achieving solubilization, stabilization, enhancement of activity, permeability and bioavailability. NS are a novel class of hyperbranched polymers exhibiting remarkable potential in pharmaceutical and biomedical sciences. Over the past decade, different NS has been developed based on CD and the crosslinker tailored for specific applications (Loftsson e Brewster, 2012; Castiglione *et al.*, 2013; Swaminathan *et al.*, 2016).

Norfloxacin is a fluoroquinolone antibiotic that have emerged as one of the preferred agent in the treatment of urinary tract infections (UTIs) that belongs to biopharmaceutical classification system (BCS) class IV drugs (O'donnell e Gelone, 2004; Breda *et al.*, 2009; Bennett *et al.*, 2014). Our previous work related besides the intestinal efflux already reported in the literature, the caption of NFX by the intestinal cells transporters, consuming the drug by binding with these uptake transporters to their inhibition and not to carry through the enterocyte. This mechanism of permeability first described by our group means that there is an additional barrier of permeability that needs to be circumvented for effective drug absorption.

Oral bioavailability is a crucial factor for drugs class IV and is a product between the available fraction of administered dose in the gut lumen, the fraction of drug that reaches the inside of the enterocyte cells and the fraction escaping gut and liver metabolism (Sjöberg *et al.*, 2013). In this context, the aim of this work was develop cyclodextrin based NS to overlap NFX biopharmaceutical problems. This study was based on previous work of the group about NFX permeability factors and cyclodextrin inclusion complexes of NFX. The previous knowledge of the group made possible the development of NFX NS as the *in vitro* and *in vivo* evaluation. For the first time, a complete study since the formulation, physicochemical characterization, release profile, permeability studies by Ussing chamber model, mucoadhesion evaluation, and *in vivo* activity was performed for a NS.

MATERIALS

β -cyclodextrin, norfloxacin and diphenyl carbonate (DC) were obtained from Sigma Aldrich (St. Louis, USA). All other analytical reagents were of analytical grade.

METHODS

Nanosponge preparation

To produce NS, β CD was put to react with melted diphenyl carbonate at 90 °C for 5h at three different proportions of CD:crosslinker (1:2, 1:4 or 1:8 MM). After, the solid obtained was ground in a mortar and Soxhlet extraction was realized with ethanol in order to remove unreacted crosslinker. The resultant solid was dried at 50 °C and stored at 25 °C.

NFX-loaded nanosponges

NFX-loaded nanosponges (NFX NS) were produced weighting NFX powder and dispersing in aqueous suspension of NS (1:4 w/w) at pH 3 to favor NFX inclusion due to the electric charges. This aqueous suspension was stirred during 24h protected by light. After 24h, the final suspension was centrifuged at 2000 rpm during 10 min to separate the uncomplexed drug. The colloidal supernatant was separated from the residue and freeze-dried to produce the NFX-loaded NS.

Determination of drug content

NFX-loaded in NS was quantified by high performance liquid chromatography. These analyses were performed in a Waters 515 pump, a Waters 717 plus autosampler (Milford, MA, USA) and UV detector Waters 486 set at 270 nm. The chromatographic system was equipped with a Phenomenex® (Torrance, CA, USA) C18 reversed-phase column (150 X 4.6 mm; 5 mm particle size) conditioned at 40 °C. The column eluted in isocratic mode using a mobile phase consisting of phosphate buffer (0.04 M, pH 3.0) and acetonitrile (84:16 v/v) at a flow rate of 1.0 mL/min and injection volume of 20 μ L (Oliveira *et al.*, 2009).

Nanosponges characterization

NS hydrodynamic mean diameter and size distribution were determined by light scattering using Nanosizer® N4 PLUS (Beckman-Couter, France) at 90° fixed angle. Samples were appropriated diluted in Milli-Q® water. The results are the mean hydrodynamic diameter corresponding to the average of three determinations.

For zeta potential analysis, the samples diluted in NaCl solution (1 mmol/L) were placed in electrophoretic cells and the zeta potential values were determined from the electrophoretic mobility measured by Laser Doppler Electrophoresis (Zetasizer Nano series, Malvern Instruments, Worcestershire, UK).

Physicochemical characterization of nanosponges

Differential scanning calorimetry (DSC) curves for NFX, β CD, DC, their physical mixtures and the NS produced were obtained on a Shimadzu DSC-60 cell (Shimadzu Corporation, Kyoto, Japan) using aluminum crucibles with around 2.0 mg of sample in a dynamic N₂ atmosphere with a flow rate of 100 mL/min. The heating rate was 10 °C/min and the temperature ranged from 30 °C to 300 °C. The DSC equipment was previously calibrated with indium (melting point 156.6 °C, $\Delta H = -28.54$ J/g) and zinc (melting point 419.5 °C), which are DSC calibration standards.

The diffuse reflectance Fourier transform infrared spectroscopy (FT-IR) spectra were recorded using a FTIR Frontier spectrophotometer (PerkinElmer, Brazil), within a scan range of 600–4000 cm⁻¹, with an average of over 32 scans, at a spectral resolution of 4 cm⁻¹. A background spectrum was obtained for each experimental condition.

Transmission Electron Microscopy (TEM) images were obtained using TEM JEOL 1400 (Imagif, France) at 60 kv transmission coupled to TEM domain center software. For the preparation, 10 μ L of the NFX-loaded NS suspension was diluted to 100 μ L of Milli-Q® water and 5 μ L of this dilution was placed on a grid. The grid was disposed on a slide and inserted in the microscope to visualize samples.

Ussing chambers experiments

This study was carried out with male Wistar rats weighing 210–250 g (Janvier Lab, Paris, France). The animals were housed in a temperature (22 \pm 2°C) and light- (12 h light/dark cycles) controlled room, with free access to water and food, submitted to fasted state 12h before the experiment. The studies were approved by ethical committee of University of Paris-Sud in accordance with European legislation on animal experiments.

Different intestinal segments of sacrificed rats were excised, washed with cold physiological saline solution and visually examined to discard sections containing Payer's patches. The tissue was mounted in the Ussing chambers (intestinal surface of 1 cm²) bathed with Ringer's Krebs Bicarbonate solution at pH 7.4, with mucosal side facing the donor compartment and serosal side facing the receptor compartment. The system was maintained at 37 °C and continuously oxygenated with O₂/CO₂ (95/5%). NFX (150 μ M) or NFX-loaded NS (equivalent of 150 μ M) were placed in the donor chamber and 500 μ L were recovered from donor side and replaced with the same volume of fresh medium each 30 min until 180 min. Samples of donor side were also recovered to verify any change in NFX concentration. All samples were analyzed by high performance liquid chromatography (HPLC) validated method as described above. Tissue viability was assessed

during the experiments by continuously recording the transmucosal potential difference. If tissue damage was suspected, the experiment was discarded.

Nanosponges adhesion experiment

Initially, a little adaptation of Ussing chamber method was used to investigate the interference of the contact between NS and the intestinal mucosa. Aiming this, the flow was evaluated in presence of a semi-permeable membrane in contact with mucosal side to avoid contact between the NS and the mucosa, in comparison to NFX drug alone. After this, the NS adhesion experiment was realized. Nanosponge (150 μ M) in Ringer's Krebs Bicarbonate solution was lead in contact with a delimited intestinal mucosa surface (2 cm²) at room temperature. Samples of supernatant (non-attached particles) were recovered carefully during 60 min and evaluated by HPLC.

***In vitro* release experiments**

Release experiments were conducted in *sink* conditions using United States Pharmacopeia apparatus 2 (paddle) with 300 mL of simulated intestinal fluid (6.8) maintained at 37 ± 0.5 °C and stirred at 75 rpm. NFX-loaded NS (equivalent to 10 mg) were placed into semi-permeable membranes (commercial dialysis cellulose membranes MW cut-off 12,000 Da, Sigma-Aldrich, St. Louis, MO, USA) and aliquots of 5 mL of the medium were withdrawn at intervals of 5, 15, 25, 30, 45, 60, 90, 120, 150 and 180 min. The samples were analyzed by HPLC and the curve of percent of NFX released from NS *versus* time was constructed.

Antimicrobial *in vivo* experiments

Animal procedure were performed in accordance with the National Institutes of Health Guidelines and approved by the Institutional Animal Care and Use Committee of Universidade Federal de Santa Catarina (CEUA/UFSC-PP00790). Sepsis was induced by cecal ligation and puncture (CLP) as previously described (Rittirsch *et al.*, 2008). Briefly, female rats (~200 g) were pre-anesthetized with xylazine (5 mg/Kg, i.p.) and tramadol hydrochloride (10 mg/Kg, i.p.), then anesthetized with isoflurine (5% for induction and 3% for maintenance). After laparotomy, the cecum was ligated distal to the ileocecal valve, punctured two times with 14-gauge needle and a small amount of cecal content was squeezed through the punctures. The cecum was placed back into the abdominal cavity and walls were sutured. All animals received saline (30 ml/kg, s.c) after the surgery.

One hour after sepsis induction, NFX (10 mg/Kg) or NFX-NS (10 mg/Kg) were administrated by gavage and then animals were kept under standard laboratory conditions, with temperature (23 ± 2 °C), light-controlled

room (12h light/dark cycle), and free access to water and food. Tramadol hydrochloride (5 mg/Kg, s.c.) was injected 12 h after surgery as analgesic procedure. Twenty four hours after treatment, animals were euthanized by anesthetic overdose (ketamine/xylazine) and then kidney were aseptically harvested, homogenized and plated. A 2 μ L of each aliquot of serial dilution (10^{-1} , 10^{-2} and 10^{-3}) was plated onto Mueller-Hinton agar plate and incubated at 32 - 35 °C for 16-18h for colony count determination (Clsi, 2009). The total count of CFU/mL in the original inoculum was used to compare NS and NFX drug alone and data are expressed as the means \pm sem. Statistical significance was analyzed by Kuskal-Wallis test followed by Dunn's post hoc test as indicated in figure legends. A p value of less than 0.05 was considered significant. Statistical tests were performed using Graph Pad Prism 5 for Windows (Graph Pad Software, La Jolla, CA).

RESULTS

Nanosponges characterization

After the NS preparation, the NFX content was evaluated by HPLC. Three different proportions of CD:crosslinker (1:2, 1:4 or 1:8 MM) were prepared and revealed a NFX content of 80, 76 and 70%, respectively. Due to the higher drug content, the proportion 1:2 was selected to produce the NS and continue the studies. NS hydrodynamic mean diameter and size distribution were determined and NS revealed a mean size of 40 nm with a potential zeta of - 19 mV.

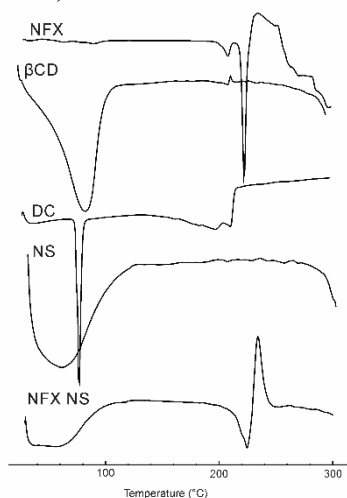
Physicochemical characterization of nanosponges

DSC curves were obtained and the results are expressed in Figure 1. NFX revealed two endothermic events at 223.85 °C (ΔH -116.52 J/g) and 209.73 °C (ΔH -14.9 J/g) corresponding to the melting point of NFX form B (Barbas *et al.*, 2006). β CD showed a wide endothermic peak at 87.72 °C (ΔH -368.57 J/g) related to the loss of water from the inner cavity and the crosslinker DC revealed an endothermic peak at 78.41 °C (ΔH_{fusion} -123.7 J/g). In NS thermal analyze it is not possible to observe the separated components, only one endothermic event at 62.23 °C (ΔH -222.86 J/g) related to the remaining water from the NS production. The same water is observed in NFX-loaded NS at 56.57 °C (ΔH -96.76 J/g) and one of NFX characteristic endothermic points could be observed at 225.73 °C (ΔH -83.05 J/g).

The FT-IR spectra of the samples are illustrated in Figure 2. NFX spectrum presents the characteristic bands at 1606 cm^{-1} (1) corresponding to pyridone keto and at 1720 cm^{-1} (2) corresponding to COOH stretching. In the spectra of the excipients (β CD) and DC are possible to verify the

characteristic bands of each one. The NS spectrum revealed an additional band not observed in the components isolated at 1612 cm^{-1} (3), which reveals the polymeric structure formation between β CD and DC. The NFX NS spectrum is very similar to NS spectrum, differing only in the intensity. It is important to notice that NFX bands could not be seen in NFX NS spectrum. TEM observations showed the spherical form of the NS (Figure 3). There is no difference of shape and size between NFX-loaded and unloaded NS.

Figure 1 - Differential scanning calorimetry curves of Norfloxacin (NFX), β -cyclodextrin (β CD), diphenyl carbonate (DC), Nanosponge (NS), NFX-loaded Nanosponge (NFX NS).



Ussing chambers experiments

Ussing chamber experiment with NFX and NFX-loaded NS mucosal-to-serosal (M-S) and serosal-to-mucosal (S-M) at $37\text{ }^{\circ}\text{C}$ are expressed as percentage of NFX that permeates in Figure 4A. The permeability values are expressed in Table 1. NFX-loaded NS presents a higher passage of NFX in both directions in comparison to NFX drug alone.

Permeability values are higher to NFX-loaded NS in comparison to NFX drug alone at duodenum and ileum ($P < 0.05$). It is important to notice that NFX passage is not statistically different when comparing mucosal-to-serosal (M-S) and serosal-to-mucosal (S-M) for NFX drug alone or loaded in NS.

Figure 2 - Fourier transform infrared spectroscopy spectra of Norfloxacin (NFX), β -cyclodextrin (β CD), diphenyl carbonate (DC), Nanosponge (NS), NFX-loaded Nanosponge (NFX NS).

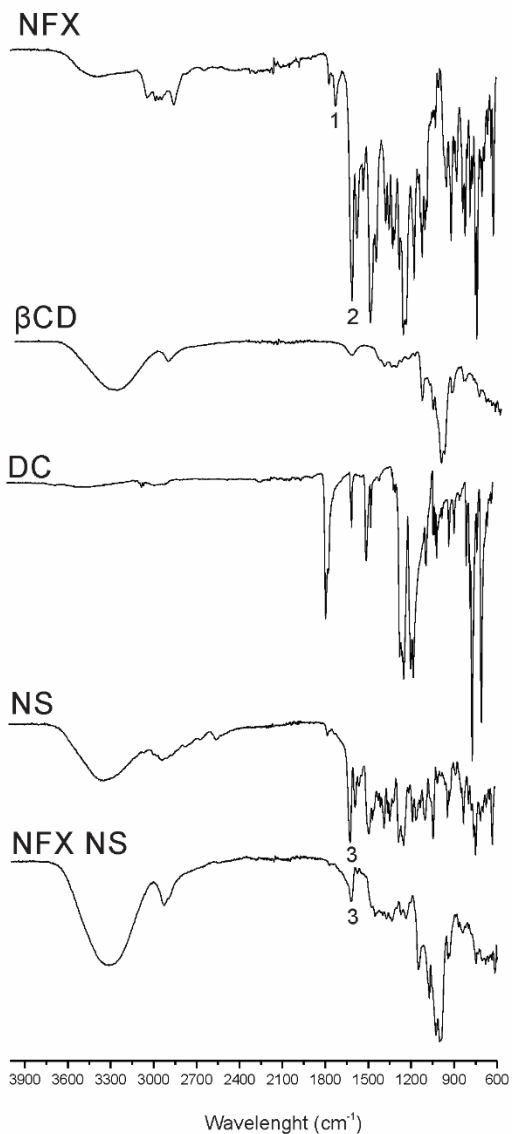


Figure 3 - TEM observations of nanosponges (NS).

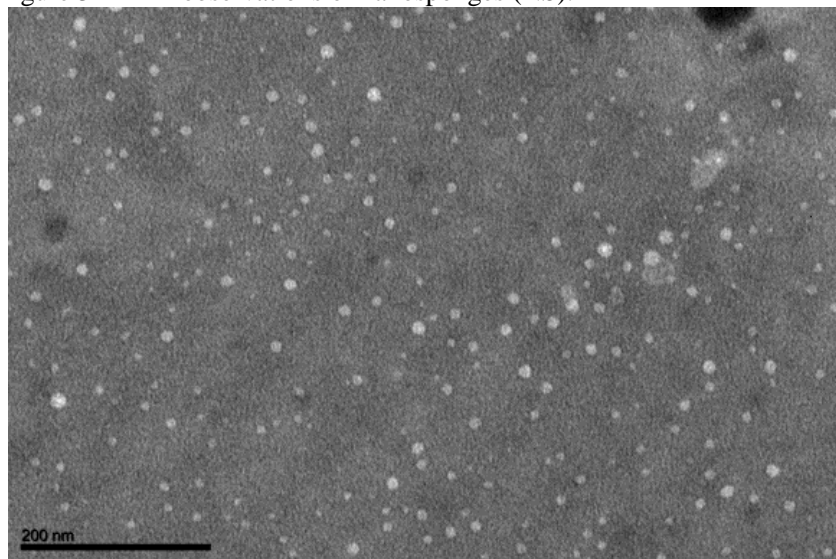
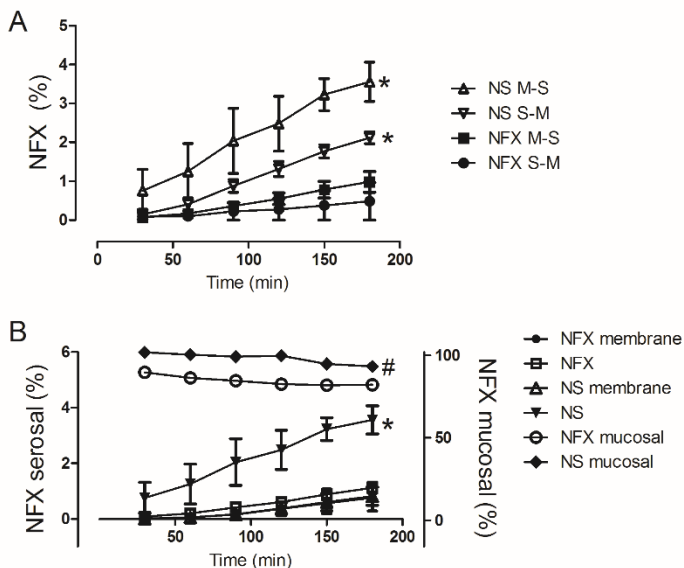


Table 1. Apparent permeability values (P_{app}) of NFX determined from Ussing chamber experiments in mucosal-to-serosal (M-S) at 37 °C, experiments realized with duodenal portions.

Sample	P_{app} ($\times 10^{-6}$ cm/s)			
	Duodenum	Jejunum	Ileum	Colon
NFX	1.07 ± 0.18	3.30 ± 0.36	3.63 ± 0.69	1.08 ± 0.73
NFX-loaded NS	3.23 ± 0.44	3.33 ± 0.43	5.26 ± 0.22	1.60 ± 0.99

NFX and NFX-loaded NS flow at different portions of rat intestine were evaluated and the results are expressed in Figure 5. It could be observed that NFX presents a flow variation between different intestinal parts, differently of NFX-loaded NS that presents an intestinal flow more similar between different regions. When comparing NFX-loaded NS to NFX at each intestinal segment, there is no statistical difference ($P > 0.05$) of flow between them.

Figure 4 - Norfloxacin (NFX) and NFX-loaded nanosponge (NS) (%) that permeates during 180 minutes at 37 °C: (A) mucosal-to-serosal (M-S) and serosal-to-mucosal (S-M), (B) in mucosal and serosal side and in presence and absence of semi-permeable membrane. (A) * $P < 0.05$ when compared NS with NFX M-S or S-M. (B) * $P < 0.05$ when compared NS with NS membrane, NFX or NFX membrane. # $P < 0.05$ when compared NS mucosal to NFX mucosal.



Nanosponge adhesion experiment

The influence of the contact with the mucus layer in NFX intestinal passage was investigated in Ussing chamber model by using a semi-permeable membrane in mucosa side. The results of NFX that permeates from NFX drug alone or NFX-loaded NS are expressed as percentage in Figure 4B. It could be observed the influence that mucus layer present in the NFX passage in the case of NS formulation. Therefore, the mucoadhesion experiment was evaluated during time in jejunum and colon due to their higher surface. The % of NFX attached is expressed in Figure 6. NFX as drug alone and inclusion complexes of NFX and β CD were evaluated also for adhesion test and revealed less than 5% of NFX attached (data not shown).

Figure 5 - Norfloxacin intestinal flow ($\times 10^{-12}$ nmol/cm²/s) at different portions of rat intestine (duodenum, jejunum, ileum and colon) from Norfloxacin drug alone (NFX) or NFX-loaded Nanosponge.

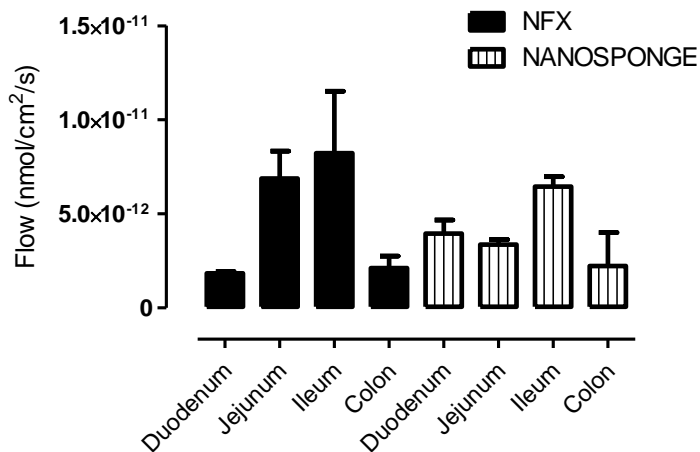
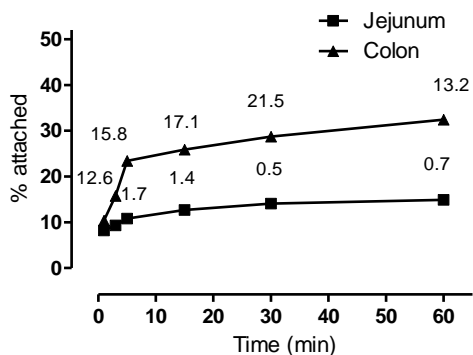


Figure 6 - Norfloxacin-loaded Nanosponge attached to the mucus layer (% attached) at jejunum and colon during 60 min.

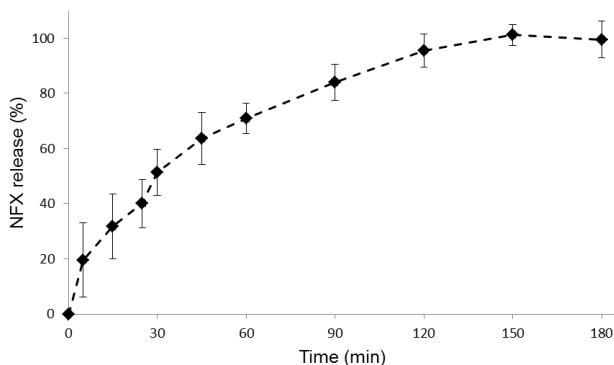


NFX-loaded NS release

In order to characterize the release of NFX from NS, the in vitro drug release was performed (Figure 7). NFX-loaded revealed a modulation in the NFX release from the NS to the dissolution media at pH 6.8, with 100% reached at 150min, confirming the strong interaction between NFX and NS,

interaction stronger than simple inclusion complexes with β CD (Mendes *et al.*, 2015a).

Figure 7 - Release profile of norfloxacin (NFX) from nanosponge (NS) in intestinal simulated fluid (pH 6.8).



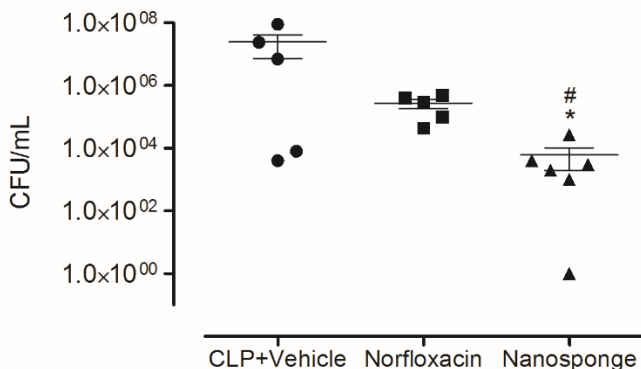
Antimicrobial *in vivo* experiments

In order to evaluate the antibacterial activity of NS, CLP model was used. According to CLP standardization, animals presented a survival of 50% after 48h. Therefore, the time of 24h was chosen to harvest the kidney due to the number of survival animals at this time point (initial of 6 animals per group). The kidney was the organ chosen to antibacterial evaluation since NFX is largely used in clinical to UTI (O'donnell e Gelone, 2004). Figure 8 presents the smaller CFU/mL detected in the kidney of animals treated with NFX-loaded NS when comparing to animals treated with NFX drug alone. It must be considered that groups CLP+vehicle and NFX was lost one animal because of the sepsis induction.

DISCUSSION

Our group revealed recently the intestinal permeability determinants of NFX in Ussing chamber model and realized that the intestinal transport of this drug is related to its zwitterionic form at biological pH. Aiming an original formulation that could overlap the biopharmaceutical problems as the intestinal transporters issues, NFX-Loaded NS at nanoscale were successfully obtained by the combination of 1:2 M/M CD:crosslinker with high NFX content.

Figure 8 - Effects of oral treatment of Nanosponge on bacterial growth. The graph shows the bacterial growth in kidney harvested 24 h after the treatment of animal treated 1h after sepsis induction by CLP. The results show the mean \pm S.E.M of 5-6 animals per group (CLP+Veh: 5; NFX: 5; NS: 6 animals). The results not showed normal distribution, Kruskal-Wallis followed by Dunn's post-test was used for statistical analysis. * $P < 0.05$ when compared NS with the CLP+Veh group and # $P < 0.05$ when compared NS with the corresponding NFX group.



DSC analysis did not show the endothermic events of NS components in the NS curve, evidencing the NS formation. NFX-loaded NS analysis showed one endothermic event of NFX fusion, confirming the HPLC loaded quantification, that NFX is not totally included in the NS. The FT-IR analyses corroborate with NS formation, being an indicative of the strong interactions between the components of NS. The absence of NFX bands reveals that there is no crystalline drug in superficial level enough to be observed in NFX-loaded NS spectrum. Photomicrographs obtained by TEM analyses revealed the globe-shape of NS formed, corroborating with the cyclic structure proposed by Swaminathan and coworkers (Swaminathan *et al.*, 2007).

In the Ussing chamber experiments, NFX-loaded NS presented higher NFX passage in comparison to drug alone in both direction, mucosal-to-serosal (M-S) and serosal-to-mucosal (S-M). Regardless of the intestinal flow was not statistically different between the intestinal segments comparing NFX-loaded NS to NFX drug alone, NFX-loaded NS presented higher permeability coefficient values in duodenum and ileum. This difference is probably related to the transporters that are expressed differently along the intestinal tract. NFX drug alone has an affinity itself to some intestinal uptake transporters to act as inhibitor, which consumes NFX

decreasing its passage. NFX-loaded in NS probably ionize differently from NFX drug alone, as already observed to β CD inclusion complexes with NFX produced by our group (Mendes *et al.*, 2015b), which could influence the ions transporters caption. If NFX-loaded in NS is not a substrate of this consumption, the amount of NFX able to permeate from NS is bigger than NFX drug alone. This hypothesis was verified by NFX quantification into the donor chamber (mucosal side). The results revealed (Figure 4B) an increased NFX quantity able to permeate of NFX-loaded in comparison to NFX drug alone, confirming our hypothesis that NS could protect NFX from uptake transporters consumption. This protection is related to the ionic charges, since the uptake transporters that consume NFX are organic cation carnitine transporters (OCTN) and organic anion transporter polypeptide (OATP). These results explain the difference observed in permeability and not observed in intestinal flow, since permeability takes into account the initial content able to permeate, which is increased for NFX-loaded NS.

The intestinal flow test in presence of semipermeable membrane revealed an important effect in the intestinal passage of NFX-loaded NS when in contact with the mucus layer. Therefore, the ability of NS to interact with mucin glycoproteins or other mucus components being immobilized in the mucus layer was evaluated. The mucoadhesion experiment verified an increasing quantity of NFX attached when loaded in NS during 60 min in jejunum and higher in colon. The higher mucoadhesion in colon is expected since it has two-layered mucus while jejunum present only one layer of mucus (Hansson, 2012). It is important to highlight that the quantity of NFX attached in the mucoadhesion experiment is at 2 cm² of the intestinal segment, extrapolating to *in vivo* system, the gastrointestinal transit will increase this percentage. The mucoadhesion ability of NS could explain the higher intestinal passage, because mucoadhesive property prolongs the residence time of NS in the mucus layer of intestinal epithelial cells, extending the quantity of NFX that permeates. The NS mucoadhesion was not caused by electrostatic interactions since the zeta potential is negative and the charge of proteins in mucus layer are also negative, therefore, the bioadhesion is probably related to hydrogen bonds and/or hydrophobic interactions between the chemical groups of NS and the mucus layer (Boddupalli *et al.*, 2010; Carvalho *et al.*, 2010).

CLP model used in the antibacterial activity has become the most widely model used for experimental sepsis and is considered a gold standard method being realistic and similar to septic human patients. Rodents with sepsis induced by CLP, like humans, also respond to antibiotics (Dellinger *et al.*, 2008; Rittirsch *et al.*, 2008; Kumar, 2011; Mayr *et al.*, 2014). After the induced sepsis, NFX-loaded NS presented an improved antibacterial activity

24h after treatment comparing to NFX drug alone. This pharmacodynamic effect is probably related to the higher solubility of the drug in NS system, higher intestinal flow observed in Ussing chambers and the mucoadhesion caused by this system. The NS as a mucoadhesive system could extend the contact time between NFX and the mucus layer, increasing its absorption, which will lead to a better antibacterial activity even after 24h.

Interestingly, antibacterial activity revealed that NFX drug alone was not different from CLP+Vehicle in the timepoint evaluated. This fact is probably related to the release profile of NS that presented a slow and modulated release of NFX than the drug already dissolved. NFX-loaded NS presented a modulation of NFX release which could extend the pharmacodynamic effect. This difference could explain the effect observed in 24h to NFX-loaded NS and not to NFX drug alone.

CONCLUSION

The association of NFX in the β CD-based NS resulted in a mucoadhesive formulation with enhanced permeation through rat intestine using Ussing chamber method. The NFX-loaded NS presented a modulated release of NFX which extend the *in vivo* antibacterial activity in rats caused by sepsis induction. In this way, NS might be suitable carrier of NFX to maximize and facilitate oral absorption, which could lead to a reduction in the dose required due to its higher antibacterial activity, increasing the therapeutic benefits as a potential alternative to the existing NFX drug formulations.

REFERENCES

BARBAS, R. et al. Polymorphism of norfloxacin: Evidence of the enantiotropic relationship between polymorphs A and B. *Crystal growth & design*, v. 6, n. 6, p. 1463-1467, 2006.

BENNETT, J. E.; DOLIN, R.; BLASER, M. J. *Principles and practice of infectious diseases*. Elsevier Health Sciences, 2014. ISBN 1455748013.

BODDUPALLI, B. M. et al. Mucoadhesive drug delivery system: An overview. *Journal of advanced pharmaceutical technology & research*, v. 1, n. 4, p. 381, 2010.

BREDA, S. A. et al. Solubility behavior and biopharmaceutical classification of novel high-solubility ciprofloxacin and norfloxacin

pharmaceutical derivatives. *International journal of pharmaceutics*, v. 371, n. 1, p. 106-113, 2009.

CARVALHO, F. C. et al. Mucoadhesive drug delivery systems. *Brazilian Journal of Pharmaceutical Sciences*, v. 46, n. 1, p. 1-17, 2010.

CASTIGLIONE, F. et al. Vibrational dynamics and hydrogen bond properties of β -CD nanosponges: an FTIR-ATR, Raman and solid-state NMR spectroscopic study. *Journal of Inclusion Phenomena and Macrocyclic Chemistry*, v. 75, n. 3-4, p. 247-254, 2013.

CAVALLI, R.; TROTTA, F.; TUMIATTI, W. Cyclodextrin-based nanosponges for drug delivery. *Journal of inclusion phenomena and macrocyclic chemistry*, v. 56, n. 1-2, p. 209-213, 2006.

CHALLA, R. et al. Cyclodextrins in drug delivery: an updated review. *AAPS PharmSciTech*, v. 6, n. 2, p. E329-E357, 2005.

CLSI, C. A. L. S. I., Ed. Methods for dilution antimicrobial susceptibility testing for bacteria that grew aerobically; approved standard. CLSI document M7-A10. Clinical and Laboratory Standards Institute, Wayne, PA Clinical and Laboratory Standards Institute, CLSI document M7-A10, Seventh Edition ed. 2009.

DEL VALLE, E. M. M. Cyclodextrins and their uses: a review. *Process Biochemistry*, v. 39, n. 9, p. 1033-1046, 2004.

DELLINGER, R. P. et al. Surviving Sepsis Campaign: international guidelines for management of severe sepsis and septic shock: 2008. *Intensive care medicine*, v. 34, n. 1, p. 17-60, 2008.

HANSSON, G. C. Role of mucus layers in gut infection and inflammation. *Current opinion in microbiology*, v. 15, n. 1, p. 57-62, 12/14 2012.

KUMAR, A. Optimizing antimicrobial therapy in sepsis and septic shock. *Critical care nursing clinics of North America*, v. 23, n. 1, p. 79-97, 2011.

LI, D.; MA, M. Nanosponges for water purification. *Clean products and processes*, v. 2, n. 2, p. 112-116, 2000.

LOFTSSON, T.; BREWSTER, M. E. Cyclodextrins as functional excipients: Methods to enhance complexation efficiency. *Journal of Pharmaceutical Sciences*, v. 101, n. 9, p. 3019-3032, 2012.

MAYR, F. B.; YENDE, S.; ANGUS, D. C. Epidemiology of severe sepsis. *Virulence*, v. 5, n. 1, p. 4-11, 2014.

MENDES et al. Investigation of β -cyclodextrin–norfloxacin inclusion complexes. Part 1. Preparation, physicochemical and microbiological characterization. *Expert review of anti-infective therapy*, v. 13, n. 1, p. 119-129, 2015a.

MENDES, C. et al. Investigation of β -cyclodextrin – norfloxacin inclusion complexes. Part 2. Inclusion mode and stability studies. *Expert Review of Anti-Infective Therapy*, v. 13, n. 1, p. 131–140, 2015b.

O'DONNELL, J. A.; GELONE, S. P. The newer fluoroquinolones. *Infectious disease clinics of North America*, v. 18, n. 3, p. 691-716, 2004.

OLIVEIRA, P. R. et al. Liquid chromatographic determination of norfloxacin in extended-release tablets. *Journal of chromatographic science*, v. 47, n. 9, p. 739-744, 2009.

RITTIRSCH, D. et al. Functional roles for C5a receptors in sepsis. *Nature medicine*, v. 14, n. 5, p. 551-557, 2008.

SJÖBERG, Å. et al. Comprehensive study on regional human intestinal permeability and prediction of fraction absorbed of drugs using the Ussing chamber technique. *European Journal of Pharmaceutical Sciences*, v. 48, n. 1, p. 166-180, 2013.

SWAMINATHAN, S.; CAVALLI, R.; TROTTA, F. Cyclodextrin-based nanosponges: a versatile platform for cancer nanotherapeutics development. *Wiley Interdisciplinary Reviews: Nanomedicine and Nanobiotechnology*, 2016.

SWAMINATHAN, S. et al. Formulation of betacyclodextrin based nanosponges of itraconazole. *Journal of Inclusion Phenomena and Macrocyclic Chemistry*, v. 57, n. 1-4, p. 89-94, 2007.

DISCUSSÃO GERAL

Grande percentual de candidatos a fármacos apresenta falhas em estudos pré-clínicos, devido às propriedades inadequadas de absorção. Fármacos que pertencem à classe IV são os que manifestam maior dificuldade para a administração oral. Compostos farmacêuticos pertencentes à classe IV tem a sua absorção limitada não só pela baixa dissolução aquosa no ambiente gastrointestinal, mas também pela sua baixa capacidade de permeação, de modo que níveis muito baixos de fármaco dissolvido levarão a uma baixa biodisponibilidade (Vasconcelos *et al.*, 2007).

Um dos desafios encontrados no desenvolvimento de formulações contendo fármacos da classe IV situa-se na dificuldade de desenvolver sistemas de liberação capazes de aperfeiçoar ambas as propriedades em deficiência. Alguns avanços tecnológicos foram propostos nesse sentido, como a redução do tamanho de partícula, emprego de dispersões sólidas e complexação com CD. Porém, estas tecnologias demonstram certas limitações e apesar de casos com sucesso, dependem em grande parte das propriedades dos fármacos (Vierstein *et al.*, 2003; Hauss, 2007).

As nanoemulsões constituem um avanço na terapêutica de fármacos com baixa solubilidade aquosa e já demonstram grande eficiência no incremento da biodisponibilidade oral. Esta tecnologia representa uma estratégia eficiente que é capaz de prolongar a estabilidade do fármaco na formulação, por meio da proteção do mesmo frente às possíveis reações de degradação. A técnica de nanoemulsificação espontânea emprega baixa energia e baixo custo para gerar as nanoemulsões e uma vez selecionados os componentes ideais da formulação, tais sistemas são de fácil preparação, manipulação e transposição para escala industrial (Gursoy e Benita, 2004; Hong *et al.*, 2006; Zhao *et al.*, 2010; Zabaleta *et al.*, 2012).

Foram propostas duas diferentes tecnologias para a obtenção de nanoemulsões de HCTZ ainda não descritas na literatura e para ambas foram avaliadas a resposta terapêutica *in vivo*. O capítulo 2 apresenta o desenvolvimento de sistemas autonanoemulsionáveis contendo a HCTZ. Foi possível obter um sistema em nanoescala com autoemulsificação em água e nos fluidos gastrointestinais simulados com reduzida quantidade de surfactante. Este sistema proporcionou um aumento na excreção de íons *in vivo* já nas primeiras horas após a administração oral de cápsulas contendo o sistema e um aumento total no volume de urina em comparação com a HCTZ pura. A presença do Cremophor EL na formulação pode auxiliar na inibição do efluxo intestinal encontrado para a HCTZ. Desta forma, foi obtida com sucesso uma formulação autonanoemulsionável para liberação da HCTZ.

O capítulo 3 descreve o desenvolvimento de uma nanoemulsão por emulsificação espontânea, um método simples e de fácil transposição para a escala industrial. Esta nanoemulsão foi revestida com um agente

mucoadesivo amplamente utilizado, a quitosana, e a sua bioadesão foi verificada objetivando o maior contato da nanoemulsão com as mucosas intestinais a fim de facilitar a absorção do fármaco. A inovação deste capítulo vem na forma da aspersão desta nanoemulsão revestida em diferentes materiais de parede para secagem e veiculação de um sistema sólido que possa ser facilmente redisperso em água.

Dadas estas premissas, pode-se notar que ambos os sistemas nanoestruturados desenvolvidos para liberação da HCTZ foram obtidos com sucesso, demonstrando uma melhora do perfil de dissolução e na atividade diurética em animais. Visando a comparação entre os sistemas, parâmetros principais de custo, facilidade de preparação, liberação do fármaco e atividade diurética foram considerados importantes e, portanto, avaliados. A HCTZ no sistema autonanoemulsionável apresentou uma liberação um pouco mais lenta que o sistema Trojan, em condições gastrointestinais simuladas. Acredita-se que a formação espontânea da nanoemulsão (*in vitro*) requer mais tempo que a solubilização do material de parede e redispersão da nanoemulsão pronta presente no sistema Trojan. A diferença observada *in vitro* no tempo de liberação do fármaco dos sistemas não pôde ser notada no estudo *in vivo*, uma vez que ambos os sistemas apresentaram aumento na excreção de íons já nas primeiras horas. O Cremophor EL utilizado no sistema autonanoemulsionável é reconhecido como inibidor do efluxo intestinal que a HCTZ comprovadamente apresenta. Porém, a melhora na absorção devido à este fato não gerou uma diferença estatística entre os sistemas. Um fato notório neste estudo foi a ação prolongada que o sistema Trojan foi capaz de proporcionar à ação diurética do fármaco. A hipótese que pode ser levantada sobre este ponto, e diferencial desta formulação, é de que a mucoadesão evidenciada para as partículas Trojan pode realmente aumentar o tempo de contato da formulação com as mucosas, estendendo significativamente seu efeito farmacodinâmico. Terapeuticamente, esta vantagem pode gerar redução de doses e/ou intervalos de administração oral do fármaco. Entretanto, vale destacar que para a produção do sistema Trojan empregam-se mais etapas e exige-se a disponibilidade de equipamento (*spray-dryer*). O maior tempo e custo de preparação do sistema Trojan pode ser compensatório se as doses e o esquema posológico puderem, por ventura, ser alterados. Uma vez de interesse público e industrial, estudos clínicos que apliquem os sistemas desenvolvidos poderão responder às questões abordadas. O presente trabalho apresenta alternativas terapêuticas frente às formas farmacêuticas convencionais disponíveis atualmente no mercado, bem como a inovação para uso da indústria, academia e comunidade científica.

Uma vez determinado o mecanismo de comportamento *in vitro* é importante a realização de estudos biológicos. Normalmente as formulações obtidas são testadas diretamente em estudos com animais ou em estudos pré-clínicos. Porém, esta conduta acarreta um maior uso de animais além de ser economicamente mais dispendiosa que a implementação de um estudo *in vitro* simples intermediário para “screening” das formulações (Barthe *et al.*, 1999). Um sistema muito utilizado para avaliação da permeabilidade intestinal são as “Ussing chambers” ou câmaras de Ussing, em que pequenas secções da mucosa intestinal são alocadas entre duas câmaras contendo solução tamponada e tanto o transporte das moléculas através do tecido como entre as câmaras pode ser medido (Lennernäs, 2007). Neste contexto, por meio da execução desta técnica torna-se possível a avaliação da permeabilidade intestinal *ex vivo* de fármacos. O capítulo 4 aborda o estudo dos fatores de permeabilidade intestinal do NFX, outro fármaco classe biofarmacêutica IV, objeto de estudo desde o projeto do mestrado. Esta parte do trabalho foi realizada durante estágio sanduíche com equipe renomada no estudo de moléculas biologicamente ativas através de barreiras biológicas.

A determinação dos fatores de permeabilidade intestinal do NFX desmistificou várias descrições da literatura revelando ainda outras informações relevantes no âmbito do desenvolvimento de fármacos bem como de interações medicamentosas. A primeira informação fundamental para o entendimento do processo de absorção oral do NFX é o conhecimento em qual porção do intestino que o fármaco apresenta uma maior absorção. Este trabalho revelou uma absorção maior na porção ílaca, seguida do jejuno, duodeno e cólon, em ordem decrescente, contrariando literaturas mais antigas que revelavam uma maior absorção das fluorquinolonas no duodeno. Foi possível ainda a confirmação do efluxo intestinal do NFX já determinado para outros fármacos da classe, sendo um dos fatores responsáveis pela sua baixa permeabilidade intestinal. O estudo inicial do mestrado de determinação dos valores de pka do fármaco viabilizou a investigação quanto à ligação do NFX aos transportadores intestinais de cátions e ânions, devido ao fato do fármaco apresentar-se zwitteriônico no pH intestinal. Desta forma, a pesquisa revelou que o NFX por si só tem uma afinidade por transportadores de influxo específicos. Esta ligação está relacionada com a passagem intestinal do fármaco bem como com a ação de inibidor que o NFX apresenta frente à alguns transportadores.

O estudo da influência dos transportadores intestinais na farmacocinética de vários princípios ativos tem despertado interesse de muitos pesquisadores nos últimos anos devido às informações valiosas que são reveladas facilitando a compreensão dos mecanismos de absorção oral de fármacos. Pouquíssimos trabalhos com este foco têm sido desenvolvidos

no país, e a utilização de tecido vivo possibilita a avaliação completa de todos os fatores presentes nos enterócitos, sendo estes morfológicos, fisiológicos ou de permeabilidade envolvendo processos mediados por transportadores. Quando cultura de células são utilizadas para estudos de permeabilidade, os fatores biológicos são estudados separadamente, não sendo possível mimetizar as condições *in vivo* que são apresentadas aos fármacos ao atravessarem as barreiras biológicas.

O conhecimento dos mecanismos de permeabilidade intestinal do NFX serve, portanto de base para a comunidade científica e clínica, de forma a auxiliar na compreensão das interações medicamentosas. Além disso, o entendimento específico da ligação do NFX com os transportadores pode ser utilizado pelas indústrias farmacêuticas para o delineamento de novas formas farmacêuticas que sejam capazes de aumentar a absorção de antimicrobianos, impactando na eficiência terapêutica, na aderência dos pacientes ao tratamento bem como no surgimento de novos micro-organismos resistentes.

A presente tese utilizou o conhecimento inicial gerado durante o mestrado no desenvolvimento de complexos de inclusão contendo NFX bem como os fatores de permeabilidade determinados para o NFX para desenvolver uma formulação inovadora e direcionada para as limitações físico-químicas deste fármaco. A NS de NFX desenvolvida é o resultado do planejamento racional de novas formulações, para que estas possam atingir resultados promissores *in vivo*. A NS apresentou uma modulação na liberação do NFX a qual foi capaz de estender a atividade antibacteriana. Com a melhora da sua atividade farmacodinâmica, a NS pode ser um carreador para o NFX capaz de maximizar e facilitar sua absorção oral. Uma melhora na biodisponibilidade pode influenciar na redução da dose aumentando os benefícios da terapia e surgindo como uma alternativa frente às formulações presentes atualmente no mercado.

A despeito do grande progresso científico, tecnológico e de inovação decorrente do avanço das ciências farmacêuticas e médicas, o desenvolvimento de sistemas ainda apresenta várias dificuldades em termos de estratégia terapêutica e de obtenção de novas formulações. Desta forma, é imperativa a busca constante de novas alternativas terapêuticas que possam modificar este panorama adverso. Neste cenário, foi possível observar o desenvolvimento de sistemas novos com princípios ativos amplamente reconhecidos de forma a explorar os efeitos benéficos dos mesmos. A presente tese fornece um estudo de sistemas nanoestruturados contendo HCTZ ou NFX bem como o estudo de permeabilidade intestinal do NFX visando a melhora das propriedades biofarmacêuticas e a consequente eficácia terapêutica que possibilite a adesão do paciente ao tratamento por meio da utilização de alternativas tecnológica e fármaco-econômica.

CONCLUSÕES

- O *screening* de pré-formulação foi obtido com sucesso por meio da construção de diagramas de fase ternários;
- O desenvolvimento e obtenção de um sistema autonanoemulsionável de liberação da HCTZ foi possível combinando-se triglicerídeos de cadeia média, Cremophor EL e Transcutol P;
- A verificação da autonanoemulsificação foi obtida nos fluidos gastrointestinais simulados para melhor prever as condições *in vivo*;
- A melhora do perfil de dissolução do sistema autonanoemulsionável contendo HCTZ foi observada e refletiu na atividade diurética nos animais apresentando natriurese, caliurese e cloriurese nos estágios iniciais com um aumento do volume total de urina em 24h após a administração do sistema em comparação com o fármaco puro;
- O delineamento de um sistema autonanoemulsionável de HCTZ produziu uma melhora na atividade farmacodinâmica devido à maior dissolução atingida juntamente com a inibição do efluxo intestinal pelo Cremophor EL que este sistema pode proporcionar, mostrando-se uma abordagem eficiente para modular a absorção da HCTZ.
- Nanoemulsões foram produzidas pelo método de nanoemulsificação espontânea combinando-se triglicerídeos de cadeia média, Lipoid S75® e Pluronic F68® com alta eficiência de encapsulação.
- Um método simples e de baixa energia foi aplicado para a obtenção de nanoemulsões mucoadesivas estáveis, apresentando vantagens em termos de produção facilitando a transposição de escala;
- As propriedades mucoadesivas foram fornecidas pelo revestimento com quitosana e a microencapsulação das nanoemulsões foi obtida com sucesso por *spray-dryer* usando Aerosil® como material de parede gerando as partículas Trojan;
- A rápida redispersão da nanoemulsão nos fluidos simulados levou a uma completa e rápida dissolução da HCTZ no meio gástrico;
- A atividade farmacodinâmica da HCTZ presente do sistema Trojan foi incrementada estendendo o efeito diurético do fármaco;
- O novo sistema mucoadesivo particulado Trojan desenvolvido para a liberação da HCTZ mostrou-se promissor para superar as limitações em termos de absorção e consequentemente melhorar a eficácia terapêutica da HCTZ;
- O estudo dos mecanismos de permeabilidade intestinal do NFX revelou que sua permeação é transporte-dependente e que a maior absorção ocorre a nível ílaco seguido do jejuno, duodeno e do cólon;

- Foi possível determinar por meio de câmara de Ussing que os transportadores BCRP e MRP estão envolvidos no efluxo intestinal do NFX e os transportadores PEPT1, PMAT e OCT no influxo do fármaco;
- Revelou-se ainda que o NFX tem uma afinidade pelos transportadores OCTN e OATP, demonstrando que o NFX pode inibir estes transportadores e influenciar na absorção de outros fármacos;
- A descrição atualizada dos fatores de permeabilidade intestinal pode contribuir para o desenvolvimento racional de novas formas farmacêuticas que podem diminuir o efluxo intestinal do NFX e ainda melhorar suas propriedades biofarmacêuticas evitando interações fármaco-fármaco;
- O estudo da permeabilidade intestinal possibilitou o desenvolvimento de uma formulação que melhore os problemas revelados pela câmara de Ussing, as nanoesponjas de norfloxacino.
- A obtenção de nanoesponjas de norfloxacino que apresentam mucoadesão refletiram na melhora da passagem intestinal do fármaco;
- A nanoesponja de norfloxacino apresentou uma liberação estendida do fármaco capaz de prolongar a atividade antibacteriana em comparação com o fármaco puro.

REFERÊNCIAS

- AL-RASHOOD, K. A. *et al.* Bioequivalence evaluation of norfloxacin 400 mg tablets (Uroxin and Noroxin) in healthy human volunteers. **Biopharmaceutics & drug disposition**, v. 21, p. 175-179, 2000.
- ALDRED, K. J.; KERNS, R. J.; OSHEROFF, N. Mechanism of Quinolone Action and Resistance. **Biochemistry**, v. 53, n. 10, p. 1565-1574, 2014.
- ALMEIDA, M. E.; TEIXEIRA, H. F.; KOESTER, L. S. Preparação de Emulsões Submicrométricas: Aspectos Teóricos sobre os Métodos Empregados na Atualidade. **Latin American Journal of Pharmacy**, v. 27, n. 5, p. 780-8, 2008.
- ALNAJJAR, A.; IDRIS, A. M.; ABUSEADA, H. H. Development of a stability-indicating capillary electrophoresis method for norfloxacin and its inactive decarboxylated degradant. **Microchemical Journal**, v. 87, n. 1, p. 35-40, 2007.
- ALVAREZ, A. I. *et al.* Fluoroquinolone efflux mediated by ABC transporters. **Journal of pharmaceutical sciences**, v. 97, n. 9, p. 3483-3493, 2008.
- AMIDON, G. L. *et al.* A theoretical basis for a biopharmaceutic drug classification: the correlation of in vitro drug product dissolution and in vivo bioavailability. **Pharmaceutical Research**, v. 12, n. 3, p. 413-20, 1995.
- ANDERSSON, M. I.; MACGOWAN, A. P. Development of the quinolones. **Journal of Antimicrobial Chemotherapy**, v. 51, n. 1, p. 1-11, 2003.
- ANDREWS, G. P.; LAVERTY, T. P.; JONES, D. S. Mucoadhesive polymeric platforms for controlled drug delivery. **European Journal of Pharmaceutics and Biopharmaceutics**, v. 71, n. 3, p. 505-518, 2009.
- ANTON, N.; BENOIT, J.-P.; SAULNIER, P. Design and production of nanoparticles formulated from nano-emulsion templates — a review. **Journal of Controlled Release**, v. 128, n. 3, p. 185-199, 2008.
- ANVISA. **Consulta a Medicamentos e Hemoderivados**. Disponível em: <<http://portal.anvisa.gov.br/medicamentos-e-hemoderivados>>. Acesso em 17 jan 2017.

AVDEEF, A.; BERGER, C. M.; BROWNELL, C. pH-metric solubility. 2: correlation between the acid-base titration and the saturation shake-flask solubility-pH methods. **Pharmaceutical research**, v. 17, n. 1, p. 85-89, 2000.

BANDYOPADHYAY, S.; KATARE, O. P.; SINGH, B. Optimized self nano-emulsifying systems of ezetimibe with enhanced bioavailability potential using long chain and medium chain triglycerides. **Colloids and Surfaces B: Biointerfaces**, v. 100, n. 0, p. 50-61, 2012.

BARBAS, R. *et al.* Polymorphism of norfloxacin: Evidence of the enantiotropic relationship between polymorphs A and B. **Crystal growth & design**, v. 6, n. 6, p. 1463-1467, 2006.

BARTHE, L.; WOODLEY, J.; HOUIN, G. Gastrointestinal absorption of drugs: methods and studies. **Fundamental & clinical pharmacology**, v. 13, n. 2, p. 154-168, 1999.

BENNETT, J. E.; DOLIN, R.; BLASER, M. J. **Principles and practice of infectious diseases**. Elsevier Health Sciences, 2014.

BODDUPALLI, B. M. *et al.* Mucoadhesive drug delivery system: An overview. **Journal of advanced pharmaceutical technology & research**, v. 1, n. 4, p. 381, 2010.

BOLON, M. K. The newer fluoroquinolones. **Infectious Disease Clinics of North America**, v. 23, n. 4, p. 1027, 2009.

BOUCHEMAL, K. New challenges for pharmaceutical formulations and drug delivery systems characterization using isothermal titration calorimetry. **Drug Discovery Today**, v. 13, n. 21, p. 960-972, 2008.

BOUCHEMAL, K. *et al.* Nano-emulsion formulation using spontaneous emulsification: solvent, oil and surfactant optimisation. **International journal of pharmaceutics**, v. 280, n. 1, p. 241-251, 2004.

BRASIL. **Resolução RDC n. 20, de 5 de maio de 2011**. AGÊNCIA NACIONAL DE VIGILÂNCIA SANITÁRIA (ANVISA). Brasília, Diário Oficial da União 09 mai 2011.

BREDA, S. A. et al. Solubility behavior and biopharmaceutical classification of novel high-solubility ciprofloxacin and norfloxacin pharmaceutical derivatives. **International journal of pharmaceutics**, v. 371, n. 1, p. 106-113, 2009.

BRUNTON, L.; CHABNER, B.; KNOLLMAN, B. **Goodman and Gilman's the pharmacological basis of therapeutics**. 12^a ed. McGraw Hill Professional, 2010.

BRUXEL, F. *et al.* Nanoemulsões como sistemas de liberação parenteral de fármacos. **Química nova**. São Paulo: Sociedade Brasileira de Química, 1978-. Vol. 35, n. 9, p. 1827-1840, 2012.

BUCKLEY, S. T. *et al.* *In vitro* models to evaluate the permeability of poorly soluble drug entities: Challenges and perspectives. **European Journal of Pharmaceutical Sciences**, v. 45, n. 3, p. 235-250, 2012.

CAGNO, M. D. *et al.* Overcoming instability and low solubility of new cytostatic compounds: A comparison of two approaches. **European Journal of Pharmaceutics and Biopharmaceutics**, v. 80, n. 3, p. 657-662, 2012.

CAO, C. X. *et al.* J774 macrophages secrete antibiotics via organic anion transporters. **Journal of Infectious Diseases**, v. 165, n. 2, p. 322-328, 1992.

CARVALHO, F. C. *et al.* Mucoadhesive drug delivery systems. **Brazilian Journal of Pharmaceutical Sciences**, v. 46, n. 1, p. 1-17, 2010.

CASTIGLIONE, F. *et al.* Vibrational dynamics and hydrogen bond properties of β -CD nanosponges: an FTIR-ATR, Raman and solid-state NMR spectroscopic study. **Journal of Inclusion Phenomena and Macrocyclic Chemistry**, v. 75, n. 3-4, p. 247-254, 2013.

CAVALLI, R.; TROTTA, F.; TUMIATTI, W. Cyclodextrin-based nanosponges for drug delivery. **Journal of inclusion phenomena and macrocyclic chemistry**, v. 56, n. 1-2, p. 209-213, 2006.

CHADHA, R. *et al.* Exploring the potential of lecithin/chitosan nanoparticles in enhancement of antihypertensive efficacy of hydrochlorothiazide. **Journal of microencapsulation**, v. 29, n. 8, p. 805-812, 2012.

CHALLA, R. *et al.* Cyclodextrins in drug delivery: an updated review. **AAPS PharmSciTech**, v. 6, n. 2, p. E329-E357, 2005.

CHENG, G. *et al.* Antibacterial Action of Quinolones: From Target to Network. **European Journal of Medicinal Chemistry**, 2013.

CHOCKALINGAM, A.; CAMPBELL, N. R.; FODOR, G. J. Worldwide epidemic of hypertension. **Canadian Journal of Cardiology**, v. 22, n. 7, p. 553-555, 2006.

CHOWDARY, K. P. R.; RAO, Y. Mucoadhesive microspheres for controlled drug delivery. **Biological and pharmaceutical Bulletin**, v. 27, n. 11, p. 1717-1724, 2004.

CLSI. **Methods for dilution antimicrobial susceptibility testing for bacteria that grew aerobically; approved standard**. CLSI document M7-A10. Clinical and Laboratory Standards Institute, Wayne, PA Clinical and Laboratory Standards Institute, CLSI document M7-A10, Seventh Edition ed. 2009.

DALHOFF, A. Resistance surveillance studies: a multifaceted problem — the fluoroquinolone example. **Infection**, v. 40, n. 3, p. 239-262, 2012.

DATE, A. A. *et al.* Self-nanoemulsifying drug delivery systems: formulation insights, applications and advances. **Nanomedicine**, v. 5, n. 10, p. 1595-1616, 2010.

DEL VALLE, E. M. M. Cyclodextrins and their uses: a review. **Process Biochemistry**, v. 39, n. 9, p. 1033-1046, 2004.

DELLINGER, R. P. *et al.* Surviving Sepsis Campaign: international guidelines for management of severe sepsis and septic shock: 2008. **Intensive care medicine**, v. 34, n. 1, p. 17-60, 2008.

DRESSMAN, J. B.; REPPAS, C. **Oral drug absorption: Prediction and assessment**. CRC Press, 2016.

DRLICA, K. *et al.* Quinolone-mediated bacterial death. **Antimicrobial agents and chemotherapy**, v. 52, n. 2, p. 385-392, 2008.

EL KHATEEB, S. Z.; ABDEL RAZEK, S. A.; AMER, M. Stability-indicating methods for the spectrophotometric determination of norfloxacin.

Journal of Pharmaceutical and Biomedical Analysis, v. 17, n. 4, p. 829-840, 1998.

EMMERSON, A.; JONES, A. The quinolones: decades of development and use. **Journal of Antimicrobial Chemotherapy**, v. 51, n. suppl 1, p. 13-20, 2003.

ESTUDANTE, M. *et al.* Intestinal drug transporters: an overview. **Advanced drug delivery reviews**, v. 65, n. 10, p. 1340-1356, 2013.

FANG, X. *et al.* Purification and identification of an impurity in bulk hydrochlorothiazide. **Journal of pharmaceutical sciences**, v. 90, n. 11, p. 1800-1809, 2001.

FARMACOPEIA BRASILEIRA. 5^a ed. Parte I, São Paulo: ATHENEU, 2010.

FLORENCE, A. T.; ATTWOOD, D. **Physicochemical principles of pharmacy**. London: Pharmaceutical Press, 2011.

FLYNN, J. T. Pharmacologic management of childhood hypertension: current status, future challenges. **American journal of hypertension**, v. 15, n. S2, p. 30S-33S, 2002.

FRANCO, A. V. M. Recurrent urinary tract infections. **Best Practice & Research Clinical Obstetrics & Gynaecology**, v. 19, n. 6, p. 861-873, 2005.

GONZÁLEZ-CHAMORRO, F. *et al.* Urinary tract infections and their prevention. **Actas Urológicas Españolas (English Edition)**, v. 36, n. 1, p. 48-53, 2012.

GOTOH, Y.; KAMADA, N.; MOMOSE, D. The advantages of the Ussing chamber in drug absorption studies. **Journal of biomolecular screening**, v. 10, n. 5, p. 517-523, 2005.

GRASS, G. M. Simulation models to predict oral drug absorption from in vitro data. **Advanced drug delivery reviews**, v. 23, n. 1, p. 199-219, 1997.

GURSOY, R. N.; BENITA, S. Self-emulsifying drug delivery systems (SEDDS) for improved oral delivery of lipophilic drugs. **Biomedicine & Pharmacotherapy**, v. 58, n. 3, p. 173-182, 2004.

HANSSON, G. C. Role of mucus layers in gut infection and inflammation. **Current opinion in microbiology**, v. 15, n. 1, p. 57-62, 2012.

HAUSS, D. J. Oral lipid-based formulations. **Advanced Drug Delivery Reviews**, v. 59, n. 7, p. 667-76, 2007.

HONG, J.-Y. *et al.* A new self-emulsifying formulation of itraconazole with improved dissolution and oral absorption. **Journal of Controlled Release**, v. 110, n. 2, p. 332-338, 2006.

JANTRATID, E. *et al.* Dissolution media simulating conditions in the proximal human gastrointestinal tract: an update. **Pharmaceutical research**, v. 25, n. 7, p. 1663-1676, 2008.

KADAM, Y. *et al.* Micelles from PEO-PPO-PEO block copolymers as nanocontainers for solubilization of a poorly water soluble drug hydrochlorothiazide. **Colloids and Surfaces B: Biointerfaces**, v. 83, n. 1, p. 49-57, 2011.

KASIM, N. A. *et al.* Molecular properties of WHO essential drugs and provisional biopharmaceutical classification. **Molecular pharmaceutics**, v. 1, n. 1, p. 85-96, 2004.

KAWAKAMI, K. Modification of physicochemical characteristics of active pharmaceutical ingredients and application of supersaturatable dosage forms for improving bioavailability of poorly absorbed drugs. **Advanced Drug Delivery Reviews**, v. 64, n. 6, p. 480-495, 2012.

KEARNEY, P. M. *et al.* Global burden of hypertension: analysis of worldwide data. **The Lancet**, v. 365, n. 9455, p. 217-223, 2005.

KHALED, K. A.; ASIRI, Y. A.; EL-SAYED, Y. M. In vivo evaluation of hydrochlorothiazide liquisolid tablets in beagle dogs. **International Journal of Pharmaceutics**, v. 222, n. 1, p. 1-6, 2001.

KOROLKOVAS, A.; FRANÇA, F. F. D. A. C. D.; CUNHA, B. C. D. A. **Dicionário terapêutico Guanabara: 2006/2007**, 2006.

KRIEGER, J. N. Urinary tract infections: what's new? **The Journal of urology**, v. 168, n. 6, p. 2351-2358, 2002.

KUMAR, A. Optimizing antimicrobial therapy in sepsis and septic shock. **Critical care nursing clinics of North America**, v. 23, n. 1, p. 79-97, 2011.

KUMAR, P.; SINGH, C. A study on solubility enhancement methods for poorly water soluble drugs. **American Journal of Pharmacological Sciences**, v. 1, n. 4, p. 67-73, 2013.

LENNERNÄS, H. Animal data: the contributions of the Ussing Chamber and perfusion systems to predicting human oral drug delivery in vivo. **Advanced drug delivery reviews**, v. 59, n. 11, p. 1103-1120, 2007.

LENNERNÄS, H.; ABRAHAMSSON, B. The use of biopharmaceutic classification of drugs in drug discovery and development: current status and future extension. **Journal of pharmacy and pharmacology**, v. 57, n. 3, p. 273-285, 2005.

LI, D.; MA, M. Nanosponges for water purification. **Clean products and processes**, v. 2, n. 2, p. 112-116, 2000.

LI, X. *et al.* Microencapsulation of nanoemulsions: novel Trojan particles for bioactive lipid molecule delivery. **International journal of nanomedicine**, v. 6, p. 1313 - 1325, 2011.

LIPINSKI, C. A. Poor Aqueous Solubility-an Industry Wide Problem in ADME Screening. **American Pharmaceutical Review**, v. 5, p. 82-85, 2002.

LOFTSSON, T.; BREWSTER, M. E. Cyclodextrins as functional excipients: Methods to enhance complexation efficiency. **Journal of Pharmaceutical Sciences**, v. 101, n. 9, p. 3019-3032, 2012.

MAYR, F. B.; YENDE, S.; ANGUS, D. C. Epidemiology of severe sepsis. **Virulence**, v. 5, n. 1, p. 4-11, 2014.

MCCLEMENTS, D. J.; RAO, J. Food-grade nanoemulsions: formulation, fabrication, properties, performance, biological fate, and potential toxicity. **Critical reviews in food science and nutrition**, v. 51, n. 4, p. 285-330, 2011.

MENDES, C. *et al.* Investigation of β -cyclodextrin–norfloxacin inclusion complexes. Part 1. Preparation, physicochemical and microbiological characterization. **Expert review of anti-infective therapy**, v. 13, n. 1, p. 119-129, 2015a.

MENDES, C. *et al.* Investigation of β -cyclodextrin – norfloxacin inclusion complexes. Part 2. Inclusion mode and stability studies. **Expert Review of Anti-Infective Therapy**, v. 13, n. 1, p. 131–140, 2015b.

MILLER, O.; HEMPHILL, R. R. UNINARY TRACT INFECTION AND PYELONEPHRITIS. **Emergency Medicine Clinics of North America**, v. 19, n. 3, p. 655-674, 2001.

MOLLICA, J. A. *et al.* Hydrolysis of benzothiadiazines. **Journal of Pharmaceutical Sciences**, v. 60, n. 9, p. 1380-1384, 1971.

NEU, H. C. Urinary tract infections. **The American Journal of Medicine**, v. 92, n. 4, Supplement 1, p. S63-S70, 1992.

NIELSEN, F. S. *et al.* Characterization of prototype self-nanoemulsifying formulations of lipophilic compounds. **Journal of pharmaceutical sciences**, v. 96, n. 4, p. 876-892, 2007.

NORRBY, S. R. Useful agents in the management of urinary tract infections. **International Journal of Antimicrobial Agents**, v. 4, n. 2, p. 129-134, 1994.

O'DONNELL, J. A.; GELONE, S. P. The newer fluoroquinolones. **Infectious disease clinics of North America**, v. 18, n. 3, p. 691-716, 2004.

OLIVEIRA, P. R. *et al.* Liquid chromatographic determination of norfloxacin in extended-release tablets. **Journal of chromatographic science**, v. 47, n. 9, p. 739-744, 2009.

PATIL, S. B.; SAWANT, K. K. Mucoadhesive microspheres: a promising tool in drug delivery. **Current drug delivery**, v. 5, n. 4, p. 312-318, 2008.

PINA, E. *et al.* Infecções associadas aos cuidados de saúde e segurança do doente. **Revista Portuguesa de Saúde Pública**, v. 10, p. 27-39, 2010.

PORTER, C. J. *et al.* Enhancing intestinal drug solubilisation using lipid-based delivery systems. **Advanced Drug Delivery Reviews**, v. 60, n. 6, p. 673-691, 2008.

PORTER, C. J.; TREVASKIS, N. L.; CHARMAN, W. N. Lipids and lipid-based formulations: optimizing the oral delivery of lipophilic drugs. **Nature Reviews Drug Discovery**, v. 6, n. 3, p. 231-248, 2007.

POUTON, C. W. Formulation of self-emulsifying drug delivery systems. **Advanced Drug Delivery Reviews**, v. 25, n. 1, p. 47-58, 1997.

POUTON, C. W. Lipid formulations for oral administration of drugs: non-emulsifying, self-emulsifying and 'self-microemulsifying' drug delivery systems. **European Journal of Pharmaceutical Sciences**, v. 11, p. S93-S98, 2000.

RABBAA, L. *et al.* Intestinal elimination of ofloxacin enantiomers in the rat: evidence of a carrier-mediated process. **Antimicrobial agents and chemotherapy**, v. 40, n. 9, p. 2126-2130, 1996.

RANG, H. P.; RITTER, J. M.; DALE, M. M., Eds. **Farmacologia**. Rio de Janeiro: Elsevier, p.386-389ed. 2012.

RAWAT, M. *et al.* Nanocarriers: promising vehicle for bioactive drugs. **Biological and Pharmaceutical Bulletin**, v. 29, n. 9, p. 1790-1798, 2006.

REVELLE, L. K. *et al.* Identification of chlorothiazide and hydrochlorothiazide UV-A photolytic decomposition products. **Journal of pharmaceutical sciences**, v. 86, n. 5, p. 631-634, 1997.

RICHTERICH, R. Natriuretic potency of hydrochlorothiazide in humans. **Experientia**, v. 14, n. 12, p. 458-458, 1958.

RITTIRSCH, D. *et al.* Functional roles for C5a receptors in sepsis. **Nature medicine**, v. 14, n. 5, p. 551-557, 2008.

SELVAMUTHUKUMAR, S. *et al.* Nanosponges: A novel class of drug delivery system-review. **Journal of Pharmacy & Pharmaceutical Sciences**, v. 15, n. 1, p. 103-111, 2012.

SHAH, P.; BHALODIA, D.; SHELAT, P. Nanoemulsion: a pharmaceutical review. **Systematic Reviews in Pharmacy**, v. 1, n. 1, p. 24, 2010.

SHILLINGFORD, C. A.; VOSE, C. W. Effective decision-making: progressing compounds through clinical development. **Drug discovery today**, v. 6, n. 18, p. 941-946, 2001.

SHUGARTS, S.; BENET, L. Z. The role of transporters in the pharmacokinetics of orally administered drugs. **Pharmaceutical research**, v. 26, n. 9, p. 2039-2054, 2009.

SJÖBERG, Å. *et al.* Comprehensive study on regional human intestinal permeability and prediction of fraction absorbed of drugs using the Ussing chamber technique. **European Journal of Pharmaceutical Sciences**, v. 48, n. 1, p. 166-180, 2013.

SMART, J. D. The basics and underlying mechanisms of mucoadhesion. **Advanced Drug Delivery Reviews**, v. 57, n. 11, p. 1556-1568, 2005.

SMETANOVÁ, L. *et al.* Caco-2 cells, biopharmaceutics classification system (BCS) and biowaiver. **Acta Medica (Hradec Kralove)**, v. 54, n. 1, p. 3, 2011.

SWAMINATHAN, S.; CAVALLI, R.; TROTTA, F. Cyclodextrin-based nanosponges: a versatile platform for cancer nanotherapeutics development. **Wiley Interdisciplinary Reviews: Nanomedicine and Nanobiotechnology**, 2016.

SWAMINATHAN, S. *et al.* Formulation of betacyclodextrin based nanosponges of itraconazole. **Journal of Inclusion Phenomena and Macrocyclic Chemistry**, v. 57, n. 1-4, p. 89-94, 2007.

SWEETMAN, S. C. **Martindale: The complete drug reference**. 36^a ed. Londres: Pharmaceutical press. 2011.

TAGNE, J.-B. *et al.* A nanoemulsion formulation of tamoxifen increases its efficacy in a breast cancer cell line. **Molecular Pharmaceutics**, v. 5, n. 2, p. 280-286, 2008.

TAKÁCS-NOVÁK, K. *et al.* Lipophilicity of antibacterial fluoroquinolones. **International Journal of Pharmaceutics**, v. 79, n. 1, p. 89-96, 1992.

TEJASHRI, G., AMRITA, B., DARSHANA, J. Cyclodextrin based nanosponges for pharmaceutical use: A review. **Acta pharmaceutica**, v. 63, n.3, p. 335-358, 2013.

TROTTA, F., CAVALLI, R. Characterization and applications of new hyper-cross-linked cyclodextrins. **Composite Interfaces**, v. 16, n. 1, p. 39-48, 2009.

TROTTA, F., ZANETTI, M., CAVALLI, R. Cyclodextrin-based nanosponges as drug carriers. **Beilstein journal of organic chemistry**, v. 8, n.1, p 2091-2099, 2012.

TSAPIS, N. *et al.* Trojan particles: large porous carriers of nanoparticles for drug delivery. **Proceedings of the National Academy of Sciences**, v. 99, n. 19, p. 12001-12005, 2002.

UEDA, S. *et al.* Evaluation of capacity-limited first-pass effect through liver by three-points sampling in portal and hepatic veins and systemic artery. **Pharmaceutical Research**, v. 19, n. 6, p. 852-7, 2002.

USP. **United States Pharmacopoeia XXX**. USP Convention Inc. Rockville. 2007.

VAN BAMBEKE, F. *et al.* Quinolones in 2005: an update. **Clinical Microbiology and infection**, v. 11, n. 4, p. 256-280, 2005.

VASCONCELOS, T.; SARMENTO, B.; COSTA, P. Solid dispersions as strategy to improve oral bioavailability of poor water soluble drugs. **Drug Discovery Today**, v. 12, n. 23-24, p. 1068-75, 2007.

VEIGA, F.; PECORELLI, C. C. M. F.; RIBEIRO, L. S. S. **As ciclodextrinas em tecnologia farmacêutica**. Coimbra: Minerva, 2006.

VIERNSTEIN, H.; WEISS-GREILER, P.; WOLSCHANN, P. Solubility enhancement of low soluble biologically active compounds temperature and cosolvent dependent inclusion complexation. **International Journal of Pharmaceutics**, v. 256, n. 1-2, p. 85-94, 2003.

WAGENLEHNER, F. M.; WEIDNER, W.; NABER, K. G. Chlamydial infections in urology. **World journal of urology**, v. 24, n. 1, p. 4-12, 2006.

WANG, L. *et al.* Formation and stability of nanoemulsions with mixed ionic–nonionic surfactants. **Physical Chemistry Chemical Physics**, v. 11, n. 42, p. 9772-9778, 2009.

WANG, X. *et al.* Synthesis of β -cyclodextrin modified chitosan-poly(acrylic acid) nanoparticles and use as drug carriers. **Carbohydrate Polymers**, v. 90, n. 1, p. 361-369, 2012.

WANG, X. *et al.* Contribution of reactive oxygen species to pathways of quinolone-mediated bacterial cell death. **Journal of Antimicrobial Chemotherapy**, v. 65, n. 3, p. 520-524, 2010.

YADAV, P. S. *et al.* Development, Characterization, and Pharmacodynamic Evaluation of Hydrochlorothiazide Loaded Self-Nanoemulsifying Drug Delivery Systems. **The Scientific World Journal**, v. 2014, 2014.

YOON, E. Y. *et al.* Medical management of children with primary hypertension by pediatric subspecialists. **Pediatric Nephrology**, v. 24, n. 1, p. 147-153, 2009.

ZABALETA, V. *et al.* Oral administration of paclitaxel with pegylated poly (anhydride) nanoparticles: permeability and pharmacokinetic study. **European Journal of Pharmaceutics and Biopharmaceutics**, v. 81, n. 3, p. 514-523, 2012.

ZHAO, Y. *et al.* Self-nanoemulsifying drug delivery system (SNEDDS) for oral delivery of Zedoary essential oil: formulation and bioavailability studies. **International journal of pharmaceutics**, v. 383, n. 1, p. 170-177, 2010.

APÉNDICE A



Inclusion complexes of hydrochlorothiazide and β -cyclodextrin: Physicochemical characteristics, in vitro and in vivo studies



Cassiana Mendes^{a,*}, Aline Buttchevitz^a, Jéssica H. Kruger^a, Jadel Müller Kratz^b, Cláudia Maria Oliveira Simões^b, Patricia de Oliveira Benedet^c, Paulo Renato Oliveira^d, Marcos Antônio Segatto Silva^a

^a Post graduation Program in Pharmaceutical Sciences, Quality Control Laboratory, Universidade Federal de Santa Catarina, JK 207, 88040-900 Florianópolis, SC, Brazil

^b Departamento de Ciências Farmacéuticas, Universidade Federal de Santa Catarina, 88040-900 Florianópolis, SC, Brazil

^c Department of Pharmacology, Universidade Federal de Santa Catarina, 88040-900 Florianópolis, SC, Brazil

^d Post graduation Program in Pharmaceutical Sciences, Universidade Estadual do Centro-Oeste/UNICENTRO, 85040-080, Guarapuava, PR, Brazil

ARTICLE INFO

Article history:

Received 9 June 2015

Received in revised form 6 November 2015

Accepted 9 December 2015

Available online 11 December 2015

Keywords:

Hydrochlorothiazide

Inclusion complex

Physicochemical characterization

Solubility

Permeability

In vivo diuretic activity

ABSTRACT

Hydrochlorothiazide is a thiazide diuretic widely used in clinics to treat arterial hypertension. It is a class IV drug according to the Biopharmaceutical Classification System, that is, it presents low solubility and low permeability and, consequently, low absorption in the gastrointestinal tract. As a strategy to improve stability and biopharmaceutical properties of hydrochlorothiazide, the use of cyclodextrins to produce inclusion complexes, applying different methods, was investigated. In the phase solubility studies, β -cyclodextrin was identified as the cyclodextrin which provided the most promising results in terms of the solubilization of the drug. The thermal analysis verified the interaction between hydrochlorothiazide and β -cyclodextrin, indicating the formation of inclusion complexes, and the thermal stability varied according to the preparation technique. The physicochemical characterization showed that in the inclusion complexes obtained by co-evaporation, kneading followed by freeze-drying and kneading followed by spray-drying the hydrochlorothiazide complexation mostly occurred with different degrees of amorphization and the drug solubility was improved. These three inclusion complexes presented better in vitro characteristics and the inclusion complex obtained by kneading followed by freeze-drying increased the in vivo diuretic activity of the drug accompanied by significant effects on natriuresis, kaliuresis and chloriguresis. The inclusion complex formation was effective in improving the biopharmaceutical properties of hydrochlorothiazide and protecting the drug from hydrolysis. This paper describes an important alternative approach to the development of liquid pharmaceutical formulations to pediatric administration, a real need of the current pharmaceutical market.

© 2015 Elsevier B.V. All rights reserved.

1. Introduction

Hydrochlorothiazide (HCTZ), a thiazide diuretic which was discovered in 1958, was the first effective drug used in arterial hypertension treatment. The drug acts on the distal tubule binding to the chloride ion site on the sodium cotransporter (Rang et al., 2012). Chemically known as 6-chloro-1,1-dioxo-3,4-dihydro-2 H-1,2,4-benzothiadiazine-7-sulfonamide ($C_7H_6ClN_2O_4S_2$), hydrochlorothiazide is an odorless white crystalline powder with a molecular weight of 297.74 g/mol, it presents aqueous solubility of 722 mg/L and two pKa values of 7.0 and 9.2 (25 °C) (Kadam et al., 2011; USP, 2007; Yalkowsky and Dannenfelser, 1992). Low absorption of HCTZ in the gastrointestinal tract occurs due to its low aqueous solubility and low permeability and based on these factors HCTZ is classified as class IV according to the Biopharmaceutical Classification System (BCS) (Amidon et al., 1995; Kasim et al., 2004; Yu et al., 2002). Consequently, it presents

low bioavailability, with a large variation in this parameter. Furthermore, the drug is associated with instability problems, such as hydrolysis in aqueous solution, as described by Mollica and coworkers (Mollica et al., 1971).

Oral administration is the first choice for many drugs, due to its convenience, simplicity and relatively low cost. The in vivo behavior of drugs following oral administration is dependent on their solubility and permeability (Ansel et al., 2010; Yu et al., 2002). The percentage of drug candidates which fail in pre-clinical trials is significant and most are due to problems associated with the absorption properties. The greatest difficulties in relation to oral administration are encountered with formulations containing class IV drugs (Vasconcelos et al., 2007).

In the pharmaceutical area, cyclodextrins (CD) are being used as a strategy to increase drug solubility, stability and bioavailability. CDs are a class of pharmaceutical excipients which contain D-glucopyranose units linked together to form cyclic conical structures. CDs with six, seven and eight units of glucose are known as α -cyclodextrin (α CD), β -cyclodextrin (β CD) and γ -cyclodextrin (γ CD), respectively. These

* Corresponding author.

E-mail address: cassi_ana@yahoo.com.br (C. Mendes).

are the so-called natural CDs and they can be obtained in relatively high yields. The torus-shaped and the outer surface of hydroxylic groups provide unique physicochemical properties to these cyclic sugars, which can be water soluble and at the same time complexed in the inner cavity by hydrophobic molecules. The stability of inclusion complexes can be provided by non-covalent interactions, such as hydrophobic interactions, electronic effects, steric factors and van der Waals forces (Brewster and Loftsson, 2007; Mady et al., 2010; Pathak et al., 2010). The formation of an inclusion complex between a drug and CD can provide the 'guest' molecule with increased bioavailability due to increased stability, solubility, dissolution rate, wettability and permeability. In general, CDs are molecular transporters which are able to transport "guest" hydrophobic molecules in solution through the lipophilic cell membrane, facilitating their absorption (Loftsson et al., 2004).

In this context, considering the problems associated with HCTZ absorption and stability, the complexation of HCTZ with different CDs was investigated with a view to improve the biopharmaceutical and stability properties. Preliminary studies on the formation of HCTZ and CD have been described in the literature (Denadai et al., 2006; Onnainty et al., 2012; Pires et al., 2011). However, these studies do not include a complete study covering from development to biological activity. To this aim, in this study inclusion complexes of HCTZ and different CDs were prepared and a complete physicochemical characterization, dissolution studies, *in vitro* permeability tests, chemical stability and *in vivo* tests were conducted to verify the efficacy of the systems developed.

2. Materials and methods

2.1. Materials

HCTZ was obtained from Valdequímica (São Paulo, Brazil) and the CDs (β -cyclodextrin, γ -cyclodextrin and 2-hydroxypropyl- β -cyclodextrin average degree of substitution DS = 0.6) were generously donated by Roquette Corporate (Labonathus Biotecnologia Internacional Ltda, São Paulo, Brazil). All other chemicals and reagents used were of analytical reagent grade.

2.2. Phase solubility studies

Solubility studies were performed according to the method reported by Higuchi and Connors (1965). Excess amounts of HCTZ were added to the solutions with increasing concentrations of β CD (β -cyclodextrin 0–16 mM), γ CD (γ -cyclodextrin 0–123 mM) and HP- β CD (2-hydroxypropyl- β -cyclodextrin 0–46 mM). The suspensions were prepared at different pH values (pH = 3.0; 4.5; 5.5 adjusted with 2% citric acid) to maintain the HCTZ stability during the complexation. These suspensions were stirred at room temperature ($25 \pm 2^\circ\text{C}$) until equilibrium was reached (24 h).

The amount of HCTZ dissolved was determined spectrophotometrically at 273 nm (Cary 50 Bio; Varian, Palo Alto, CA, USA). The CDs did not interfere with the spectrophotometric assaying of HCTZ. All experiments were carried out in triplicate.

The apparent stability constants (K_c) for the complexation were calculated using Eq. (1), where S_0 is the solubility of the drug in the absence of CD.

$$K_c = \frac{\text{slope}}{S_0(1 - \text{slope})} \quad (1)$$

2.3. Preparation of solid complexes

The solid complexes of HCTZ (molecular weight 297.74 g/mol) and β CD (molecular weight 1135.0 g/mol) were prepared by different processes: co-evaporation, freeze-drying, and kneading followed by freeze-drying or spray-drying. For the control, physical mixtures of

HCTZ and β CD were prepared by blending equimolar amounts of HCTZ and β CD in a mortar until a homogeneous mixture was obtained.

2.3.1. Co-evaporation

Equimolar quantities of HCTZ and β CD (1:1) were solubilized in a hydroalcoholic solution (1:1 M/M), adjusted to pH 3.3 with citric acid 2% and mixed by magnetic stirring at room temperature ($25^\circ\text{C} \pm 2^\circ\text{C}$) for 24 h. This solution was then filtered (0.45 μm) and the solvent removed under vacuum at 50°C .

2.3.2. Freeze-drying

This procedure involved dissolving and mixing equimolar amounts of HCTZ and β CD (1:1 M/M) in water, adjusting the pH to 3.3 with 2% citric acid and stirring at room temperature ($25^\circ\text{C} \pm 2^\circ\text{C}$) for 24 h. The filtrate (0.45 μm) was then frozen at -40°C and freeze-dried (Terroni LD 1500 freeze-dryer; Terroni LTDA, São Carlos, SP, Brazil) for 24 h.

2.3.3. Kneading

Stoichiometric amounts of HCTZ and β CD (1:1 M/M) were mixed for 20 min in a mortar, 1 mL of water was then added, the paste was mixed again for 5 min and then this last procedure was repeated. In the next step, 50 mL of water at 40°C was added to the paste formed, the pH was adjusted to 3.3 with 2% citric acid and the solution was stirred for 20 min at 40°C . The solution was filtered and dried in a freeze-dryer or spray-dryer.

2.3.3.1. Freeze-dryer. The solution obtained by kneading was frozen at -40°C and freeze-dried (Terroni LD 1500 freeze-dryer; Terroni LTDA, São Carlos, SP, Brazil) for 24 h.

2.3.3.2. Spray-dryer. The resultant solution was placed in a Mini Spray Dryer Buchi B-290 (BUCHI Labortechnik AG, Flawil, Switzerland) with an inlet temperature of 180°C , outlet temperature of 62°C , air flow rate of 30 mL/min and air pressure of 1.5 bar.

2.4. Solid analysis of inclusion complexes

2.4.1. Differential scanning calorimetry

Differential scanning calorimetry (DSC) curves for HCTZ, the HCTZ/ β CD physical mixture and the inclusion complexes produced by the different methods were obtained on a Shimadzu DSC-60 cell (Shimadzu Corporation, Kyoto, Japan) using aluminum crucibles with around 2.0 mg of sample in a dynamic N_2 atmosphere with a flow rate of 50 mL/min. The heating rate was $10^\circ\text{C}/\text{min}$ and the temperature ranged from 30°C to 300°C . The DSC equipment was previously calibrated with indium (melting point 156.6°C , $\Delta H = -28.54 \text{ J/g}$) and zinc (melting point 419.5°C), which are DSC calibration standards.

2.4.2. Diffuse reflectance Fourier transform infrared spectroscopy

The diffuse reflectance Fourier transform infrared spectroscopy (FT-IR) spectra were recorded using a Shimadzu FTIR IR-Prestige-21 spectrophotometer (Shimadzu Corporation, Kyoto, Japan), within a scan range of $400\text{--}4000 \text{ cm}^{-1}$, with an average of over 32 scans, at a spectral resolution of 4 cm^{-1} in KBr. A background spectrum was obtained for each experimental condition.

2.4.3. X-ray powder diffraction

X-ray powder diffraction (XRPD) patterns of samples were obtained using a Philips diffractometer, model X'Pert (Philips Analytical, Almelo, Netherlands), with a $\text{CuK}\alpha$ tube, operating at 40 kV and 40 mA, in the range of 5° to 40° (2θ) with a pass time of 5 s.

2.5. Drug content determination

The technique used to verify the true complex formation and determine the free drug in solid state is known as the "acetone wash" method (Hussein et al., 2007). This method is based on the insolubility of β CD and its complexes in acetone; however, the free HCTZ is soluble. For the determination of the free drug, 5 mg of each dry product was shaken with acetone (5 mL). The supernatant was separated out, dried under reduced pressure at 50 °C and the residue was dissolved in mobile phase and analyzed by HPLC.

For the determination of the drug content, the previously washed complex was dissolved in 400 μ L of dimethyl sulfoxide and 9.6 mL of methanol. After 12 h, the β CD precipitated and the supernatant was centrifuged at 3000 rpm for 10 min and quantified by HPLC.

The HCTZ content was calculated according to the following formula (Eq. (2)):

$$\text{Included HCTZ (\%)} = \frac{\left[\frac{\text{Complexed amount of HCTZ}}{\text{(Free amount + complexed amount)}} \right] \times 100}{(2)}$$

2.6. High performance liquid chromatography

A previously validated methodology for high performance liquid chromatography (HPLC) was used to quantify the drug. Validation parameters such as specificity, linearity, precision, accuracy, robustness, limit of detection and quantification were within the acceptable range according to the International Conference on Harmonization (ICH, 2005). Validation parameters all were (unpublished data).

All of the analysis was performed on a Shimadzu liquid chromatograph (Kyoto, Japan) consisting of a LC-10A VP quaternary pump and UV-VIS detector, model SDP-10AVP, managed by a SCL-10AVP controller. The chromatograph was equipped with a Luna 5 μ m Phenomenex (Torrance, CA, USA) C₁₈ column (150 \times 4.60 mm, 5 μ m) conditioned in a SPD-10AVP column oven at 40 °C and UV-VIS detection at 260 nm. The column was eluted with an isocratic mobile phase consisting of water (pH 3 adjusted with phosphoric acid) and acetonitrile (80:20 v/v) at a flow rate of 1.0 mL/min with an injection volume of 50 μ L.

2.7. In vitro dissolution study

Dissolution studies ($n = 6$) were performed with 900 mL of simulated intestinal fluid without enzymes (0.05 M potassium phosphate, pH 6.8), maintained at 37 °C \pm 0.5 °C using the United States Pharmacopoeia apparatus I (basket) and stirred at 75 rpm. For the dissolution studies, samples equivalent to 50 mg of HCTZ were collected and the amount of HCTZ dissolved was measured by spectrophotometry (Cary 50 Bio; Varian, USA) at 273 nm.

After the assays, the similarity factor (f_2) was calculated according to the following equation (Eq. (3)):

$$f_2 = 50 \cdot \log \left\{ \left[1 + \left(\frac{1}{n} \right) \sum_{i=1}^n (Rt - Tt)^2 \right]^{-0.5} \cdot 100 \right\} \quad (3)$$

where Rt and Tt are the cumulative percent dissolved at each time point, t , for the reference and test dissolution profiles, respectively.

Values of between 50 and 100 for f_2 ensure the sameness of the release profiles. Only one measurement should be considered after 85% dissolution of the drug (Ahuja et al., 2007; Moore and Flanner, 1996).

2.8. Evaluation of intestinal permeability

The intestinal epithelial permeability was determined from transport rates across Caco-2 cell monolayers (apical to basolateral). Cells

(ATCC:HTB-37) were cultured in high glucose (4.5 g/L) Dulbecco's modified Eagle's medium (Gibco, Carlsbad, CA, USA) supplemented with 10% fetal bovine serum and 1% non-essential amino acids (Gibco, Carlsbad, CA, USA). Cultures were maintained at 37 °C in a humidified 5% CO₂ atmosphere. For the transport experiments, cells (passages #114–116) were harvested and seeded on 0.4 μ m polycarbonate inserts (Millipore, Billerica, MA, USA), at a density of 1.66×10^5 cells/cm², and were allowed to grow and differentiate for 21–28 days in the culture medium.

Prior to the experiments, cell monolayers were equilibrated for 30 min at 37 °C with transport buffer, consisting of Hank's balanced salt solution (HBSS) pH 6.8 (apical side) and pH 7.4 (basolateral side). Monolayer integrity was assessed before and after the experiments by measuring the transepithelial electrical resistance (TEER). Only monolayers with TEER values above 200 Ω cm² were considered for the data analysis.

Samples of the free drug, and the corresponding amount of the drug-loaded complex and the physical mixture, were obtained from dissolution studies conducted in HBSS at pH 6.8, for 180 min, as described in Section 2.7. Samples were added to the apical sides of the inserts and incubated for 180 min at 37 °C under constant stirring (150 rpm). Receiver chambers were sampled at 0, 45, 90, 120 and 180 min, and promptly replenished with an equivalent amount of pre-heated transport buffer ($n = 6$). The apparent permeability coefficients (P_{app}) were calculated from the following equation (Eq. (4)):

$$P_{app} = \frac{\Delta Q}{\Delta t} \times \frac{1}{AC_0} \quad (4)$$

where $\Delta Q/\Delta t$ is the steady-state flux (mol/s), C_0 is the initial concentration in the donor chamber at each time interval (mol/mL), and A is the surface area of the filter (0.6 cm²).

The dissolution–absorption relationship for each sample was investigated by plotting the fraction of drug absorbed (F_a) against the fraction of drug dissolved (F_d – dissolution profiles obtained under the same conditions as those applied in the permeability study), paired according to identical times. F_a was considered as the fraction of permeated drug relative to the total amount of drug in the receiver chamber after 180 min, which is approximately the mean residence time of the drug in the small intestine. Additionally, this approach takes into account the mean dissolution time required to compute the absorption time (Ginski and Polli, 1999; Polli et al., 1996).

2.9. Chemical stability

The stability of HCTZ, physical mixture and inclusion complexes in water were evaluated. Samples equivalent to 10 mg of HCTZ were placed into amber flasks containing 50 mL of water and stored at ambient temperature (25 °C). In the intervals of 0, 5, 10, 15 and 30 days, samples were diluted to 10 μ g/mL in mobile phase and the total of HCTZ content was analyzed by HPLC as described above to verify the CD capacity to protect the included molecule.

2.10. In vivo studies

2.10.1. Animals

Female Wistar rats (weighing 210–250 g) were housed in a temperature (22 \pm 2 °C) and light (12 hour light/dark cycles) controlled room, with free access to water and food. All animal care and experimental procedures were approved by the University Institutional Ethics Committee and are in accordance with CONCEA (National Council for the Control of Animal Experimentation) guidelines.

2.10.2. Evaluation of the diuretic activity

The diuretic activity was determined according to a previously described method (Kau et al., 1984), with minor modifications. Rats were distributed randomly into four groups of 6 animals each: Group

1 received HCTZ inclusion complexes; Group 2 received the physical mixture; Group 3 received free HCTZ (all at 10 mg/kg, p.o.) and Group 4 (control) animals were not submitted to any treatment. The rats were then placed individually in a metabolic cage for 24 h, with free access to water and food. At different time intervals after treatment (2, 8 and 24 h) urinary excretion was measured. Cumulative urine excretion was calculated in relation to body weight and expressed as mL/100 g. Electrolyte concentrations (Na^+ , K^+ , and Cl^-) of the urine samples of each rat were also measured, using the ion selective method on a Dade-Behring Dimension RXL analyzer.

2.10.3. Statistical analysis

The results were expressed as mean \pm standard error of mean (S.E.M.) of 4–6 animals per group. Statistical analysis was performed using one-way analysis of variance (ANOVA) followed by the Tukey test. A *p* value less than 0.05 was considered statistically significant. The graphs were drawn and the statistical analysis was performed using GraphPad Prism, version 6.0 for Windows (GraphPad Software, San Diego, CA, USA).

3. Results and discussion

3.1. Phase solubility studies

In order to verify that the addition of cyclodextrin improved the solubility of HCTZ the first step was to carry out phase solubility studies, originally developed by Higuchi and Connors (1965). The time required to reach the thermodynamic equilibrium was experimentally determined and found to be 24 h. The graphic representations of the variation in the solubility of HCTZ as a function of the increase in CD (β CD, γ CD and HP β CD) are given in the phase diagrams (Fig. 1A and B). These diagrams were obtained at different acidic pH levels, since HCTZ could undergo hydrolysis under basic pH conditions (Mendes et al., 2013; Yamana et al., 1969).

The phase diagrams obtained for γ CD and HP β CD (Fig. 1A) are type B, that is, the inclusion complexes formed presented limited solubility, which was lower than that of CD. The phase diagram obtained in the presence of β CD (Fig. 1B), however, at different pH values, was type A_L (linear). This indicates soluble inclusion complexes, with an increase in the HCTZ solubility when β CD was added. HCTZ presents two different pK_a values (7.0 and 9.2 – Fig. 1C) (Kadam et al., 2011). Thus, the ionization of the molecule will be dependent on the solution pH. The minimum ionizable fraction of HCTZ occurs at pH 3.3, and the presence of the non-ionizable molecules favors the formation of the inclusion complexes due to the apolar characteristic of the β CD cavity. This study reveals interactions with both ionizable and non-ionizable molecules; however, in the case of ionizable molecules the interaction is weaker. Similar results were obtained by Veiga and coworkers for tolbutamide (Veiga et al., 1996). A pH of 3.3 was chosen due to its proximity to the pH of the maximum chemical stability of the drug (Mollica et al., 1971). The linear segment of the phase diagram reveals the formation of a 1:1 (M/M) inclusion complex.

The stability constants (K_c), intrinsic solubility (S_0), maximum solubility (S_{max}) and solubility efficiency (SE, S_{max}/S_0) of the HCTZ: β CD inclusion complexes were determined based on the phase solubility diagram and are shown in Table 1. The pH value was measured in the end of the experiment and there were no differences after the equilibrium time.

It can be noted that the stability constants decreased with increasing pH, which reveals a low interaction with the ionized form of the molecule. Consequently, a high degree of ionization presented better aqueous solubility, as observed through the intrinsic solubility (S_0). It was possible to identify β CD as the CD which provided the best results in terms of the HCTZ solubilization and thus it was used in the subsequent experiments of this study.

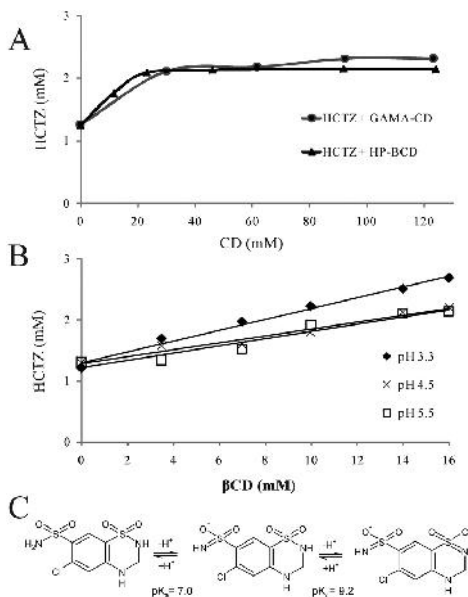


Fig. 1. (A) Phase solubility diagrams of HCTZ and γ CD or HP β CD at pH = 3.3, and (B) with β CD at pH 3.3, 4.5 and 5.5, all of them in aqueous solution (25 °C). (C) Schematic representation of hydrochlorothiazide ionization and pK_a values, adopted from Kadam and coworkers (2011). β CD: β -cyclodextrin; γ CD: gamma-cyclodextrin; HP β CD: hydroxypropyl- β -cyclodextrin; HCTZ: hydrochlorothiazide.

3.2. Solid analysis

The DSC curves obtained for the HCTZ, physical mixture and inclusion complexes prepared by different methodologies (co-evaporation, freeze-drying and kneading followed by freeze-drying or by spray-drying) are shown in Fig. 2. HCTZ revealed a fusion event at 265.17 °C ($\Delta H = 123.38$ J/g) and β CD (Fig. 2B) exhibited an endothermic event at 115.58 °C ($\Delta H = 163.22$ J/g), related to the loss of water from the inner cavity of β CD. The water loss was verified by heating the β CD up to 200 °C followed by cooling to room temperature and reheating up to 300 °C. In the second heating, no further endothermic event could be observed due to the total loss of water in the first heating (data not shown).

The DSC curves obtained for the 1:1 (w/w) physical mixture of HCTZ and β CD, as seen in Fig. 2C, showed two different endothermic events (at 114.32 °C and 262.3 °C).

All DSC curves (Fig. 2D–G) demonstrated the possible formation of an inclusion complex between β CD and HCTZ due to the absence or reduction of the characteristic HCTZ fusion event. The inclusion complex

Table 1

Data from phase solubility studies between HCTZ: β CD 1:1 (M/M). K_c (stability constant), S_0 (intrinsic solubility), S_{max} (maximum solubility), ES (solubility efficiency).

System	pH	K_c (M^{-1})	S_0 (1 G/mL)	S_{max} (1 G/mL)	ES
HCTZ: β CD	3.3	177	0.36	0.80	2.2
HCTZ: β CD	4.5	45	0.38	0.65	1.7
HCTZ: β CD	5.5	36	0.39	0.63	1.6

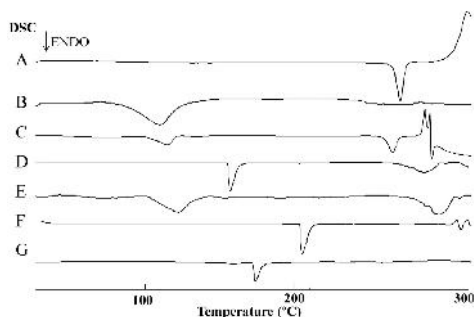


Fig. 2. DSC curves obtained for HCTZ (A), β CD (B), physical mixture (C) and different techniques of preparation: co-evaporated (D), freeze-drying (E), kneading followed by freeze-drying (F) and kneading followed by spray-drying (G).

obtained by freeze-drying, however, revealed one fusion event close to the temperature of HCTZ fusion, which indicates weak interaction between β CD and HCTZ. As seen in Fig. 2, new endothermic events for the complexes obtained applying the different methods were observed at 166.24 °C ($\Delta H = 68.35$ J/g) for co-evaporation (2D), 123.58 °C ($\Delta H = 52.51$ J/g) for freeze-drying (2E), 205.1 °C ($\Delta H = 50.38$ J/g) for kneading followed by freeze-drying (2F) and 184.21 °C ($\Delta H = 129.98$ J/g) for kneading followed by spray-drying (2G). These results indicate that the inclusion of the HCTZ molecule into the β CD cavity replaced previously bound water molecules, which led to variations in the strength of the interaction between HCTZ and β CD depending on the preparation technique. Thus, the technique employed influenced the thermal stability of the inclusion complex obtained, as shown by the endothermic events reported above.

The FT-IR spectra were obtained for the samples and the main bands are indicated (supplementary material). The physical mixture showed the superposition of bands mainly related to HCTZ and β CD. With regard to the inclusion complexes, that obtained by freeze-drying showed characteristic signals of HCTZ and β CD, in contrast to the inclusion complexes obtained by the other techniques. For the other methods a reduction or the total absence of the characteristic band of HCTZ was noted, which indicates that most of the HCTZ replaced the water molecules in the β CD cavity. For the inclusion complexes, the spectra revealed the inclusion of the heterocyclic moiety and the almost complete inclusion of the aromatic ring. This is in agreement with the molecular modeling between HCTZ and β CD described by Onnainty and co-workers, which performed theoretical and experimental methods to characterize the inclusion complex between HCTZ and β CD, however, the study did not include different production methods and drug content determination (Onnainty et al., 2012).

The diffraction patterns for HCTZ, β CD, the physical mixture and the inclusion complexes were obtained (supplementary material). The diffraction pattern for HCTZ and β CD was marked by the presence of crystalline peaks while the physical mixture revealed crystalline peaks of HCTZ and β CD with reduced intensity. The product obtained by the co-evaporation technique demonstrated some characteristic peaks of β CD, however, the most intense peaks of HCTZ could not be observed in the spectrum, which indicates a reduction in the crystallinity of this sample and the inclusion of HCTZ in the β CD cavity. The product obtained by freeze-drying demonstrated an important reduction in the crystallinity of the sample, while, it was possible to note the crystalline peak of β CD. This result is in agreement with the FT-IR and DSC analyses that the freeze-drying method resulted in the formation of the inclusion complex in the presence of HCTZ and β CD in the free form. The inclusion complexes obtained by kneading followed by freeze-drying or spray-

drying revealed a high degree of sample amorphization. The drying process increased the degree of amorphization, although the previously applied kneading also contributes greatly to this characteristic. This could be evidenced by comparing the XRPD patterns, showing that only the freeze-drying process was not able to provide that degree of sample amorphization. Besides changing the crystallinity of the sample, the kneading process was responsible for the high level of interaction between HCTZ and β CD, which will influence the physicochemical properties of the inclusion complex.

3.3. Drug content

Many studies on inclusion complexes have been carried out but few studies have used HPLC to guarantee the correct quantification of free and complexed drug. The content of HCTZ in the inclusion complex was evaluated by the wash method, which allows the determination of the free drug content and also the complexed form. The principle behind this method is the solubilization of the drug that is not included in β -CD cavity (uncomplexed form or free drug) in acetone and the non-solubilization capacity of β -CD and its complexes in the same solvent.

The solubility of the free HCTZ in acetone was performed to ensure the necessary solubility to this test and it was found to be 0.7 mg/mL. This value is higher than that necessary for 5 mg of inclusion complex used in the test. The inclusion complex solubility in acetone is minimal (<0.00023 mg/mL) and therefore it would not interfere significantly with the determination of the free drug content, in other words, β -CD and its complexes still remain practically insoluble in acetone.

To determine the content of HCTZ in the complexed form, dimethyl sulfoxide was used to destabilize the inclusion complex and methanol to solubilize HCTZ, which could then be quantified. The HCTZ in the complexed form was analyzed by HPLC and the results are shown in Table 2. HCTZ and the physical mixture (1:1 w/w) were used to verify the recovery of the HCTZ by this wash method. It can be seen that the previous process was efficient due to high levels of HCTZ amount when used alone or in the physical mixture.

A high quantity of HCTZ in the complexed form can be noted for all preparation techniques, with the exception of freeze-drying. The complex obtained by this method revealed, in the physicochemical characterization, a low degree of interaction between HCTZ and β CD, showing the melting point of HCTZ in the DSC analysis, and characteristic bands of HCTZ and β CD in the FT-IR analysis. Thus, low drug content was present in the complexed form, and this complex was not included in subsequent experiments. The other preparation techniques generated inclusion complexes with high contents of HCTZ.

3.4. Dissolution profile

Fig. 3 shows the dissolution profiles plotted from the experimental values for HCTZ, the physical mixture and the inclusion complexes

Table 2

HCTZ included content, solubility in water, solubility in simulated intestinal fluid and permeability as a free drug (HCTZ), in the physical mixture (PM) and inclusion complexes obtained by co-evaporation (COE), freeze-drying (FD), kneading followed by freeze-drying (KFD) and kneading followed by spray-drying (KSD).

	HCTZ included content (%)	Water solubility (25 °C) (μ g/mL)	Simulated intestinal fluid solubility pH 6.8 (37 °C) (μ g/mL)	P_{app} ($\times 10^{-7}$ cm/s)
HCTZ	–	37.2 \pm 0.1	60.1 \pm 0.1	6.64 \pm 1.7
PM	–	38.8 \pm 0.1	61.2 \pm 0.0	8.04 \pm 3.9
COE	85 \pm 2.2	70.7 \pm 0.0	97.1 \pm 0.1	–
FD	23 \pm 3.1	40.1 \pm 0.1	72.9 \pm 0.1	–
KFD	78 \pm 1.1	75.2 \pm 0.1	137.9 \pm 0.1	5.06 \pm 0.7
KSD	84 \pm 1.2	68.4 \pm 0.0	105.1 \pm 0.0	–

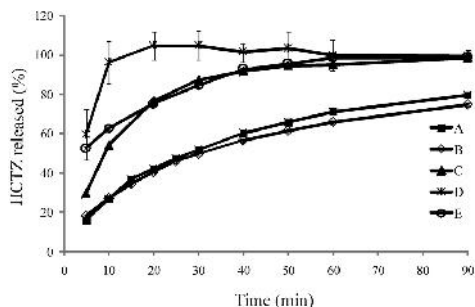


Fig. 3. Dissolution profile of HCTZ (A), physical mixture (B) and inclusion complexes obtained by co-evaporation (C), kneading followed by freeze-drying (D) and kneading followed by spray-drying (E).

obtained by co-evaporation, kneading followed by freeze-drying and kneading followed by spray-drying. Three different types of curves can be observed in the figure. HCTZ and the physical mixture (Fig. 3A and B) have very similar dissolution profiles, which reveal that HCTZ dissolution was not affected by the presence of β CD. Another type of curve was observed for the co-evaporated product (Fig. 3C), which is comprised of small crystals, as verified on the photomicrograph and in the XRPD analysis. Due to this crystalline characteristic, this inclusion complex revealed a gradual-release profile, with the release of around 30% after the first interval (5 min), higher than the corresponding value for HCTZ (16%). The HCTZ released in this inclusion complex exceeded 80% after 30 min, demonstrating an improvement in the dissolution of HCTZ included in the β CD cavity proportionate to the free hydroxyls localized externally on the β CD.

In contrast, the physicochemical techniques revealed a high degree of amorphization for the inclusion complexes obtained by kneading followed by freeze-drying and kneading followed by spray-drying, which leads to a high degree of wettability of the solid and is reflected in the dissolution profile (Fig. 3D and E). An initial release of >50% of HCTZ was noted in both cases, reaching almost 100% in only 10 min in the case of kneading followed by freeze-drying. The product obtained by kneading followed by spray-drying demonstrated a release of 80% in 30 min, similar to results for the co-evaporated product. In order to compare the dissolution profiles, an independent model based on the calculation of the similarity factor (f_2) was used (Moore and Flanner, 1996). The factor f_2 represents the closeness between the two profiles. The US FDA has set a standard range for f_2 values which indicate that the curves can be considered as similar, which is 50 to 100 (Moore and Flanner, 1996; Shah et al., 1998). Thus, HCTZ and the physical mixtures presented very similar profiles ($f_2 = 94.15$), which confirms that the β CD did not affect the HCTZ dissolution profile. On comparing the HCTZ with the products obtained by co-evaporation and kneading followed by spray-drying the f_2 values obtained were 28.15 and 14.87, respectively, that is, the release profiles for the inclusion complexes differed from that for the HCTZ. Due to the fast release of a high content from the inclusion complex obtained by kneading followed by freeze-drying, it was not necessary to determine the correlation in this case.

3.5. *In vitro* permeability study

The HCTZ permeability across Caco-2 cells was evaluated and Table 2 provides a summary of the results. For all samples, the total amount of permeated drug was below 1%, which is consistent with a permeation-limited oral absorption (BCS IV). The presence of, or complexation with β CD, did not interfere with HCTZ permeability coefficients (ANOVA, $p > 0.05$). This result is relevant since recent studies

revealed that improvement in the solubility could lead to reduction in the permeability, resulting in a null balance between gains and losses (Dahan and Miller, 2012; Loftsson et al., 2004; Miller and Dahan, 2012).

Additionally, dissolution–absorption relationships were studied, according to the approach described by Ginski and Polli (1999). To this aim, permeability and dissolution profiles were obtained under the same conditions (HBSS pH 6.8, 180 min). The graphical idea of this approach is to highlight the impact of complexation on both phenomena ruling the oral absorption of HCTZ.

The differences among dissolution profiles were less evident under these conditions (less discriminative assay), but again the complex obtained by kneading followed by freeze-drying showed a faster release profile, with high amounts of HCTZ dissolved (Fig. 3, supplementary material).

When the fraction absorbed (F_a) was plotted against the fraction dissolved (F_d), HCTZ and the physical mixture presented an intermediate ‘hockey stick’ profile, with an initial linear phase combined with an ascending phase in the latter part. This type of profile indicates that both dissolution and permeability play important roles in the overall drug absorption (dissolution and permeability rate-limited absorption), and is in good agreement with the pharmacokinetics of a BCS class IV drug (Ginski and Polli, 1999; Kasim et al., 2004).

In the case of kneading followed by freeze-drying, the complex showed a ‘reverseL’ pattern, characteristic of permeability rate-limited absorption (Ginski and Polli, 1999) (Fig. 3, supplementary material). The fast dissolution profile obtained with this complexation technique surpassed the dissolution–rate limitation, and could represent a shift in the *in vivo* absorption kinetics, since the drug is rapidly dissolved, and could be promptly available for permeation across the intestinal mucosa.

3.6. Chemical stability

The literature reports a chemical instability commonly observed for thiazides in aqueous media. In the case of HCTZ, the bell-shaped pH-dependent hydrolysis proceeds irreversibly to a ring-opened product (aminochlorobenzenedisulfonamide) (Mendes et al., 2013; Mollica et al., 1971). The chemical stability was evaluated in water in order to verify if the inclusion complex with the best formation could protect HCTZ from the hydrolysis. The results are presented in Fig. 4. It can be seen that HCTZ drug alone or in the presence of β CD hydrolyses, which reveals that the presence of β CD do not interfere in the degradation process. This degradation is accentuated in the first days for HCTZ and physical mixture; however, the inclusion complex obtained by kneading followed by freeze-drying is able to maintain the HCTZ content even after 30 days. These results provided support to the

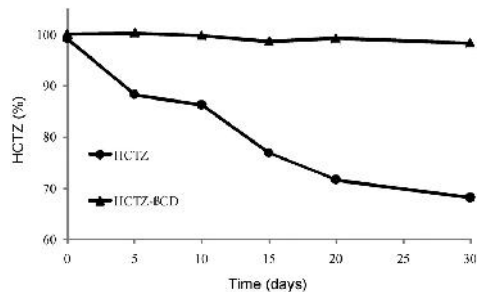


Fig. 4. HCTZ content (%) determined in the chemical stability study of HCTZ, physical mixture and inclusion complex obtained by kneading followed by freeze-drying in water at ambient temperature (25 °C) for 30 days.

hypothesis that HCTZ instability can be overcome by the production of an inclusion complex by kneading followed by freeze-drying.

3.7. Diuretic activity of inclusion complexes of hydrochlorothiazide

HCTZ, despite its low solubility and low permeability characteristics, has played an important role in hypertension therapy, acting as a diuretic alone or in combination in clinics. The pharmacological activity based on the inhibition of $\text{Na}^+ \text{Cl}^-$ transport in the distal tubule generates diuresis with a loss of these ions, which normally only reabsorbs about 5% of filtered sodium, making this diuretic less efficacious than other diuretics (loop diuretics for example) in producing diuresis, however there is also an expressive loss of potassium ions (K^+) (Brunton et al., 2010; Rang et al., 2003; Sean and Sweetman, 2002). Due to the significant improvement in the dissolution profile and given the hypothesis that the inclusion complex obtained by kneading followed by freeze-drying could lead to a shift in the in vivo absorption kinetics, this complex was chosen for the in vivo studies. Diuretic activity in animals was evaluated to observe the in vivo effect of the inclusion complex and the electrolyte concentrations (Na^+ , K^+ , and Cl^-) were also measured for comparison with the free HCTZ and its physical mixture.

The volume of urine obtained 2, 8 and 24 h after oral administration, along with the ion concentrations, is shown in Fig. 5. No statistically significant difference between the free HCTZ and the physical mixture was observed, and thus the presence of βCD has no diuretic effect. Fig. 5A shows that the oral administration of the inclusion complexes of HCTZ increases the volume of urine after 2 h when compared to the control. In other words, HCTZ included in the βCD cavity presented an anticipated pharmacological activity (statistically different) considering equimolar doses of HCTZ, the therapeutic effect of inclusion complex was faster than HCTZ free drug or physical mixture. This result can be explained by the true inclusion complex formation and the amorphization of the preparation method which reflect in the improvement of dissolution profile when compared with the HCTZ as a free drug, as observed in the dissolution studies and evidenced by the “reverseL” pattern in the fraction absorbed (Fa) plotted against the fraction dissolved (Fd –

supplementary material). Concerning drug class BCS IV which solubility hinders drug bioavailability, the inclusion complex provides high amounts of HCTZ in the intestinal lumen which is able to be promptly absorbed by the passive drug absorption, once permeability is gradient concentration dependent.

Quantification of sodium and chloride ions in urine is one of the best methods to determine the diuretic effect of drugs (Opie et al., 1991). It can be seen in Fig. 5B the natriureses caused by the administration of HCTZ in 2 and 8 h, physical mixture in 8 h and inclusion complex in 2, 8 and 24 h. In the same figure, it is noted the statistical difference ($p < 0.05$) when compared inclusion complex and HCTZ free drug alone or physical mixture. So, the inclusion complex induces natriureses at the same time of HCTZ (2 h) and it has the capacity to the maintenance of the natriureses even after 24 h.

The blockade of sodium reabsorption by HCTZ results in increased renal sodium to collecting ducts, where the absorption creates a favorable electrochemical gradient for excretion of K^+ (Tannen, 1996). As can be seen from Fig. 4C, the inclusion complex induced an important kaliuresis 2 and 24 h after the treatment. Though that the inclusion complex did not exhibit excretion of K^+ significantly different in 8 h, the kaliuresis was greater mean in 30% and 17% when compared with HCTZ free and physical mixture groups respectively. This result is probably due to variability of excretion of K^+ in groups. It is important to note that this effect produced by the inclusion complex was higher than in HCTZ free and physical 2 h after the treatment. As discussed above, this is probably because HCTZ included in βCD could be faster absorbed than HCTZ as free drug.

Relating to the excretion of Cl^- , Fig. 5D shows the chloriguresis of the inclusion complex in all times comparing to HCTZ free drug and physical mixture. As well established in the literature, one dose of HCTZ augments the urinary excretion of chloride during the first 6 h after administration with no or mildly increase between 6 and 24 h after dosing (Reyes and Leary, 1993).

These results suggest that a single dose of the inclusion complex increased the effectiveness of HCTZ as a diuretic by increasing the urine output, accompanied by significant effects on natriuresis, kaliuresis

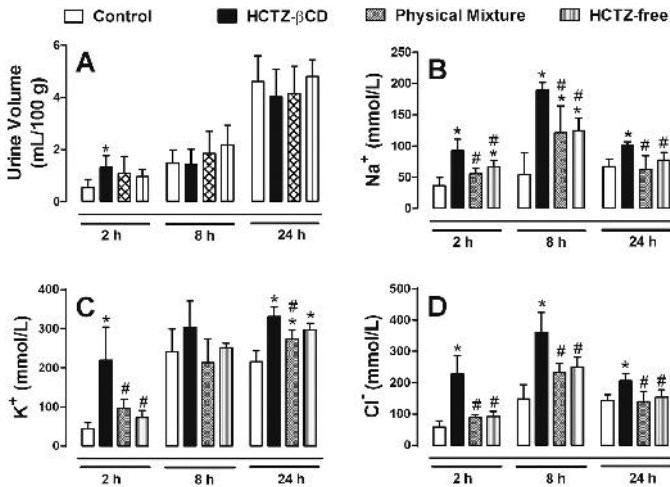


Fig. 5. Time course of diuresis (Panel A) and electrolyte excretion (Panels B, C, D) in rats treated with inclusion complexes of hydrochlorothiazide produced by kneading followed by freeze-drying. The animals were treated with inclusion complexes HCTZ- βCD (black bars), physical mixture (cross-hatched) or HCTZ-free (striped bars). Control animals were not submitted any treatment (white bars). The volume of excreted urine was measured at 2–24 h after the treatment. Hydrochlorothiazide (HCTZ-free) was administered to the positive control group. The results show the mean \pm S.E.M of 4–6 animals per group. Statistical analyses were performed by means of one-way analysis of variance (ANOVA) followed by Tukey post-test. *P.P.

and chloriuresis. This highlights the improvement in the biopharmaceutical characteristics obtained by the inclusion of HCTZ in the inner cavity of β CD applying kneading followed by freeze-drying, as observed in the physicochemical characterization, the results of all in vitro tests and the in vitro–in vivo correlation obtained from the cell culture experiments.

4. Conclusions

The solubilization and complexation of β CD and HCTZ were achieved applying different techniques to produce inclusion complexes. Based on the complete physicochemical characterization, the formation of inclusion complexes in the molar proportion of 1:1 was obtained. According to the dissolution profile, the inclusion complex obtained by kneading followed by freeze-drying demonstrated superior release characteristics in simulated intestinal fluid. Permeability studies showed non-significant difference in the apparent permeability of complexed HCTZ in relation to the free drug. The correlation of in vitro dissolution/permeability data revealed that complex obtained can present different in vivo absorption kinetics. Based on in vivo performance, it is possible to verify that HCTZ included in the β CD cavity presented an anticipated pharmacological activity considering equimolar doses of HCTZ. HCTZ instability in water can be overcome by the production of an inclusion complex by kneading followed by freeze-drying. In this way, the inclusion complex formation was effective in improving the biopharmaceutical properties of HCTZ and protecting the drug from the hydrolysis. The inclusion complex of HCTZ: β CD shows an alternative material to the development of drug delivery systems with better therapeutic benefits.

Acknowledgments

The authors would like to thank LCME/UFSC for the technical support during electron microscopy analysis, Flora Lucena Sant'ana for her skillful assistance with the in vivo studies and Dr. José Eduardo da Silva Santos, who kindly allowed the use of the metabolic cages. This study was supported by the National Council for Scientific and Technological Development (CNPq) and Coordination for the Improvement of Higher Education Personnel (CAPES).

Appendix A. Supplementary data

Supplementary data to this article can be found online at <http://dx.doi.org/10.1016/j.ejps.2015.12.015>.

References

Ahuja, N., Katara, O.P., Singh, B., 2007. Studies on dissolution enhancement and mathematical modeling of drug release of a poorly water-soluble drug using water-soluble carriers. *Eur. J. Pharm. Biopharm.* 65, 26–38.

Amidon, G.L., Lennernas, H., Shah, V.P., Crison, J.R., 1995. A theoretical basis for a biopharmaceutical drug classification: the correlation of in vitro drug product dissolution and in vivo bioavailability. *Pharm. Res.* 12, 413–420.

Ansel, H.C., Popovich, N.G., Allen, L.V., 2010. *Farmacotécnica: formas farmacéuticas e sistemas de liberação de fármacos*. Premier, São Paulo.

Brewster, M.E., Loftsson, T., 2007. Cyclodextrins as pharmaceutical solubilizers. *Adv. Drug Deliv. Rev.* 59, 645–666.

Brunton, L., Chabner, B., Knollman, B., 2010. *Goodman and Gilman's The Pharmacological Basis of Therapeutics*. 12th ed. McGraw Hill Professional.

Dahan, A., Miller, J.M., 2012. The solubility–permeability interplay and its implications in formulation design and development for poorly soluble drugs. *AAPS J.* 14, 244–251.

Denadai, A., Santoro, M., Da Silva, L., Viana, A., Santos, R., Sinisterra, R., 2006. Self-assembly characterization of the β -cyclodextrin and hydrochlorothiazide system: NMR, phase solubility, ITC and QELS. *J. Incl. Phenom. Macrocycl. Chem.* 55, 41–49.

Ginski, M.J., Polli, J.E., 1999. Prediction of dissolution–absorption relationships from a dissolution/Caco-2 system. *Int. J. Pharm.* 177, 117–125.

Higuchi, T., Connors, K.A., 1965. Phase-solubility techniques. *Adv. Anal. Chem. Instrum.* 4, 117–212.

Hussein, K., Turk, M., Wahl, M.A., 2007. Comparative evaluation of ibuprofen/ β -cyclodextrin complexes obtained by supercritical carbon dioxide and other conventional methods. *Pharm. Res.* 24, 585–592.

ICH, 2005. *Validation of Analytical Procedures: Text and Methodology Q2 (R1)*. Geneva.

Kadam, Y., Yerramilli, U., Bahadur, A., Bahadur, P., 2011. Micelles from PEO–PPO–PEO block copolymers as nanocontainers for solubilization of a poorly water soluble drug hydrochlorothiazide. *Colloids Surf. B* 83, 49–57.

Kasim, N.A., Whitehouse, M., Ramachandran, C., Bermejo, M., Lennernas, H., Hussain, A.S., Junginger, H.E., Stavchansky, S.A., Midha, K.K., Shah, V.P., 2004. Molecular properties of WHO essential drugs and provisional biopharmaceutical classification. *Mol. Pharm.* 1, 85–96.

Kau, S., Keddie, J., Andrews, D., 1984. A method for screening diuretic agents in the rat. *J. Pharmacol. Methods* 11, 67–75.

Loftsson, T., Brewster, M.E., Måsson, M., 2004. Role of cyclodextrins in improving oral drug delivery. *Am. J. Drug Deliv.* 2, 261–275.

Mady, F.M., Abou-Taleb, A.E., Khaled, K.A., Yamasaki, K., Johara, D., Taguchi, K., Anraku, M., Hirayama, F., Uekama, K., Otagiri, M., 2010. Evaluation of carboxymethyl- β -cyclodextrin with acid function: improvement of chemical stability, oral bioavailability and bitter taste of famotidine. *Int. J. Pharm.* 397, 1–8.

Mendes, C., Costa, A.P., Oliveira, P.R., Tagliari, M.P., Silva, M.A.S., 2013. Physicochemical and microbiological stability studies of extemporaneous antihypertensive pediatric suspensions for hospital use. *Pharm. Dev. Technol.* 18, 813–820.

Miller, J.M., Dahan, A., 2012. Predicting the solubility–permeability interplay when using cyclodextrins in solubility-enabling formulations: model validation. *Int. J. Pharm.* 430, 388–391.

Mollica, J.A., Rehm, C.R., Smith, J.B., Govan, H.K., 1971. Hydrolysis of benzothiadiazines. *J. Pharmacol. Sci.* 60, 1380–1384.

Moore, J.W., Flanner, H.H., 1996. Mathematical comparison of curves with an emphasis on in-vitro dissolution profiles. *Pharm. Technol.* 20, 64–74.

Onnainty, R., Schenfeld, E.M., Quevedo, M.A., Fernández, M.A., Longhi, M.R., Granero, G.E., 2012. Characterization of the hydrochlorothiazide/ β -cyclodextrin inclusion complex. Experimental and theoretical methods. *J. Phys. Chem. B* 117, 206–217.

Opie, L.H., Sonnenblick, E.H., Kaplan, I. Jr., N.M., 1991. Beta blocking agents. In: *Opie [ur.] Drugs for the Heart*. Philadelphia, Saunders, pp. 1–30.

Pathak, S.M., Musmade, P., Denge, S., Karthik, A., Bhat, K., Udupa, N., 2010. Enhanced oral absorption of saquinavir with Methyl- β -Cyclodextrin-Preparation and in vitro and in vivo evaluation. *Eur. J. Pharm. Sci.* 41, 440–451.

Pires, M.A.S., Souza dos Santos, R.A., Sinisterra, R.D., 2011. Pharmaceutical composition of hydrochlorothiazide: β -cyclo-dextrin: preparation by three different methods, physico-chemical characterization and in vivo diuretic activity evaluation. *Molecules* 16, 4482–4499.

Polli, J.E., Crison, J.R., Amidon, G.L., 1996. Novel approach to the analysis of in vitro–in vivo relationships. *J. Pharm. Sci.* 85, 753–760.

Rang, H., Dale, M.M., Ritter, J., Moore, P., 2003. *Pharmacology* Churchill Livingstone. New York.

Rang, H.P., Ritter, J.M., Dale, M.M., 2012. *Farmacologia*, in: ed (Ed.). Elsevier, Rio de Janeiro, pp. 386–389.

Reyes, A.J., Leary, W.P., 1993. Renal excretory responses to single and repeated administration of diuretics in healthy subjects: clinical connotations. *Cardiovasc. Drugs Ther.* 7, 29–44.

Sean, C., Sweetman, M., 2002. *The Complete Drug Reference*. Pharmaceutical Press, London.

Shah, V.P., Tsong, Y., Sathie, P., Liu, J.P., 1998. In vitro dissolution profile comparison — statistics and analysis of the similarity factor. *Int. J. Pharm.* 15, 889–896.

Tannen, R., 1996. Potassium disorders. *Fluids Electrolytes* 3, 127–129.

USP, 2007. *United States Pharmacopeia XXX*, USP, 30 ed. USP Convention Inc., Rockville.

Vasconcelos, T., Sarmiento, B., Costa, P., 2007. Solid dispersions as strategy to improve oral bioavailability of poor water soluble drugs. *Drug Discov. Today* 12, 1068–1075.

Veiga, F., Teixeira-Dias, J., Kedzierewicz, F., Sousa, A., Maincent, P., 1996. Inclusion complexation of toltamamide with β -cyclodextrin and hydroxypropyl- β -cyclodextrin. *Int. J. Pharm.* 129, 63–71.

Yalkowsky, S.H., Dannenfelser, R.M., 1992. *Aquasol Database of Aqueous Solubility*. College of Pharmacy, University of Arizona, Tucson, AZ.

Yamana, T., Mizukami, Y., Tsuji, A., Ichimura, F., 1969. Studies on the stability of drugs. XX. Stability of benzothiadiazines. Studies on the hydrolysis of hydrochlorothiazide in the various pH solutions. *Yakugaku Zasshi* 89, 740–744.

Yu, L.X., Amidon, G.L., Polli, J.E., Zhao, H., Mehta, M.U., Gouner, D.P., Shah, V.P., Lesko, L.J., Chen, M.L., Lee, V.H., Hussain, A.S., 2002. Biopharmaceutics classification system: the scientific basis for biowaiver extensions. *Pharm. Res.* 19, 921–925.